



**Liquefaction and erosion of mud
due to waves and current**

Experiments on Westwold Clay

P.J. de Wit

Report no. 2-93

May 1994

Hydromechanics Section
Hydraulic and Geotechnical Engineering Division
Department of Civil Engineering
Delft University of Technology
Delft, The Netherlands

Abstract

A research project was carried out at the Delft University of Technology in order to study the interaction between waves as well as a current and a muddy bed. For this purpose several experiments were made on two artificial clays, namely China Clay and Westwald Clay. The results of the experiments on China Clay were reported by De Wit (1994). In the present report only flume experiments on Westwald Clay are discussed. In the experiments made special attention was paid to the liquefaction mechanism and the influence of liquefaction on the wave damping.

Mineralogical analysis and rheological measurements showed that Westwald Clay is a more cohesive sediment than the China Clay used in the foregoing experiments. However, because of the unfavourable consolidation characteristics of this sediment, the average bed concentrations in the experiments were roughly half the value of the concentrations encountered in the China Clay beds.

The experiments in the wave/current flume showed, among other things, that a layer of fluid mud was generated when the first waves had reached the test section.

The waves were damped when a layer of fluid mud was generated. The damping was only little influenced by a current. Furthermore, it was observed that the fluid mud was transported very easily by a current.

As the Westwald Clay stucked firmly to the glass sidewalls it must be concluded that in general observations and pressure measurements made at a transparent sidewall of a set-up are not representative of the actual physical processes away from the sidewalls. Only measurements carried out far from a wall give a quantitative description of the processes inside the bed.

Pore-pressure measurements showed a transient decrease, possibly caused by the break down of the aggregate structure, succeeded by a build-up of an excess pore pressure so as to compensate for the decreased effective stress. Subsequently, the excess pore-pressure decreased gradually with time.

The measured velocity amplitudes in the fluid mud agreed well with the calculated results using a modified version of Gade's model (1958). However, the measured wave damping was underestimated by the calculated wave damping by approximately 15 per cent.

Acknowledgements

This research project was partly funded by the Commission of the European Communities, Directorate General for Science, Research and Development under MAST2 (G8 Morphodynamics research programme) and supported financially by Rijkswaterstaat. It was conducted in the framework of the Netherlands Centre of Coastal Research.

The extensive laboratory experiments could not be carried out without the continuous support of the staff of the Hydromechanics Laboratory of the Delft University of Technology. In particular I wish to thank Dirk Post, for his always enthusiastic assistance in the preparation and making of the experiments, just as Karel de Bruin, Fred van der Brugge, Mr. J. Groeneveld, Hans Tas, Frank Kalkman and Arie den Toom whose support always could be counted on. Special thanks go to Manon Moot for her continuous help during my employment as a PhD student.

Delft Hydraulics is acknowledged for making available their Haake viscometer. The suggestions of ir. Han Winterwerp and ir. John Cornelisse of Delft Hydraulics are highly appreciated.

However, most of all I would like to thank dr.ir. Cees Kranenburg who provided continuous guidance, valuable comments and highly appreciated constructive criticism throughout this research project.

Contents

Abstract	iii
Acknowledgements	v
Contents	vii
1. Introduction	1
2. Characterisation of the Westwald Clay	3
2.1 Physical and chemical properties	3
2.2 Rheological properties of suspensions	5
3. The first experiment on Westwald Clay	9
3.1 Experimental set-up	9
3.2 Preparation of the bed	10
3.3 Experimental procedure and program	14
3.4 Results	18
3.4.1 Concentration measurements prior to the tests	18
3.4.2 Test 1	19
3.4.3 Test 2	23
3.4.4 Test 3	24
3.4.5 Test 4	25
3.4.6 Test 5	29
3.4.7 Test 6	30
3.4.8 Test 7	31
3.4.9 Test 8	33
3.4.10 Test 9	34
3.4.11 Test 10	36
3.5 Conclusions	40
4. The second experiment on Westwald Clay	43
4.1 Preparation of the bed	43
4.2 Experimental procedure and program	44
4.3 Results	46
4.3.1 Concentration measurements prior to the tests	46
4.3.2 Test 1	47
4.3.3 Test 2	50
4.3.4 Test 3	55
4.3.5 Test 4	59

4.3.6	Concentration measurements prior to test 5	63
4.3.7	Test 5	64
4.3.8	Test 6	65
4.3.9	Test 7	68
4.3.10	Test 8	73
4.4	Conclusions	76
5.	General conclusions	79
Appendices		81
A	Traversing unit	81
A.1	Specifications of the traversing unit	81
A.2	Traversing program used in the experiments on Westwald Clay	83
A.3	Operation of the DA-converter	87
B	Additional information on the first experiment	89
C	Additional information on the second experiment	93
References		95

Chapter 1

Introduction

During the last decades the complex behaviour of cohesive sediments has been attracting much attention as a result of social and economic developments. The growing awareness of the disastrous effects of the accumulation of contaminated cohesive sediments in areas of great environmental importance, for instance, or the increasing costs of the removal and disposal of accumulated muds in harbours and other developments contribute to the growing interest in the behaviour of these sediments.

As a result, various research projects have been initiated in laboratories across the world, including the Hydromechanics Laboratory, to study the complex behaviour of mud under several hydraulic conditions. One of the research projects in the Hydromechanics Laboratory was started some four years ago and focused on the erosion and liquefaction of mud due to waves and current. In the framework of this project experiments were carried out in an existing flume which was adapted for this purpose. During the experiments pore pressures and velocities in the bed, and wave heights, among other things, were accurately measured when waves and/or current were present in the flume. Two artificial muds were used in these experiments, namely China Clay and Westwald Clay. Three experiments were made on China Clay and two experiments on Westwald Clay. The results of the experiments on China Clay were reported by De Wit (1994). In the present report the results of the two experiments on Westwald Clay are discussed.

The characterisation of the Westwald Clay used in the experiments is discussed in chapter 2. The experimental set-up, procedures and results of the first experiment are presented in chapter 3. Chapter 4 is concerned with the results of the second experiment and this report is concluded by summarizing the main results of the experiments on Westwald Clay (chapter 5).

Chapter 2

Characterisation of the Westwald Clay

The sediment used in this series of experiments was an artificial clay called Westwald Clay. It is a dry, greyish powder packed in sacs with a content of c. 50 kg. Altogether two major experiments were carried out on Westwald Clay from one single lot.

A clay sample was taken at random prior to the experiments. This sample was analyzed by Delft Geotechnics and by the X-ray Laboratory of the Department of Mining and Petrol Engineering (D.U.T.) in order to determine several physical and chemical parameters. The experimental procedures used by these laboratories are described by De Wit (1994). The results of these analyses are given in section 2.1. The results are compared with the specifications as given by the supplier Johnson Matthey B.V., Colour and Print Division, Maastricht, The Netherlands. The clay used can be ordered under product code RM 239. Some rheological properties of suspensions of this sediment in water were measured using a Haake rotational viscometer, made available by Delft Hydraulics. The results of these measurements are presented in section 2.2.

2.1 Physical and chemical properties

The bulk density of this sediment was determined using a so-called pycnometer. Hexane was used as a filling solution. The bulk density found was $(2.644 \pm 0.001) \cdot 10^3 \text{ kg} \cdot \text{m}^{-3}$. This value is somewhat greater than the bulk density of China Clay, which was used in preceding experiments (De Wit, 1994).

The particle size distribution was measured using a Micromeritics Sedigraph 5000 D, the principle

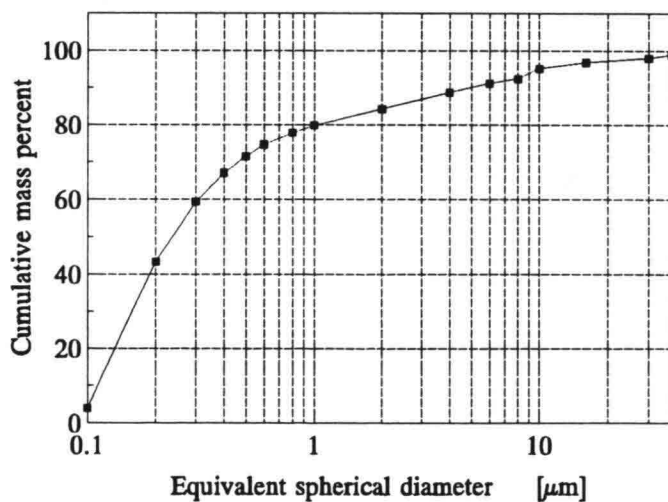


Figure 2.1.1 Particle size distribution of the Westwald Clay used.

of operation of which is based on Stokes' settling law for spherical particles. For this purpose the sediment was suspended in a peptising solution of 0.2 % sodium pyrophosphate in de-ionised water. The results show (figure 2.1.1) that this sediment is rather uniform and contains a large fraction of small particles ($< 1\mu\text{m}$).

The specific surface area was determined on the bases of the adsorption of Ethylene Glycol Monoethyl Ether (EGME) onto the particles outer surface or into the interlayer regions and was found to be $1.22 \text{ m}^2\cdot\text{g}^{-1}$, which is a rather low value.

The determination of the Cation Exchange Capacity (C.E.C.) of this sample, carried out by Delft Geotechnics, was questionable. The C.E.C. value was determined several times and the value found varied between 8.3 and 27.1 meq per 100 g dry substance. The concentrations of several cations in the sample were also determined and the results are listed in table 2.1.1.

Table 2.1.1 Concentrations of various cations in Westwald Clay.

cation	concentration [meq/100g]
calcium (Ca)	5.7
magnesium (Mg)	4.5
potassium (K)	0.4
sodium (Na)	0.3

The chemical composition was determined using an X-ray spectrometer by the X-ray laboratory of the Department of Mining and Petrol Engineering (D.U.T.). The results are listed in table 2.1.3. According to the supplier the chemical formula with which the sediment can be characterised is $\text{Al}_2\text{O}_3 \cdot 2 \text{SiO}_2 \cdot 2 \text{H}_2\text{O}$. The manufacturer also specifies the chemical composition, see table 2.1.2, which show some agreement with the results found by the X-ray laboratory.

The mineralogical composition was qualitatively determined using an X-ray diffractometer and it was found that the following minerals were present; feldspar and/or rutile, kaolinite, muscovite and α -quartz.

Table 2.1.2 Chemical composition according to supplier.
(accuracy unknown)

Substance	percentage by weight	Substance	percentage by weight
SiO_2	57.35	K_2O	1.50
Al_2O_3	26.85	CaO	0.40
TiO_2	2.21	MgO	0.20
Fe_2O_3	1.87	Na_2O	0.10
LOI	9.42		

Table 2.1.3 Chemical composition of the Westwald Clay.

Substance	percentage by weight	standard deviation	Substance	percentage by weight	standard deviation
SiO ₂	52.3	0.2	ZrO ₂	0.031	0.005
Al ₂ O ₃	28.5	0.2	V ₂ O ₅	0.027	0.006
K ₂ O	2.48	0.07	Rb ₂ O	0.026	0.003
Fe ₂ O ₃	2.30	0.07	CuO	0.024	0.004
TiO ₂	1.90	0.05	Cr ₂ O ₃	0.020	0.005
MgO	0.36	0.06	Au	0.017	0.004
Na ₂ O	0.30	0.09	ZnO	0.016	0.003
CaO	0.20	0.01	SrO	0.011	0.003
BaO	0.18	0.03	MnO	0.010	0.005
P ₂ O ₅	0.076	0.014	Ga ₂ O ₃	0.009	0.003
Cs ₂ O	0.067	0.023	Hg	0.008	0.003
LOI	10.92				

2.2 Rheological properties of suspensions

The rheological behaviour of suspensions of Westwald Clay in saline tap water was determined using a Haake rotational viscometer which comprised the Rotovisco RV 100 and the Measuring System CV 100. This instrument is capable of measuring rheological characteristics as for instance the viscosity over a wide range by using various sensor systems. A description of this instrument and some of the sensor systems that can be used during the employment is given by De Wit (1992a). Measurements were made under both steady rotational shearing and oscillatory motion (dynamic tests).

The sensor systems DA 45 and Q 30 were used to determine the flow curves of 7 suspensions with suspended sediment concentrations varying from 50 to 600 kg·m⁻³. In all of these tests the shear rate continuously increased in three minutes from zero to a maximum preselected value (about 100 s⁻¹). When the maximum shear rate was reached, the shear rate decreased to zero in the same time interval, see figure 2.2.1. The distance between the two plates of the Q 30 sensor system was set at 2 mm. The results are shown in figures 2.2.2 (sensor system DA 45) and 2.2.3 (sensor system Q 30).

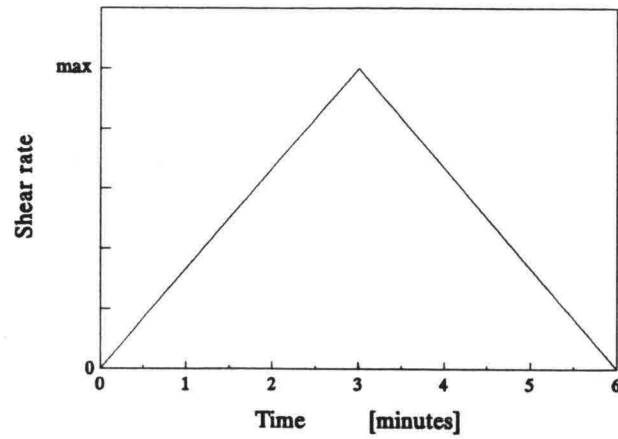


Figure 2.2.1 The shear rate as a function of the time.

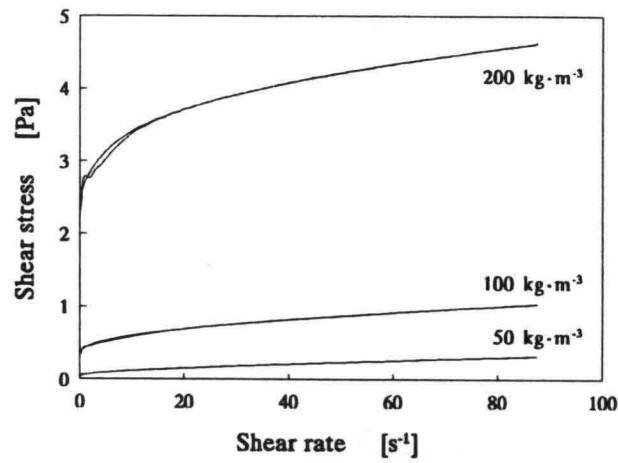


Figure 2.2.2 Flow curves of Westwald Clay suspensions measured using sensor system DA 45.

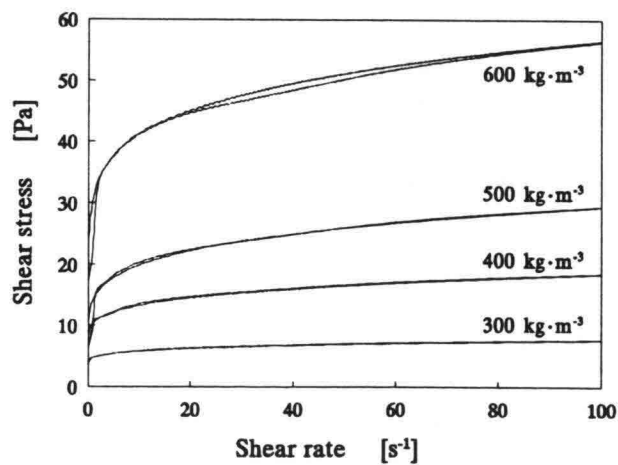


Figure 2.2.3 Flow curves of Westwald Clay suspensions measured using sensor system Q 30.

Dynamic tests were made in order to determine viscoelastic properties of some of the suspensions. The sensor systems used were PK 45, DA 45 and Q 30 and the angular frequency was set at 0.66 Hz. However, Winterwerp (1994) showed that the Haake CV100 roto-viscometer is not equipped to determine the so-called storage modulus G' and the loss modulus G'' , for the phase difference between the strain θ and the stress cannot be determined properly. For an explanation of the parameters mentioned before see De Wit (1992a). Winterwerp also showed that the complex shear modulus G^* defined as the ratio of the stress amplitude and the strain amplitude determined using the Haake viscometer may be of the correct order of magnitude. In figure 2.2.4 the calculated complex shear modulus is shown for various concentrations.

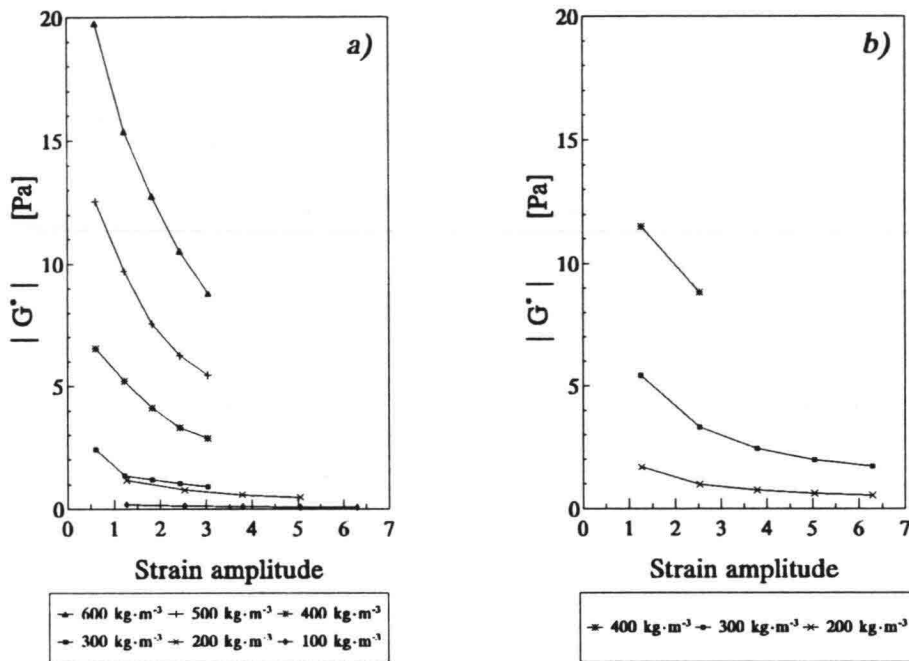


Figure 2.2.4 The complex modulus of elasticity versus the imposed strain amplitude.

a) sensor types: DA 45 & Q 30

b) sensor type: PK 45

Chapter 3

The first experiment on Westwold Clay

Around the first quarter of 1993 preparations were made for the first experiment on Westwold Clay. In section 3.1 a description is given of the experimental set-up. The preparation of the bed is discussed in section 3.2 and the experimental procedure and program are discussed in section 3.3. The experimental results are presented in section 3.4 and finally the main conclusions drawn from the first experiment on Westwold Clay are summarized in section 3.5.

3.1 Experimental set-up

In the Hydromechanics Laboratory of the Delft University of Technology an existing flume, the so-called "sediment transport flume", was adapted for the research on cohesive sediments. The flume was approximately 40 m long, 0.80 m wide and 0.8 m high. This flume was modified in order to study experimentally the behaviour of cohesive sediments under waves and current. A sketch of the flume is shown in figure 3.1.1. A recirculation pipe was installed below the flume to be able to generate a steady current. At the downstream end the fluid was withdrawn from the flume and subsequently the fluid passed an electromagnetic flowmeter and a centrifugal pump before it reentered the flume. For further information about the electromagnetic flowmeter see De Wit (1992b).

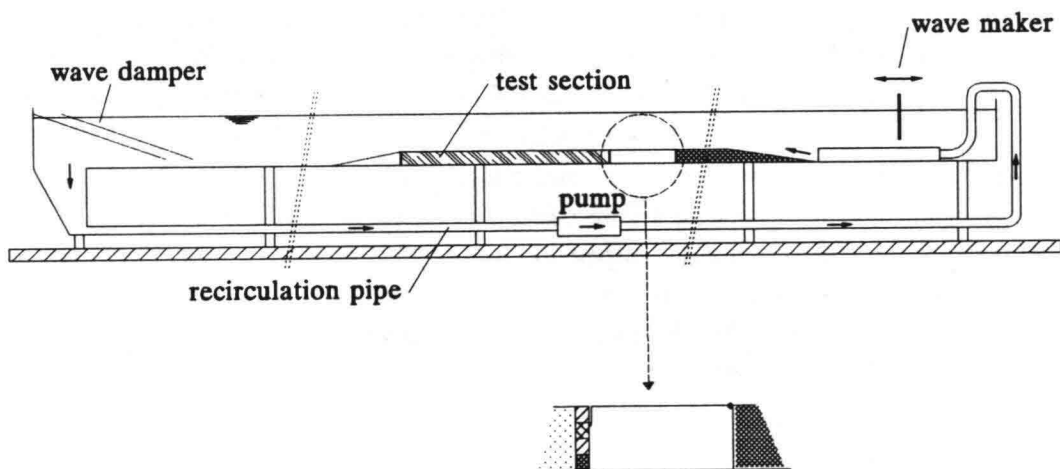


Figure 3.1.1 Sketch of the experimental set-up.

The fluid reentered the flume via a smooth stainless steel duct which was installed just below the mechanical wave generator. The duct was 0.20 m high and approximately 4 m long. The upstream, circular (\varnothing 22 cm) cross-section of the duct smoothly evolved to a rectangular ($0.20 \times 0.80 \text{ m}^2$) cross-section at the downstream side. The mechanical wave generator, which was designed and built

in the Hydro-mechanics Laboratory, was only capable of generating regular waves. The wave paddle was sinusoidally translated using a Scotch Yoke construction. During the translation the wave paddle was also able to undergo a rotation. The period of oscillation, the amplitudes of translation and the rotation were variable.

At the other end of the flume a wave damper was installed to reduce wave reflection. The wave damper was constructed in such a way that the waves were dampened and a possible current would not be hindered by the wave damper structure.

The test section which held the sediment was 8.0 m long. The vertical endwalls of the test section were 0.20 m high and were formed by stacking four beams of which three were removable during an experiment. The downstream and upstream endwalls were connected to the bottom and the upstream cement false bottom, respectively, by 2.0 m long asbestos-cement plates which were made adjustable by means of hinges. In this way the height of the test section could be adjusted during an experiment by removing a beam and lowering the free side of the plate. See for more detailed information about the experimental set-up De Wit (1994).

Prior to the experiments on Westwald Clay, tests were carried out to measure the wave decay, the wave reflection and the velocity distribution in the flume. For this purpose a temporary false bottom, made of cement, was placed over the test section. Measurements were also made in this configuration when both waves and current were present. The results showed that there was no significant wave reflection and no significant wave decay above the closed test section. Furthermore, the velocity distribution for a steady current was almost uniform. See De Wit (1994) for further information on these tests and the results.

3.2 Preparation of the bed

The Westwald Clay was provided as a dry powder. The powder was mixed with tap water in which sodium chloride was dissolved (salinity 5 ‰). The salt was added to increase the flocculation and to eliminate the possible influence of small quantities of other chemicals on the characteristics of the Westwald Clay, as for instance the settling velocity. As soon as the Westwald Clay is mixed with water several processes will be initiated, e.g. some material of the Westwald Clay will dissolve and diffuse double layers will form around a clay particle (Van Olphen, 1977). However, at a certain moment an equilibrium condition of the suspension will be established. The physical properties of such a suspension are strongly depended on the state in which the suspension is. As long as no equilibrium condition is reached the physical properties of the suspension will not be constant. In order to get reproducible measurements it is therefore very important to mix the Westwald Clay long enough.

As the consolidation characteristics of a suspension depend, among other things, on the chemical conditions of the suspension, it was tried to determine the minimal mixing period of Westwald Clay from consolidation tests. For that purpose a series of consolidation tests were made in the physico-chemical laboratory, which is situated within the Hydromechanics Laboratory.

A Westwald Clay suspension with a concentration of approximately $135 \text{ kg}\cdot\text{m}^{-3}$ and a salinity of 5 ‰ was mixed daily for at least 2 hours. A sample was taken at regular time intervals and put into a glass graduated measuring cylinder with a volume of 1 dm^3 and a diameter of about 5.9 cm. The initial height h_0 of the suspension was about $36.00 \pm 0.05 \text{ cm}$. Another sample was taken in order to determine the exact concentration of the suspension. The tests were carried out in a temperature controlled room in which the temperature was set at $21.5 \text{ }^\circ\text{C}$. Then the suspension was allowed to

consolidate. After a few seconds an interface became visible and the position of the interface h as a function of time was monitored. As soon as the position of the interface did not change any more the height of the final mud layer was measured. The results of these tests are shown in figures 3.2.1 and 3.2.2. Figure 3.2.1 shows the final height of the consolidated mud layer as a function of the mixing time. The thickness of the consolidated mud layer initially increases with the mixing time. However, after a mixing period of about 3 weeks the height of the consolidated mud layer gets fairly constant.

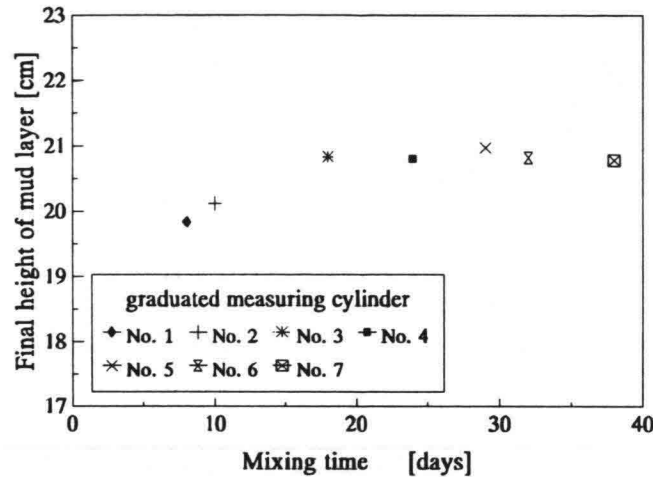


Figure 3.2.1 Final height of completely consolidated mud layer as a function of the mixing time of the initial suspension.

The monitored positions of the water-mud interface as a function of time of some of the measuring cylinders are shown in figure 3.2.2. It can be seen that the position of interface did not change any more after approximately 900 hours.

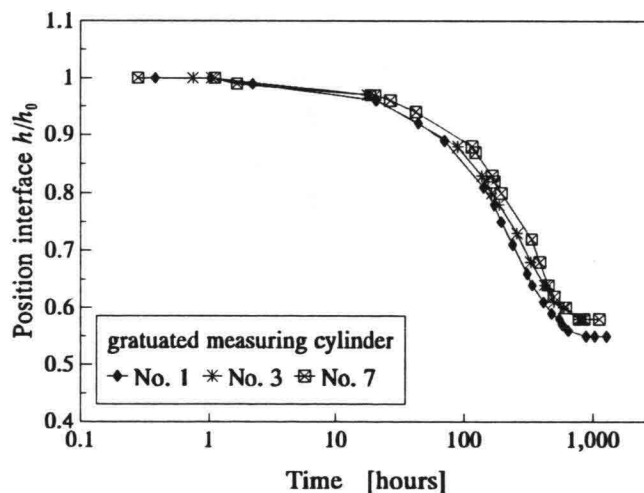


Figure 3.2.2 The position of the water-mud interface during consolidation.

Using the conductivity probe, the concentration was measured as a function of the height above the bottom of the cylinder (figure 3.2.3). According to the specifications of this device the accuracy was estimated at 10 % of the local concentration (De Wit, 1992b). These concentration profiles were used to verify the accuracy of the probe. The total dry weight of the clay in a measuring cylinder was determined using the measured concentration and the amount of initial suspension. The total dry

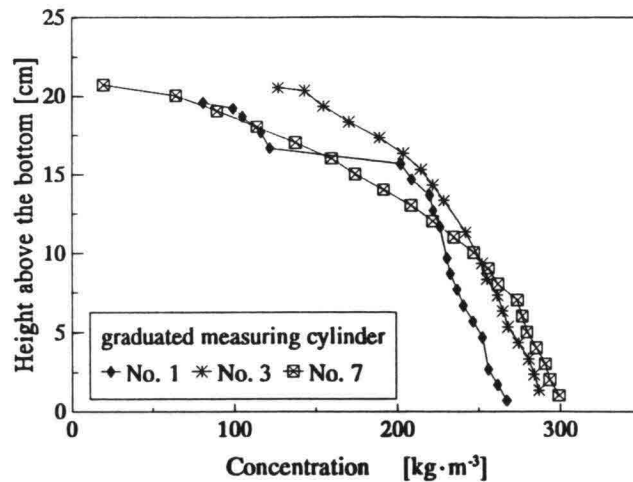


Figure 3.2.3 Concentration profiles after consolidation.
(The uppermost data points were measured below the water-mud interface.)

weight of clay was also calculated from the results found using the conductivity probe. The apparent accuracy for Westwald Clay agreed with the accuracy according to the specifications, namely a maximum error of 10 % of the local concentration.

The conclusion drawn from these results was that the Westwald Clay had to be mixed for at least 3 weeks to form an equilibrium suspension.

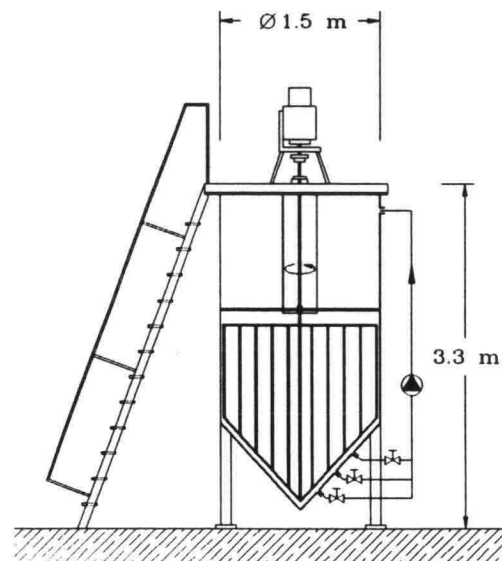


Figure 3.2.4 Sketch of the mixing tank.

The results of these consolidation tests were used to estimate the amount of clay needed to completely fill the test section with a deposited bed from a Westwald Clay suspension with a concentration of c. $135 \text{ kg}\cdot\text{m}^{-3}$. It was found that about 3 m^3 of such a suspension was necessary to fill the test section. In order to mix such a large quantity of mud a bulk mixing device was built. A sketch of the device is shown in figure 3.2.4. It was a large tank in which a revolving grid was installed. Three outlets were made in the lower part of the tank. Through these outlets fluid was

withdrawn from the tank using a sludger and was reentered at the top of the tank. A riser pipe was installed to monitor the actual amount of fluid in the tank. The top of the tank was closed, except for a small hatch, in order to prevent the escape of dust when the tank was filled. The content of the tank was approximately 4.0 m^3 .

The mixing procedure of the Westwald Clay was as follows. The tank was filled with 2.94 m^3 of tap water, then the grid was started to revolve and 14.7 kg of sodium chloride was slowly added. When the sodium chloride had dissolved, 441 kg of Westwald Clay was added and then the sludger was started. During the whole procedure the grid inside was continuously revolving. The suspension was kept inside the tank for 4 weeks. During this period the grid was continuously revolving except for the week-ends. The sludger was only running during office-hours.

At the end of the mixing period the test section was separated from the rest of the flume by installing two coated boards in the cross-section of the flume at both ends of the test section. The content of the mixing tank was pumped to the separated test section using the sludger until the height of the suspension in the test section was approximately 44.5 cm . The remaining part of the flume was filled with tap water in order to decrease the leakage of mud out of the test section. The suspension in the test section was mixed again using a mixer, which was installed on a remote-controlled measuring carriage mounted on top of the flume. The position of the mixing rod relative to the bottom and the sidewalls was varied during the mixing period. As soon as the mixing had stopped four pore-pressure transducer were positioned at several levels above the flume bottom in the middle of the test section. For further details about these pore-pressure transducers see section 3.3. Then the suspension was allowed to consolidate.

Only a few minutes after the mixing had stopped an interface was formed between the mud and the clear water. At the surface of the water-mud interface small craters were formed through which the water was pressed out of the mud. After approximately one week, cracks became visible on the mud surface, especially near the walls. The position of the water-mud interface measured in the middle of the test section during the consolidation process is shown in figure 3.2.5. After about two weeks the tap water in the remaining parts of the flume was replaced with saline tap-water (salinity 5‰) which was mixed in the mixing tank and a few days later the boards, separating the test section from the rest of the flume, were removed.

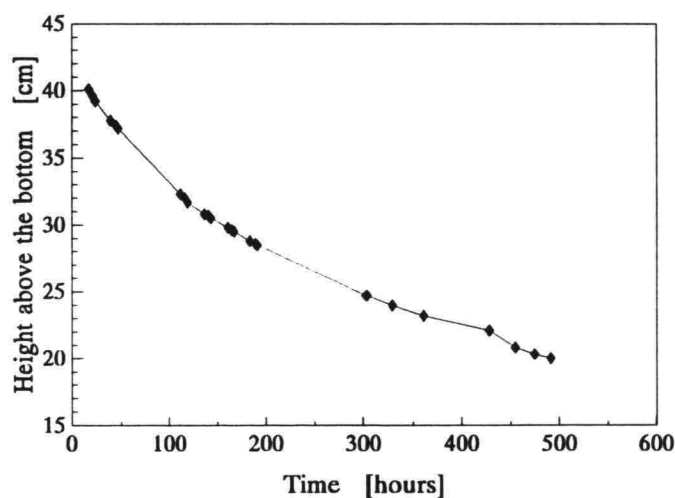


Figure 3.2.5 *The position of the water-mud interface during the consolidation in the flume versus time.*

As soon as the flume was filled, leakage of mud at the temporal boards was observed. Furthermore, small leakages were observed between the downstream end of the test section and the wave damper. After one night the water depth had decreased by 14 cm. The leakage caused a flow from the upstream part of the flume via the test section to the downstream end of the flume. As a result the consolidation of the mud was far from ideal.

3.3 Experimental procedure and program

Prior to and during the consolidation process of the mud several instruments were installed. First of all four pore-pressure transducer (Druck PDCR81, range 75 mbar) were fixed at several levels above the bottom of the flume roughly in the middle of the test section. A detailed description of this instrument is given by De Wit (1992b). The transducer was clamped in a custom-made PVC holder. A drawing of this holder is shown in figure 3.3.1. The holder was screwed on top of a stainless steel rod (diameter 5 mm). The latter was mounted on a bracket (figure 3.3.2), which was fixed in the mud suspension as soon as the mixing was stopped.

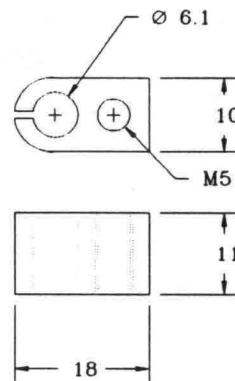


Figure 3.3.1 *Top and side views of the PVC holder which was used to position the pore-pressure transducer (dimensions in mm).*

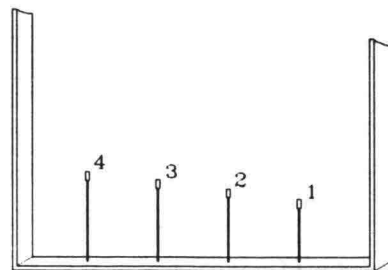


Figure 3.3.2 *Pressure transducers fixed on a frame. (Height above the bottom; no. 1: 15.0 cm, no. 2: 17.3 cm, no. 3: 19.3 cm and no. 4: 21.0 cm)*

Furthermore, six wave height meters (WHM), three electromagnetic current meters (ECM) and three optical suspended-sediment concentration meters (OCM) were installed in the centre-line of the flume. Two of the electromagnetic current meters used measured the velocity components in the longitudinal as well as in the transverse direction. The other electromagnetic current meter measured the velocity components in the longitudinal as well as in the vertical direction. The optical concentration meters were used in combination with a peristaltic pump which continuously withdrew and returned fluid (flow rate $\pm 7 \text{ cm}^3 \cdot \text{s}^{-1}$) from and into the flume via stainless steel tubes. These tubes were installed perpendicularly to the direction of the flow (transverse suction). Each electromagnetic current meter and the stainless steel tubes of each optical concentration meter were fixed to automatic traversing units, which made it possible to alter automatically the vertical measuring position during the experiment. The locations of these instruments during the experiment are schematically shown in figure 3.3.3. A detailed description of the automatic traversing units is given in appendix A. For further information about the instruments used see De Wit (1992b).

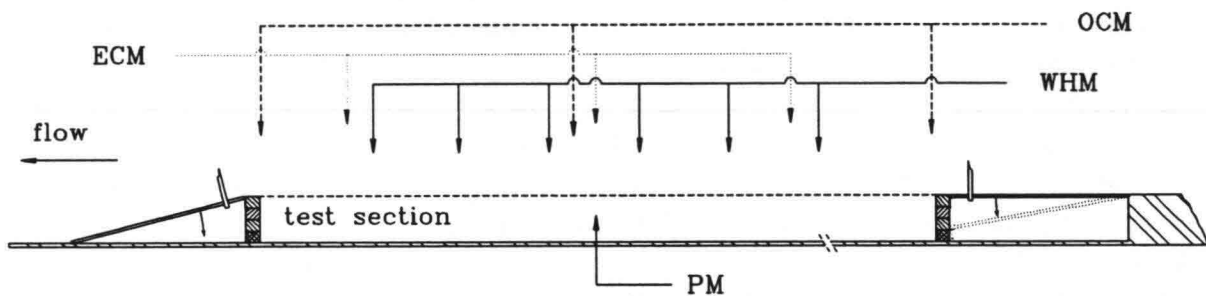


Figure 3.3.3 *Positions of the instruments.*
WHM: wave height meter, OCM: optical concentration meter,
ECM: electromagnetic current meter, PM: pressure meter.

The measurements were logged on the hard disk of a personal computer using the DACON data-acquisition software (ver. 1.2) designed for the Data Acquisition Processor DAP 2400 and the Simultaneous Sampling Board of Microstar Laboratories. The resolution of the processor was 12 bits (signed) for input voltages ranging from c. -10 V to c. 10 V and maximal 16 input signals could be logged simultaneously. The signals were logged in realtime as two's complement binary data. For further information see Dacon (1990a, 1990b).

Video recordings were made during the tests using two recording units. One stationary camera was used to record a small part of the upper part of the bed. The other camera was used to make recordings at several locations during the tests.

Prior to the experiment several actions took place. The wave height meters had to be calibrated on every range which could be used during the experiment. See for the calibration procedure De Wit (1992b). Furthermore, the output signal of the electromagnetic current meter, when it was immersed in the quiescent water, had to be adjusted to zero. This signal was logged in order to correct the measurements to be made for the zero-flow drift (See De Wit, 1992b). The maximal concentration to be measured with the optical concentration meter had to be set, after the output voltage was set to zero when clear water was pumped through the sensor. Finally, concentration profiles of the consolidated bed were measured at several locations using a conductivity probe. For additional information on the exact locations and the calibrations of the instruments used, for instance, see

appendix B.

After the preliminary measurements were made, the first experiment on Westwald Clay was started on April 22nd, 1993. This experiment comprised 10 tests, spread over three days.

The first test was started with the generation of waves with a constant wave height for approximately half an hour. The wave period was set at 1.5 s. Then the pump was started and a steady current was generated. The flow rate was set at approximately $12 \text{ dm}^3 \cdot \text{s}^{-1}$ which corresponded with an average velocity of $5 \text{ cm} \cdot \text{s}^{-1}$ in the flume. After about 5 minutes the flow rate was increased until the average velocity in the flume was c. $10 \text{ cm} \cdot \text{s}^{-1}$. This procedure was repeated again until the average velocity in flume was c. $15 \text{ cm} \cdot \text{s}^{-1}$. Then the average velocity in the flume was carefully reduced to zero.

Subsequently the wave height was increased and the whole procedure was repeated twice for increasing wave heights; test 2 and test 3. Then the mud was allowed to consolidate for 12 days and the tests were resumed on May 3rd, 1993.

Four tests were carried out with the objective to measure velocity amplitudes in a liquefied layer. In these four tests (4-7) the wave height was increased step by step approximately every half an hour. No current was present in the flume during these tests. An electromagnetic current meter was used to measure velocity amplitudes in the fluid-mud layer during test 7, which was the concluding test on May 3rd.

May 6th, 1993 the tests were started again. Test 8 started with the generation of waves for approximately half an hour. As a result a layer of fluid mud was formed. Then the wave height was increased (test 9) and after approximately half an hour the pump was started and the flow rate was set at $24 \text{ dm}^3 \text{ s}^{-1}$. Velocity measurements were carried out in the fluid mud when both waves and current were present in the flume. The final test (test no. 10) was started as soon as the average flow rate was reduced to zero. In this test the wave height was increased again and after half an hour the pump was started and a flow rate was set. Similar to test 9 velocities were measured in the fluid-mud layer for two settings of the flow rate. The experimental program of this experiment is summarized in table 3.3.1.

Table 3.3.1 Experimental program of the first experiment on Westwald Clay.

test no.	details
1 (22 April 1993)	<ul style="list-style-type: none"> * No net current. Generation of waves for half an hour; <i>average wave height 31 mm.</i> * Both waves and current. Flow rate increased step by step every five minutes. Settings of flow rate: 12, 24 and 36 dm³·s⁻¹.
2 (22 April 1993)	<ul style="list-style-type: none"> * No net current. Generation of waves for half an hour; <i>average wave height 52 mm.</i> * Both waves and current. Flow rate increased step by step every five minutes. Settings of flow rate: 12, 24 and 36 dm³·s⁻¹.
3 (22 April 1993)	<ul style="list-style-type: none"> * No net current. Generation of waves for half an hour; <i>average wave height 62 mm.</i> * Both waves and current. Flow rate increased step by step every five minutes. Settings of flow rate: 12, 24 and 36 dm³·s⁻¹.
4 (3 May 1993)	<ul style="list-style-type: none"> * No net current. Generation of waves for half an hour; <i>average wave height 24 mm.</i>
5 (3 May 1993)	<ul style="list-style-type: none"> * No net current. Generation of waves for half an hour; <i>average wave height 43 mm.</i>
6 (3 May 1993)	<ul style="list-style-type: none"> * No net current. Generation of waves for half an hour; <i>average wave height 54 mm.</i>
7 (3 May 1993)	<ul style="list-style-type: none"> * No net current. Generation of waves for half an hour; <i>average wave height 67 mm.</i> * Both waves and current. Flow rate set at 24 dm³·s⁻¹.
8 (6 May 1993)	<ul style="list-style-type: none"> * No net current. Generation of waves for half an hour; <i>average wave height 45 mm.</i>
9 (6 May 1993)	<ul style="list-style-type: none"> * No net current. Generation of waves for half an hour; <i>average wave height 57 mm.</i> * Both waves and current. Flow rate set at 24 dm³·s⁻¹.
10 (6 May 1993)	<ul style="list-style-type: none"> * No net current. Generation of waves for half an hour; <i>average wave height 70 mm.</i> * Both waves and current. Flow rate set at 24 and 48 dm³·s⁻¹.

3.4 Results

The results of the separate tests are discussed in the next sections. For all of the results presented in this report the moment at which each test was started is defined as $t=0$. If a test was started with the generation of waves, the moment at which the first waves reached the test section is defined as $t=0$. If a test was started with the generation of a steady current, the moment at which the preselected flow rate was set is defined as $t=0$.

3.4.1 Concentration measurements prior to the tests

Prior to the tests concentration profiles were measured in the bed using a conductivity probe. These measurements were made at several locations in the test section.

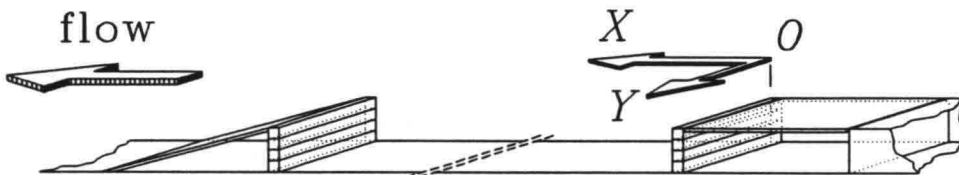


Figure 3.4.1 Cartesian coordinate system used to pinpoint the measuring positions.

Consider a cartesian coordinate system, the origin of which is at the upstream end of the test section at the right-hand sidewall of the flume when looking in downstream direction, see figure 3.4.1. This coordinate system is used to pinpoint the positions of the concentration measurements. The results of these measurements are shown in figures 3.4.2, and 3.4.3. The bed was not quite uniform. The variation in concentration in a cross-section was significant and the surface of the bed was not horizontal. The leakages were probably the cause of these inhomogeneities.

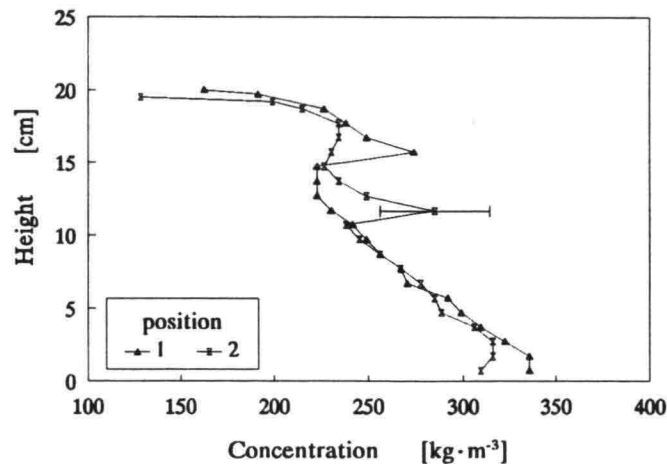


Figure 3.4.2 Concentration profiles in the bed at $x=4.25$ m.
(Position 1: $y=0.2$ m, position 2: $y=0.6$ m)

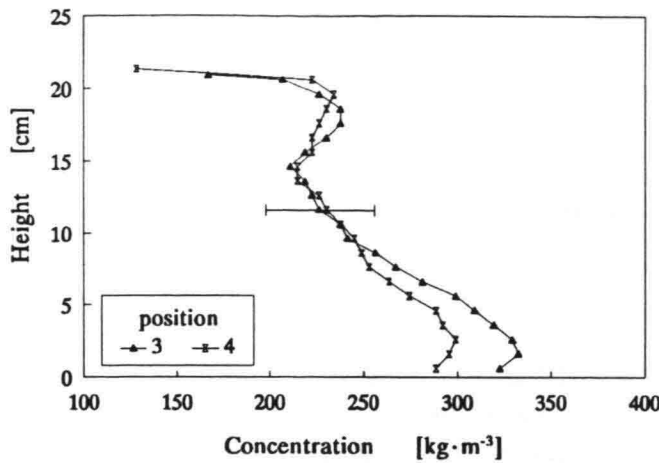


Figure 3.4.2 Concentration profiles in the bed at $x=6.01$ m. (Position 3: $y=0.2$ m, position 4: $y=0.6$ m)

3.4.2 Test 1

The wave period was set at 1.5 s and the wave height was slowly increased until the average wave height was approximately 31 mm. As soon as the first waves had reached the test section, it was observed that the upper part of the bed started to oscillate in the horizontal direction. At first the structures in the upper part were preserved, although the upper part of the bed was oscillating. Subsequently, small patches of fluid mud were formed at random. The size of these patches and also the number of patches increased with time and the cracks in the upper part of the bed disappeared. At a certain moment the entire bed surface appeared to be fluid, except for a thin layer of mud, approximately 2-3 mm thick, directly at the glass sidewall. Here the mud stuck to the glass so that no movement was observed at the glass sidewall.

Waves were generated for approximately 90 minutes. The one minute-averaged wave heights measured at six locations over the test section at several points of time during this period are shown in figure 3.4.3. This figure shows that wave damping was significant and more or less constant during the test.

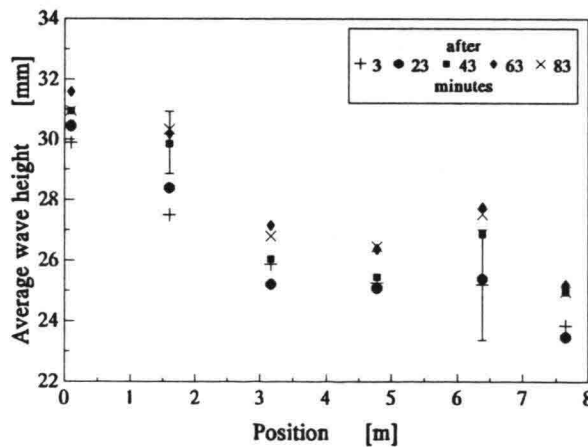


Figure 3.4.3 Average wave heights during test 1 (waves only).

Three pore-pressure transducers were fixed at three levels in the bed and one pressure transducer was fixed just above the bed as a reference (section 3.3). An example of the actual pressure changes as measured after approximately 14 minutes is shown in figure 3.4.4. The variations in pressures were almost sinusoidal. The wave-averaged pressure changes measured at the start of test 1 are shown in figure 3.4.5. The pressure measurements were averaged using a Fast Fourier Technique: the oscillations were filtered out by removing the harmonic and first-harmonic frequencies from the spectrum generated by a forward Fourier transform. This filtered spectrum was inversely transformed and subsequently this signal was filtered using a 10 point filter. Four signals are shown in figure 3.4.5: the upmost graph shows the pressure changes measured just above the bed. The other three graphs show the pore-pressure changes measured in the bed. The vertical positions at which these signals were measured are also shown in the figure. The maximum error in these signals is approximately ± 7 Pa. The reference measurement at $z=21.0$ cm shows that there was no significant change in pressure, which means that the average water depth was constant. The pore pressures in the bed showed a decrease in the average pressure followed by a transient build-up of an excess pore-pressure, which next decreased slowly with time. This trend was clearly noticeable at $z=17.3$ and $z=15.0$ cm, and was somewhat less clear at $z=19.3$ cm.

Pressure changes during the initial 400 s are shown in figure 3.4.5. In figure 3.4.6 the averaged pressures measured during the entire waves-only part of test 1 are shown. The mean pore pressures decrease significantly and at the end of the test they are lower than the pore pressures measured just before the test was started. This result seems to indicate that there was an excess pore-pressure in the bed when the test was started, which may be possible for the consolidation process was not completed at the beginning of this test (see figure 3.2.5). The average pressure amplitudes during test 1 are fairly constant as can be seen in figure 3.4.7.

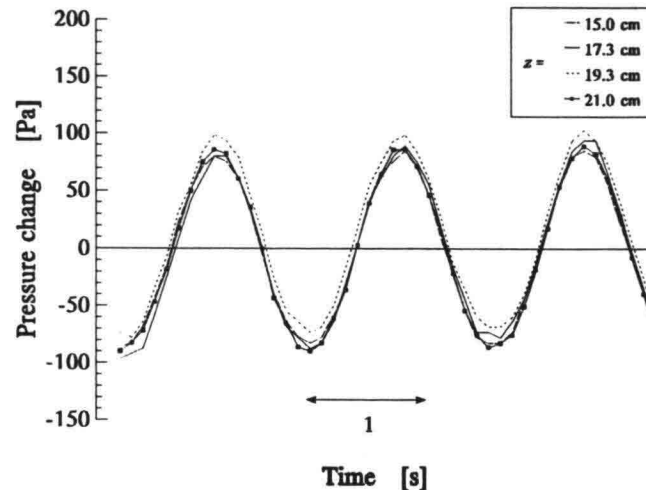


Figure 3.4.4 A representative example of the average pressure variations measured during test 1 (waves only).

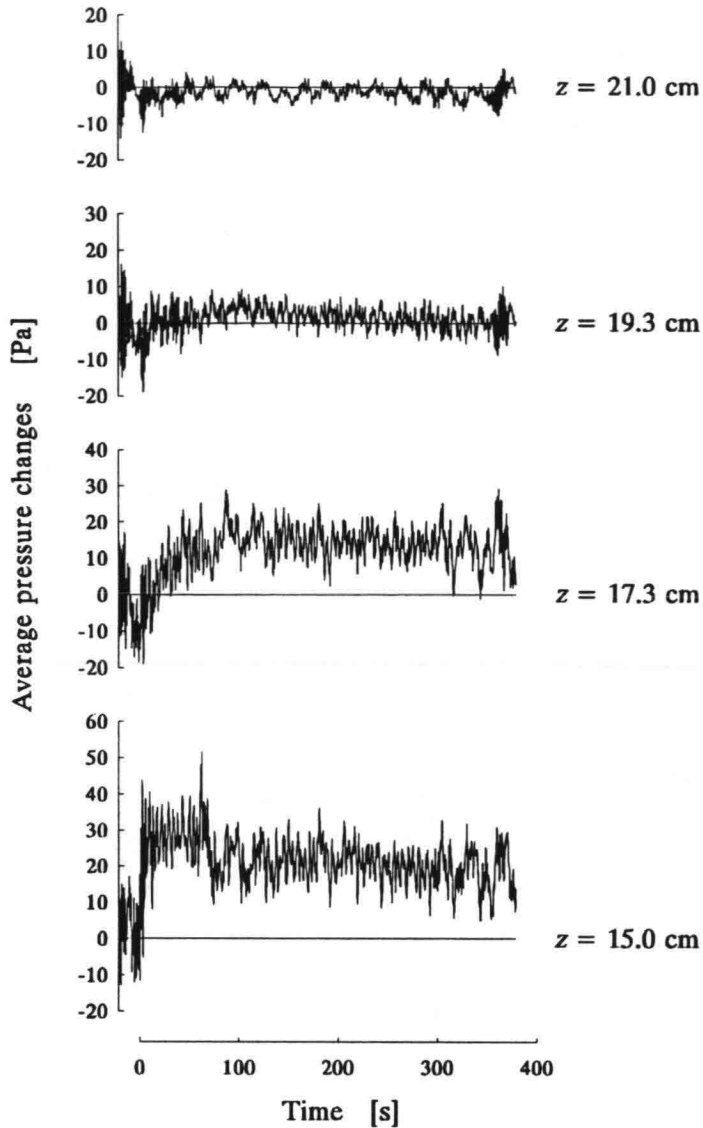


Figure 3.4.5 *Wave averaged pressure changes at the start of test 1. The bed surface was at $z=20$ cm.*

After approximately 90 minutes the pump was started and the average flow velocity was increased three times approximately every five minutes. Then the flow rate was slowly reduced to zero. The traversing systems were used to measure automatically the velocity and suspended sediment concentrations at several levels in the water column during the entire test. The positions of the measurements were logged using the data-acquisition set via a custom made digital-to-analogue converter (see appendix A). However, during the processing of the data logged on April 22nd it was found that this digital-to-analogue converter used to locate the position of the traversing units had broken down approximately 15 minutes after the start of test 1. As a result, non of the measurements made using the traversing units, i.e. the velocity and concentration measurements, could be processed, for the position at which the measurements were made could not be recovered. Consequently, only pore pressure and wave height measurements and no velocity and concentration measurements can be presented for tests (1-3) carried out on April 22nd.

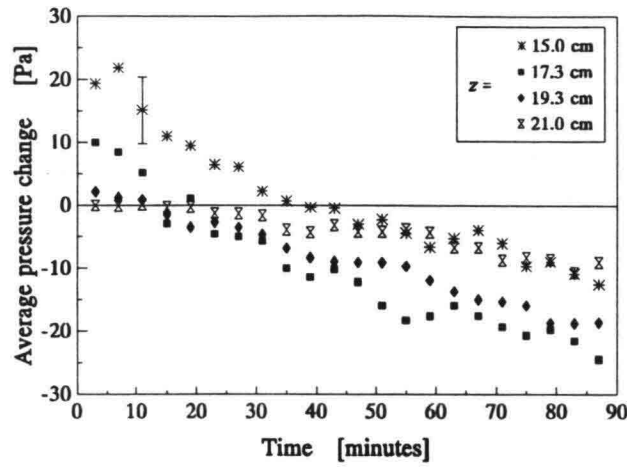


Figure 3.4.6 Wave-averaged pressure changes during the waves-only part of test 1.

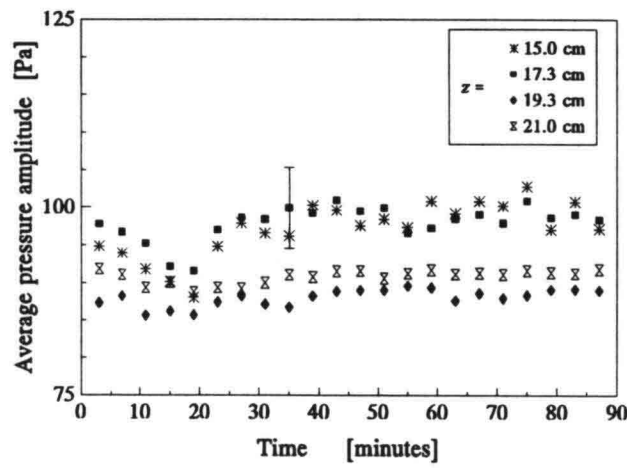


Figure 3.4.7 Average pressure amplitudes versus time during test 1 (waves only).

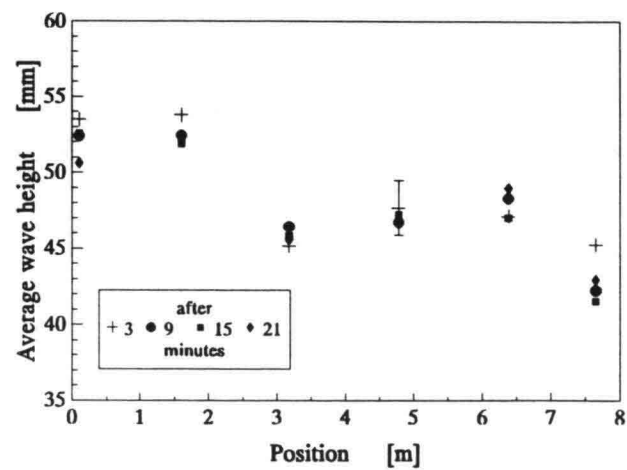


Figure 3.4.8 Average wave heights during test 2 (waves only).

3.4.3 Test 2

In test 2 the wave height was slowly increased until the average wave height was approximately 52 mm. The average wave height as a function of time during this test is shown in figure 3.4.8. No current was present in the flume during the first half an hour of test 2. The damping was fairly constant over the measuring period.

Unlike the average pore-pressures measured in test 1 (figure 3.4.6), there was almost no change in the average pore-pressure changes test 2, as can be seen in figure 3.4.9. This was probably caused by the fact that the excess pore-pressures, which were present before the experiment was started, dissipated during test 1, due to the increased permeability of the liquefied mud. The average pressure amplitudes, including the reference pressure amplitude, seem to decrease a little, which is probably caused by a slight decrease in the average wave height (figure 3.4.10).

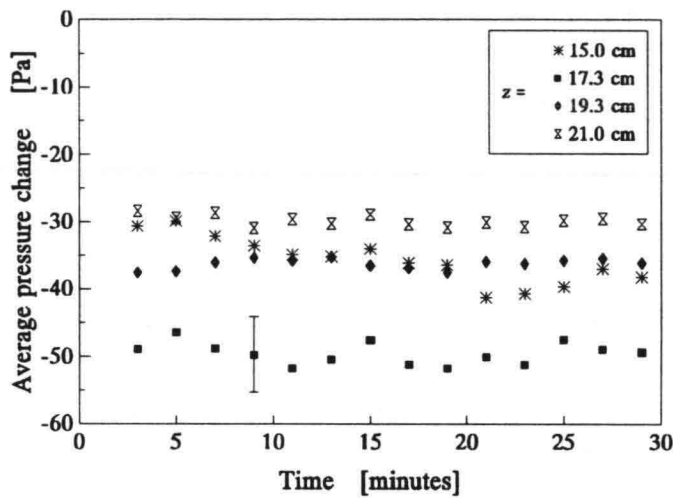


Figure 3.4.9 Average pressure changes during test 2 (waves only).

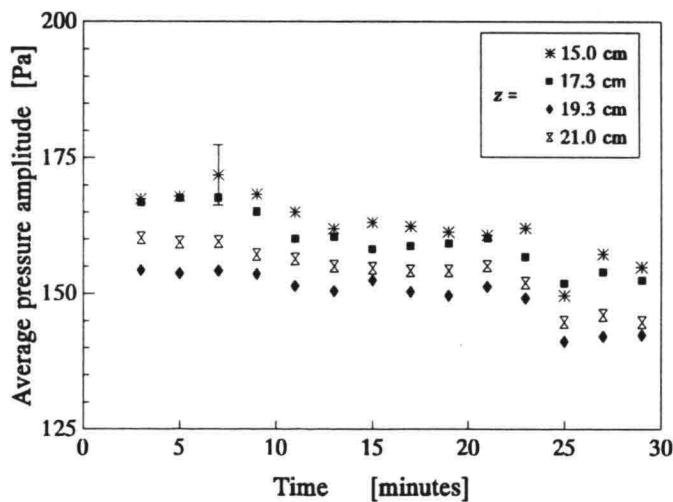


Figure 3.4.10 Average pressure amplitudes in test 2 (waves only).

3.4.4 Test 3

The final test on April 22nd was started by increasing the average wave height to approximately 63 mm. Waves were generated for approximately a quarter of an hour. The measured average wave heights during the waves-only part of this test are shown in figure 3.4.11. A similar result was found as in test 2; the damping was fairly constant over the measuring period.

The wave averaged pressure changes and pressure amplitudes (figures 3.4.12 and 3.4.13, respectively) were almost constant during the waves-only part of test 3.

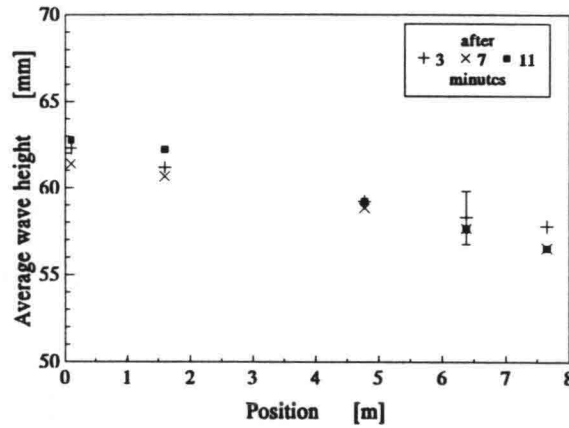


Figure 3.4.11 Average wave heights during the waves-only part of test 3.

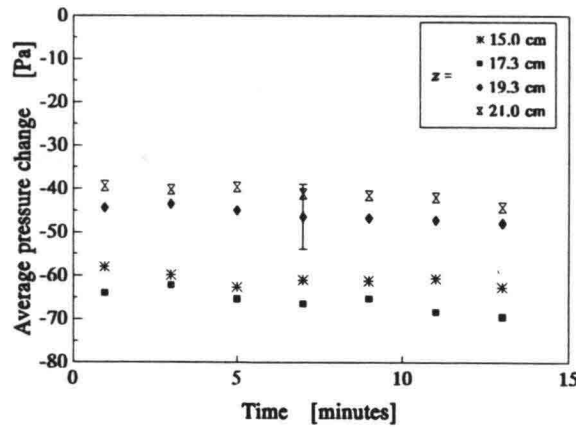


Figure 3.4.12 Average pressure changes during test 3 (waves only).

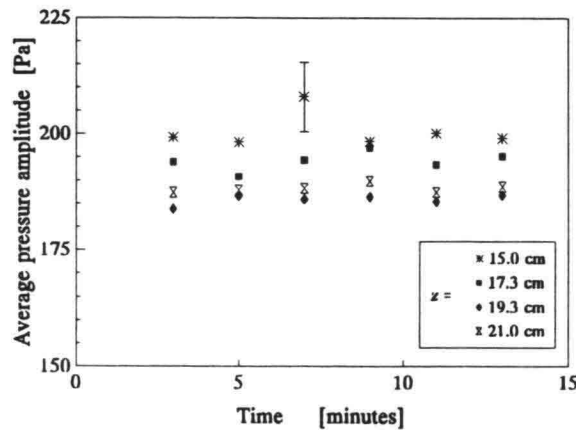


Figure 3.4.13 Average pressure amplitudes during the waves-only part of test 3.

3.4.5 Test 4

After a consolidation period of approximately 12 days the tests were continued on May 3rd, 1993. In this period the digital-to-analogue converter, which generated an analogue signal proportional to the position of the traversing unit, was repaired. A malfunction in the internal power supply was found to be the cause of the problems.

The bed surface was not smooth, for randomly spread lumps of mud which apparently had not been liquefied in the previous tests, protruded above the previously liquefied part of the bed.

Prior to test 4 concentration profiles were measured at four positions in the bed using a conductivity probe. The results of these measurements are shown in figures 3.4.14 and 3.4.15. The profiles measured at the downstream end show a local increase in concentration at approximately 12.5 cm (position 4) and 7.5 cm (position 3) above the bottom of the flume. Such a local increase in concentration may be caused by the rapid consolidation of the fluid mud formed in tests 1-3 on top of a non-liquefied mud layer. Furthermore, the bed is thicker in the downstream cross-section, for fluid mud was transported in the downstream direction at the end of test 3 and some of the mud was trapped by the downstream endwall, which had been a little too high. The profiles measured at the upstream part of the test section (positions 1 and 2) did not show such a local increase in concentration.

The concentration measurements showed that the bed was approximately 15 cm thick and as a result three pore-pressure transducers were not positioned in the bed. The fourth pore-pressure transducer seemed to be just at the surface of the bed.

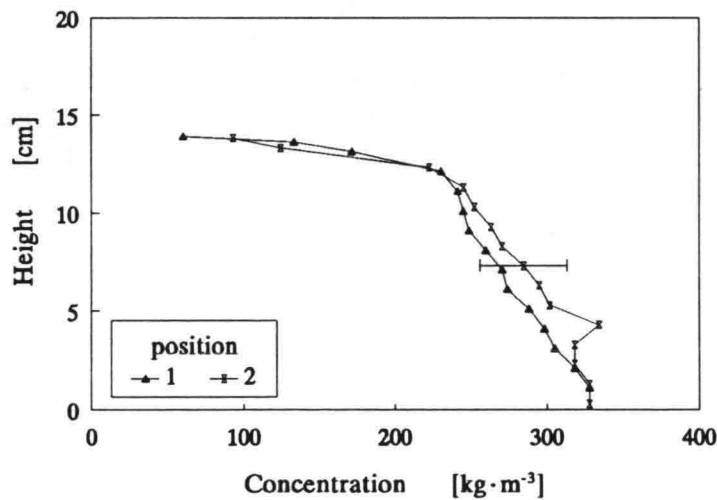


Figure 3.4.14 Concentration profiles in the bed at $x=2.47$ m prior to test 4. (Position 1: $y=0.2$ m, position 2: $y=0.6$ m)

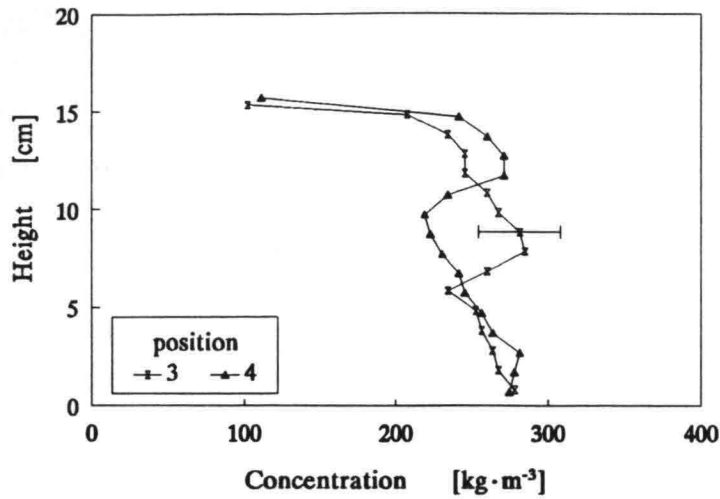


Figure 3.4.15 Concentration profiles in the bed at $x=6.02$ m prior to test 4. (Position 3: $y=0.2$ m, position 4: $y=0.6$ m)

In test 4 waves with an average wave height of about 24 mm were generated for approximately half an hour. As soon as the first waves had reached the test section similar observations were made as in test 1; first small patches of fluid mud were formed, which increased in number and size with time. After a few minutes the complete upper part of the bed seemed to be liquefied. The average wave heights measured at 6 positions in the test section during this test are shown in figure 3.4.16. No significant wave damping was observed. Consequently, only little wave energy was dissipated in the fluid-mud layer which indicates that the fluid-mud layer was thin and/or the fluid mud had a low viscosity.

The wave-averaged pressure changes measured at $z=15.0$ cm and at $z=17.3$ cm during the first 400 s of test 4 are almost constant (figure 3.4.17), although liquefaction of mud was observed visually. Therefore it is likely that the pressure transducer fixed at 15 cm above the flume bottom was not in the mud layer. The average pressure changes and average pressure amplitudes during the rest of test 4 were also almost constant, as can be seen in figures 3.4.18 and 3.4.19, respectively.

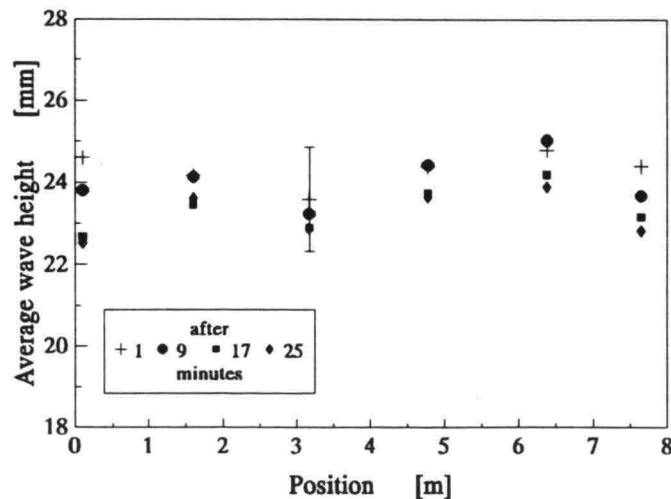


Figure 3.4.16 Average wave heights measured during test 4.

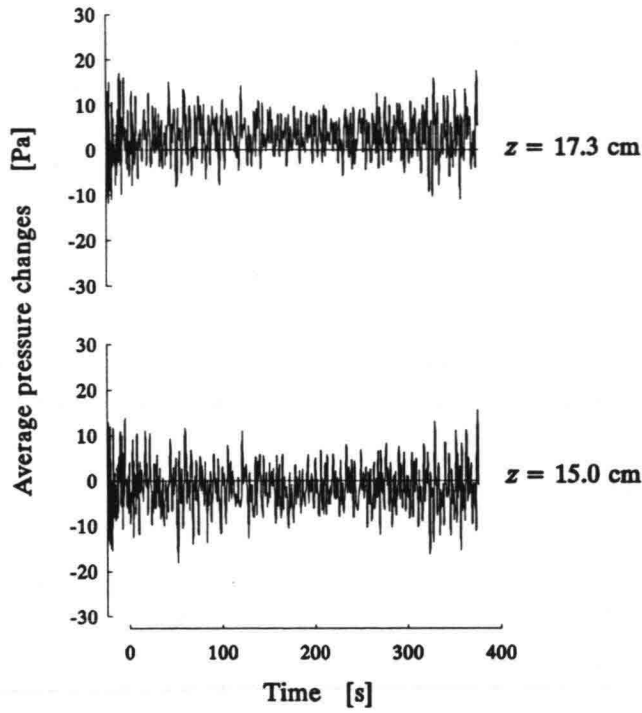


Figure 3.4.17 Wave-averaged pressure changes during the begin phase of test 4.

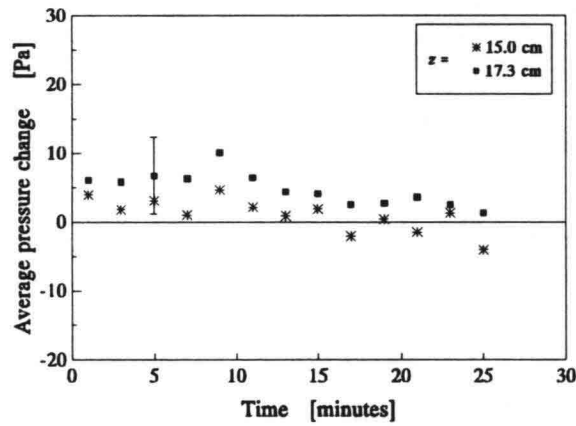


Figure 3.4.18 Wave-averaged pressure changes during test 4.

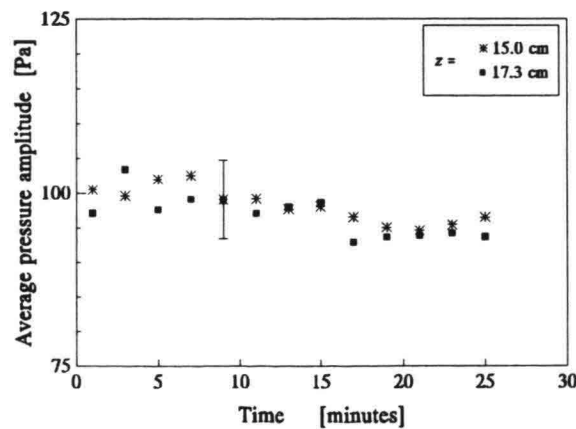


Figure 3.4.19 Average pressure amplitudes during test 4.

During this test and all of the other undermentioned tests, the traversing units were almost continuously running. As a result velocity and suspended concentration measurements were made at several levels in the water column. For reasons of brevity only the most interesting results are presented here.

Typical examples of the velocity amplitudes measured in test 4 are shown in figures 3.4.20 and 3.4.21. All three velocity components were measured: u , v , and w are the velocity components in x , y and z direction, respectively (see figure 3.4.1). Here z is positive in upward direction. The velocity amplitudes measured in x and z direction measured at $x=4.16$ m are presented in figure 3.4.21. The u and v velocity amplitude measured at $x=7.02$ m are shown in figure 3.4.20. The u velocity amplitudes measured at both locations match very well. The velocity component in y -direction was fairly small but seemed to be significant. An incorrect alignment of the gauge was probably the cause.

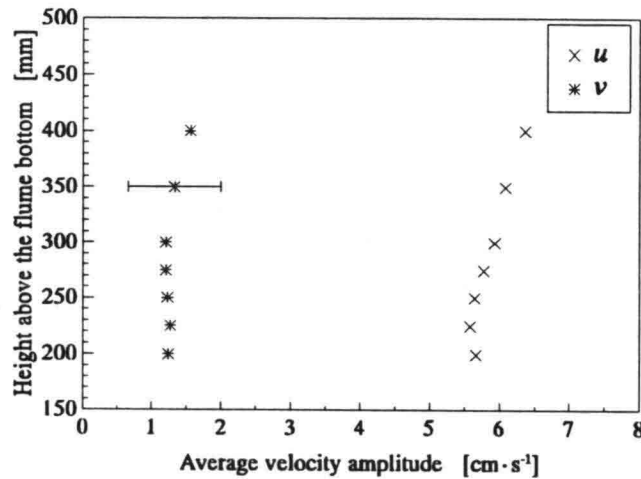


Figure 3.4.20 Velocity amplitudes measured in the centre-line of the flume at $x=7.02$ m. (The bed surface was at c. 150 mm above the flume bottom)

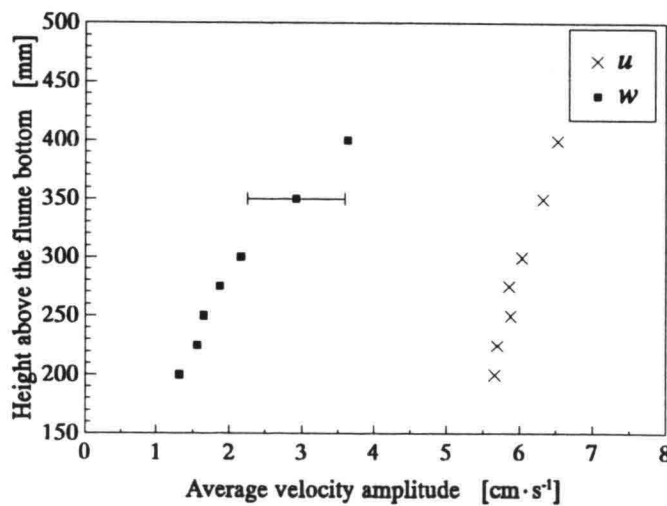


Figure 3.4.21 Velocity amplitudes measured at $x=4.16$ m. (The bed surface was c. 150 mm above the flume bottom)

3.4.6 Test 5

The wave height was increased to c. 43 mm and similar to test 4 waves were generated for half an hour. The averaged wave heights measured at six locations in the test section during this test are shown in figure 3.4.22. No significant wave damping can be observed.

The pressure amplitudes increased due to the increase in wave height (figure 3.4.23). Furthermore, no change in the average pressures were observed (not shown). Typical results of the velocity amplitudes measured during this test can be found in figure 3.4.24.

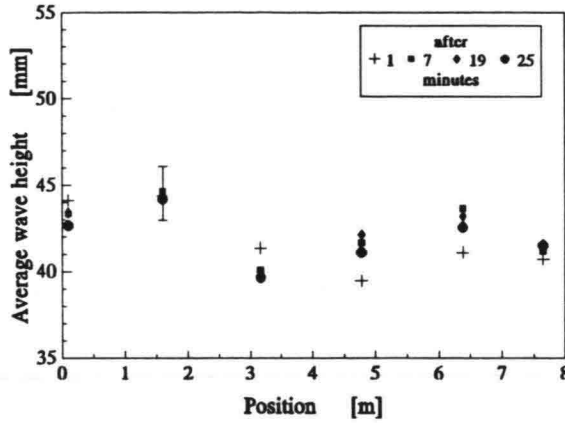


Figure 3.4.22 Average wave heights during test 5.

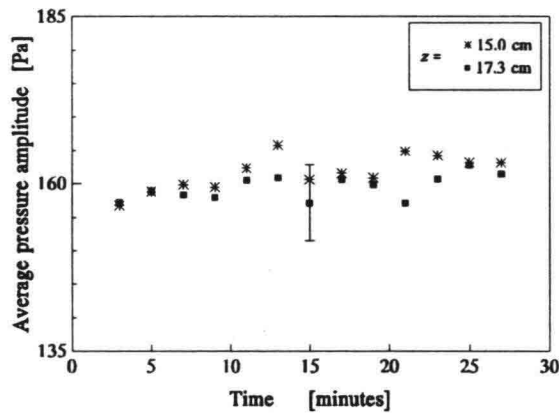


Figure 3.4.23 Average pressure amplitudes during test 5.

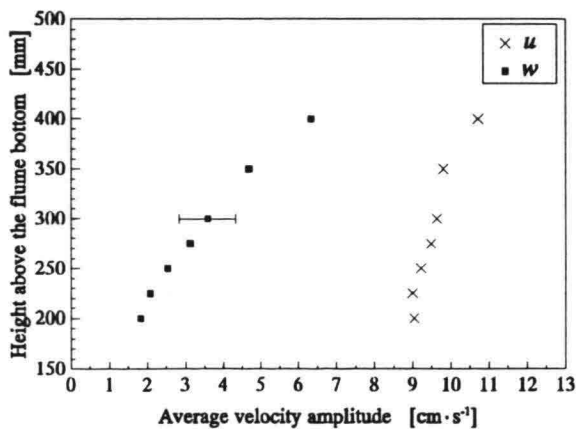


Figure 3.4.24 Velocity amplitudes measured during test 5. The bed surface was at c. 15.0 cm above the flume bottom.

3.4.7 Test 6

The wave height was increased again and set at c. 53 mm. The average wave heights and average pressure amplitudes are presented in figures 3.4.25 and 3.4.26, respectively.

The results of the velocity measurements at several levels in the water column can be found in figure 3.4.27.

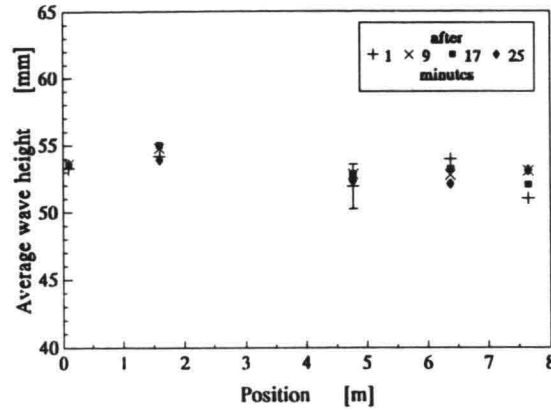


Figure 3.4.25 Average wave heights during test 6.

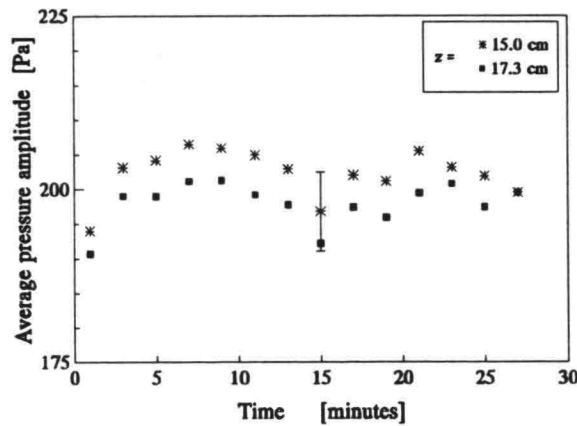


Figure 3.4.26 Average pressure amplitudes measured during test 6.

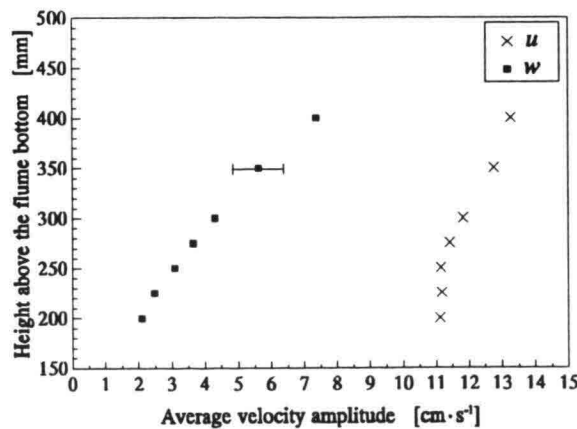


Figure 3.4.27 Velocity amplitudes in test 6. (The bed was c. 15.0 cm thick)

3.4.8 Test 7

The final test on May 3rd was started with generating waves (average wave height c. 67 mm) for half an hour. The average wave heights are shown in figure 3.4.28. Similar to the previous tests (4-6) no significant wave damping was observed although a layer of fluid was present. The average pressure amplitudes were c. 240 Pa and constant during this test.

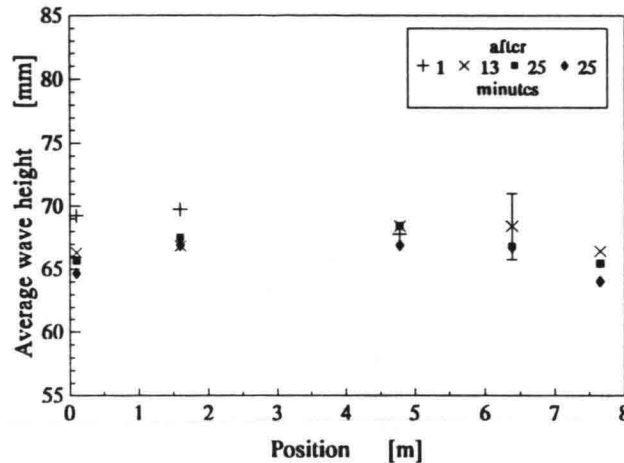


Figure 3.4.28 Average wave heights during test 7.

The electromagnetic current meter at $x=7.02$ m was used to measure velocity amplitudes in the fluid-mud layer. The tubes needed for the optical concentration meter fixed to the custom-made frame (figure A.1.3) were replaced by a conductivity probe. With this frame it was possible to measure simultaneously the velocity amplitude and the concentration at the same height above the bottom of the flume.

As already mentioned before, the Westwold Clay firmly stuck to the glass sidewalls. Consequently no estimation could be made of the thickness of the fluid-mud layer. However, the velocity measurements (figure 3.4.30) in combination with the concentration measurements (figure 3.4.31) showed that there was a fluid-mud layer of about 3 cm thick.

The velocity amplitudes calculated according to the modified Gade (1958) model are also shown in figure 3.4.40. In this model the fluid mud is considered as a viscous fluid and the water is assumed to be non-viscous. The hydrostatic model of Gade was extended to account for arbitrary wavelengths and is described by De Wit (1994). As can be seen the velocity amplitudes calculated using the model agree quite well with the measured velocity amplitudes. The input parameters for the calculation were determined from the rheological measurements in combination with the concentrations measured in the bed and the flow characteristics. These parameters were: $\bar{h}_1=0.03$ m, $\bar{h}_0=0.38$ m, $\eta_0=0.035$ m, $\rho_1=1000$ kg·m⁻³, $\rho_2=1186$ kg·m⁻³ and $\nu_2=5.94 \cdot 10^{-4}$ m²·s⁻¹. For an explanation of the parameters used see De Wit (1994).

This model can also be used to calculate the wave height as a function of the distance travelled over the test section. When the parameters mentioned above are entered it is found that the value of the imaginary part of the complex wave number is 0.020 m⁻¹, which corresponds with a decrease in wave height of roughly 13% over a distance of 8 metres. However, the wave height measurements showed no significant wave damping, which may be explained by the fact that the value of the

calculated complex wave number varies quite strongly for these small heights \bar{h}_1 of the fluid-mud layers. As an example, keeping the other parameters constant it is found that the value of the imaginary part of the complex wave number is 0.005 m^{-1} for a 0.015 m thick fluid-mud layer. As a result this wave damping could not be measured in the experiment because of the low accuracy of the instruments used.

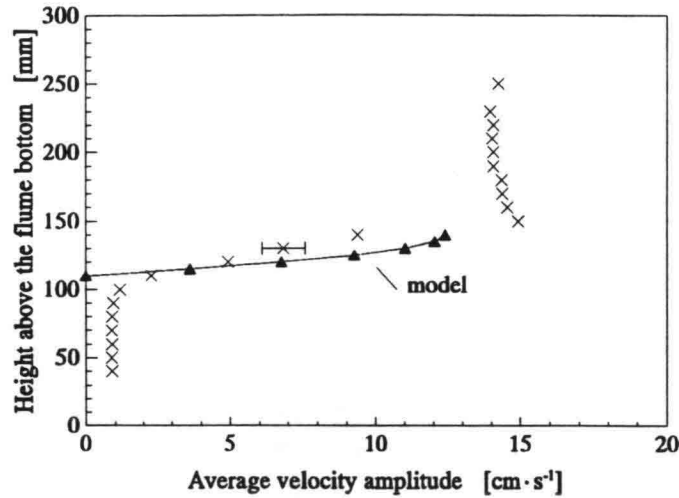


Figure 3.4.30 *Velocity amplitudes measured in and above the bed at $x=7.02 \text{ m}$ and model results during test 7.*

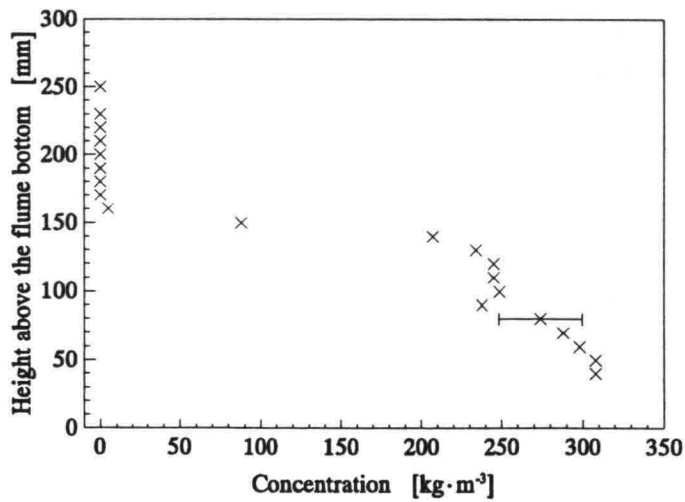


Figure 3.4.31 *Concentration profile measured at $x=7.24 \text{ m}$ in test 7.*

3.4.9 Test 8

On May 6th the final tests of the first experiment on Westwold Clay were carried out with the objective to measure velocities in fluid mud when both waves and current were present. Test 8 was started by generating waves for half an hour in order to generate a fluid-mud layer. The wave period was 1.5 s and the average wave height was c. 45 mm. No concentration profiles were measured in the bed prior to test 8. As soon as the first waves were generated the very thin layer of mud, which had been deposited in the entire flume during the previous tests, was resuspended.

The velocity amplitudes measured at several levels in the water column are shown in figure 3.4.32. Mud was resuspended in the end phase of this test. The concentration profile measured in this phase is shown in figure 3.4.33.

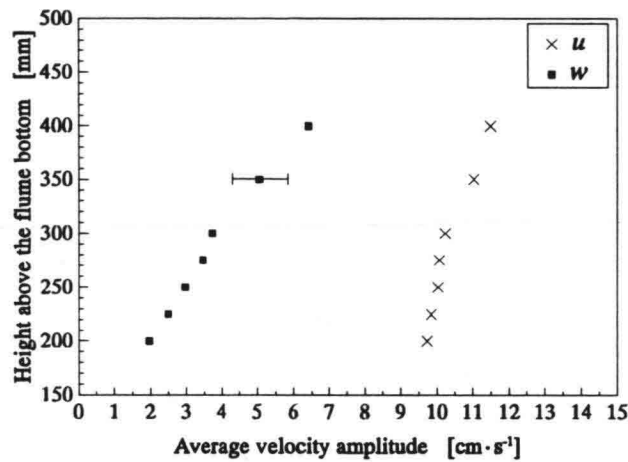


Figure 3.4.32 Velocity amplitudes measured in test 8.

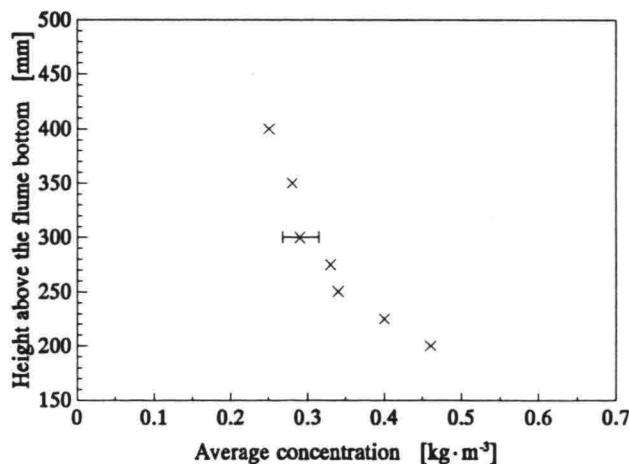


Figure 3.4.33 Concentration profile measured at $x=7.24$ m in the end phase of test 8. (The bed was c. 12 cm thick)

3.4.10 Test 9

In test 9 the wave height was increased to c. 57 mm. After generating waves for half an hour the electromagnetic current meter positioned at $x=7.02$ m was used to measure velocity amplitudes in the fluid-mud layer. Furthermore, the conductivity meter was used to measure simultaneously the concentration at the same level.

The average velocity amplitudes measured at various heights above the bottom of the flume are plotted in figure 3.4.34. The concentration profile measured at the same time is presented in figure 3.4.35. The bed was approximately 12 cm thick and a local peak in concentration was observed at about 8 cm above the bottom of the flume. This peak was probably caused by the consolidation of the fluid mud generated in the tests carried out on May 3rd. From the velocity measurements it can be concluded that the fluid-mud layer was approximately 2 cm thick.

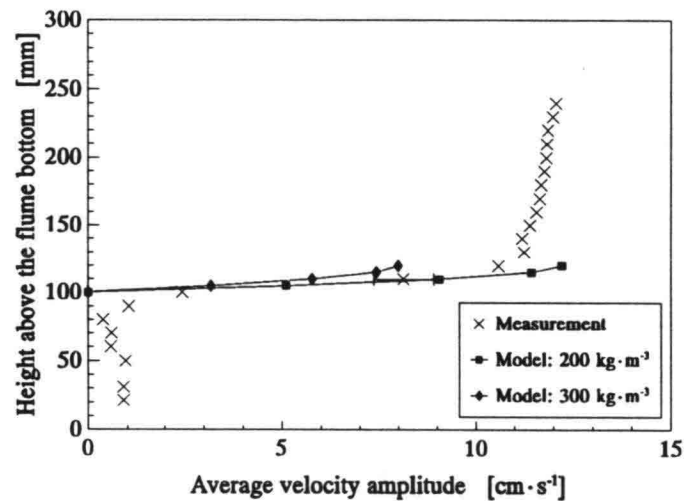


Figure 3.4.34 Average velocity amplitudes in and above a partly liquefied bed.

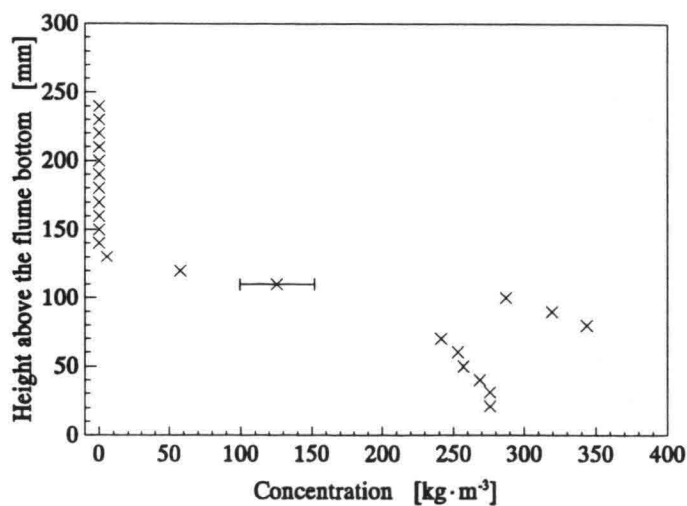


Figure 3.4.35 Concentration profile measured during the waves-only part of test 9.

The pump was started as soon as the velocity profile had been measured. The average flow rate was set at $24 \text{ dm}^3 \cdot \text{s}^{-1}$. The settings of the wave generator were not changed. Consequently, both waves and current were present in the flume. The traversing unit positioned at $x=7.02 \text{ m}$ was started as soon as the flow rate was set. The wave-averaged velocity amplitudes are shown in figure 3.4.36. The average velocities and the concentration profile measured are plotted in figures 3.4.37 and 3.4.38, respectively. The mud layer was approximately 12 cm thick, including a c. 2 cm thick fluid-mud layer. The peak in concentration in the upper part of the bed was still present (figure 3.4.38). The velocity measurements clearly show that an oscillating flow as well as a net current were present in the fluid-mud layer.

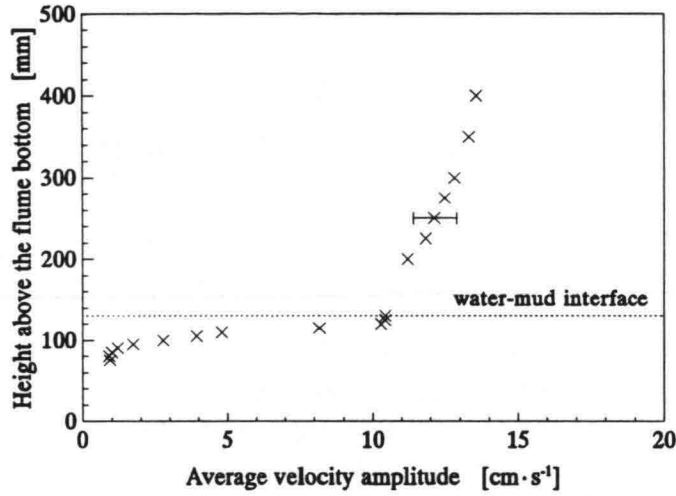


Figure 3.4.36 Velocity amplitudes in and above the bed (test 9, waves and current).

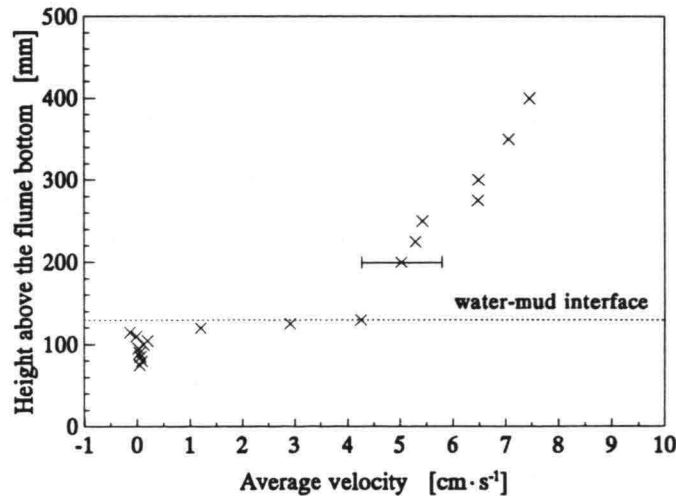


Figure 3.4.37 Average velocities in and above the bed (test 9, waves and current).

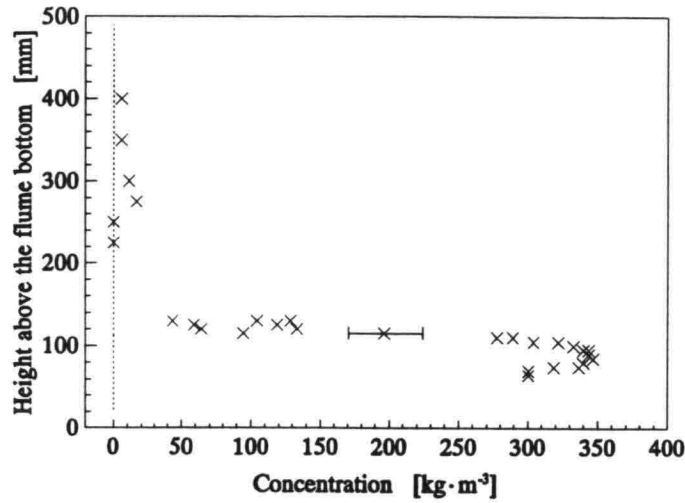


Figure 3.4.38 Concentration profile (test 9, waves and current).

3.4.11 Test 10

The final test of the first experiment on Westwold Clay was started with generating waves with an average wave height of about 70 mm for approximately half an hour. Subsequently, velocities and concentrations were measured in and above the mud layer. The traversing set was moved in upstream direction for 30 cm. The bed was approximately 11 cm thick (figure 3.4.40) and from the velocity measurements (figure 3.4.39) it may be concluded that the upper 2 cm of the bed consisted of fluid mud.

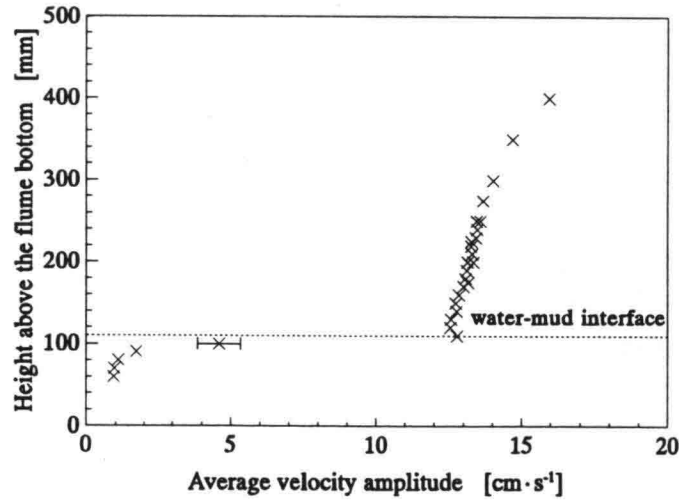


Figure 3.4.39 Average velocity amplitudes measured at $x=6.70$ m during the waves-only part of test 10.

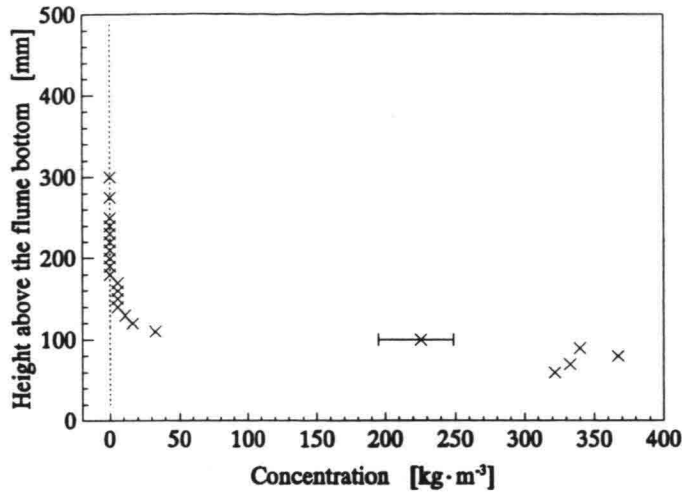


Figure 3.4.40 Concentration profile measured at $x=6.93$ m (test 10, waves only).

The pump was started as soon as the velocity profile was measured. The flow rate was set at $24 \text{ dm}^3 \cdot \text{s}^{-1}$ and the velocity and concentration profiles were measured again. The bed was about 10 cm thick (figure 3.4.43). Figure 3.4.41 indicates that there was some oscillation in the upper part of the bed. However, a significant average velocity was not measured at the same level (figure 3.4.42).

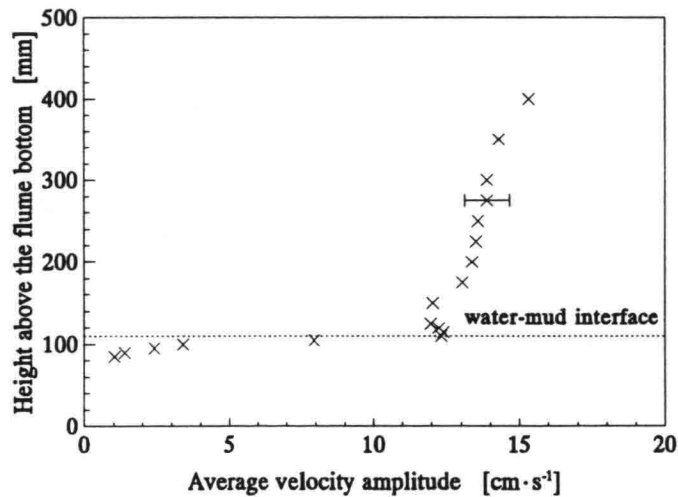


Figure 3.4.41 Average velocity amplitudes measured at $x=6.70$ m. (test 10, waves and current, flow rate: $24 \text{ dm}^3 \cdot \text{s}^{-1}$)

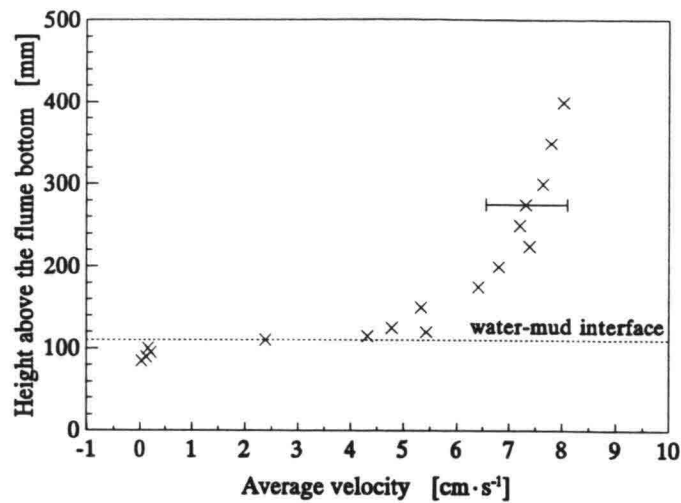


Figure 3.4.42 Average velocities measured at $x=6.70$ m.
(test 10, waves and current, flow rate: $24 \text{ dm}^3 \cdot \text{s}^{-1}$)

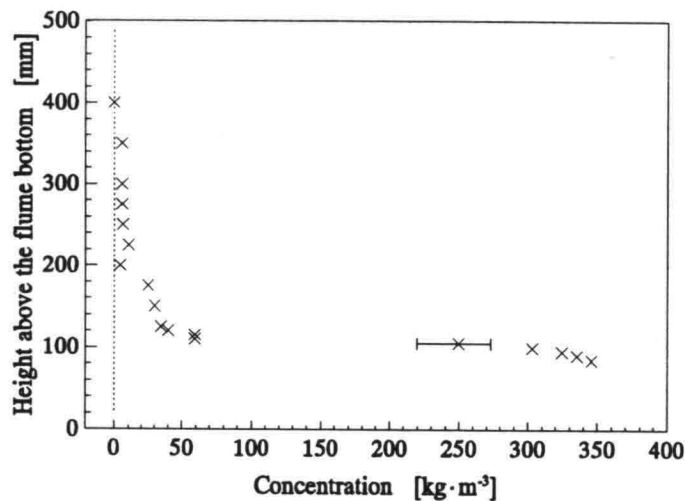


Figure 3.4.43 Concentration profile measured at $x=6.93$ m during test 10.
(waves and current, flow rate $24 \text{ dm}^3 \cdot \text{s}^{-1}$)

Finally, the flow rate was set at $48 \text{ dm}^3 \cdot \text{s}^{-1}$. The settings of the wave generator were not altered. Due to the increase in flow rate the average wave height decreased. Consequently the average velocity amplitude decreased which can be seen by comparing figures 3.4.41 and 3.4.44. Velocity amplitudes (figure 3.4.44) and average velocities (figure 3.4.45) were measured in a layer of only c. 0.5 cm thick in the uppermost part of the bed (figure 3.4.46). These results are similar to those obtained for a flow rate of $24 \text{ dm}^3 \cdot \text{s}^{-1}$.

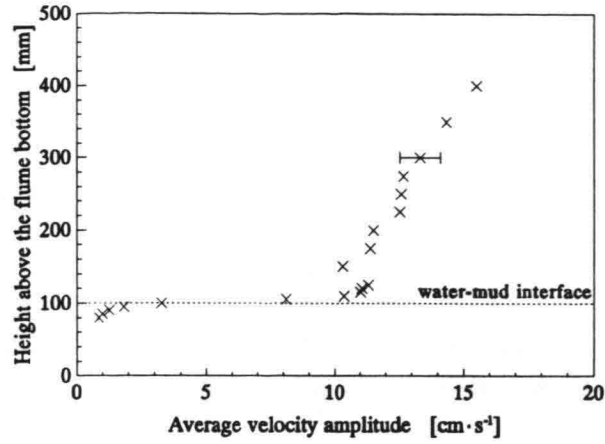


Figure 3.4.44 Average velocity amplitudes measured at $x=6.70 \text{ m}$. (test 10, waves and current, flow rate: $48 \text{ dm}^3 \cdot \text{s}^{-1}$)

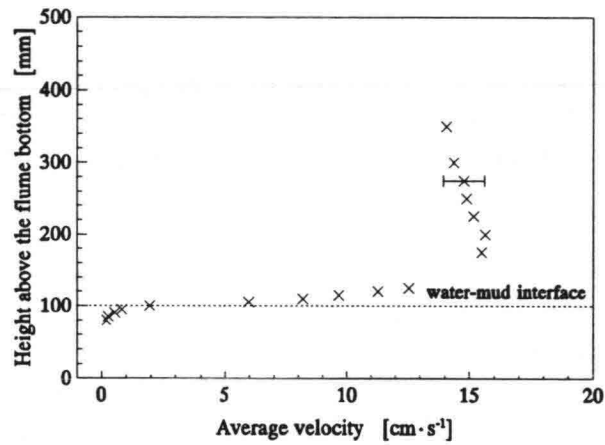


Figure 3.4.45 Average velocities measured at $x=6.70 \text{ m}$ in test 10. (waves and current, flow rate: $48 \text{ dm}^3 \cdot \text{s}^{-1}$)

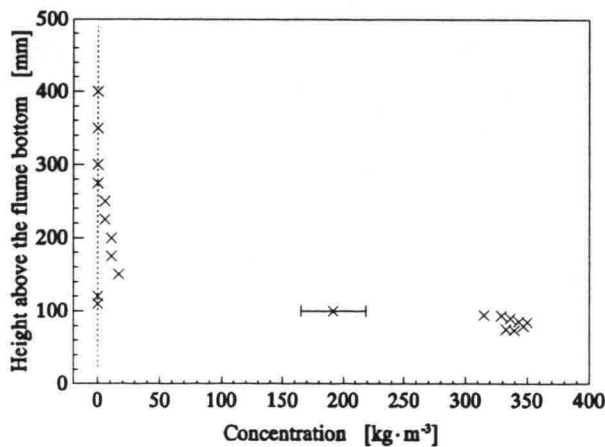


Figure 3.4.46 Concentration profile measured at $x=6.93 \text{ m}$ in test 10. (waves and current, flow rate: $48 \text{ dm}^3 \cdot \text{s}^{-1}$)

3.5 Conclusions

The following conclusions may be drawn from the results of the first experiment on Westwald Clay.

- The experiments on Westwald Clay were made with the objective to create a link between the results of the experiments on the relatively weak cohesive China Clay and more cohesive natural muds. Rheological measurements showed Westwald Clay suspensions were more cohesive than China Clay suspensions with the same suspended sediment concentration. However, due to the unfavourable consolidation characteristics of Westwald Clay the average concentration of the bed was half the bed concentration in the experiments on China Clay. As a result, the yield strength of the Westwald Clay was rather low and consequently the mud started to liquefy as soon as the first waves travelled over the test section.
- The preparation of the bed was far from ideal, which was caused by leakage. As a result the bed was not uniform in vertical, transverse and longitudinal directions, which could be concluded from the concentration measurements in the bed using the conductivity probe.
- The bed started to liquefy directly after the first waves had reached the test section. The pore pressures measured during the liquefaction process showed initially a decrease in the average pressure, followed by a transient build-up of an excess pore pressure. This excess pore-pressure decreased gradually with time. These measurements may be explained by the following scenario: the initial decrease in the pore pressure was probably caused by a break-up of the aggregate structure. Such a break-up will be provoked when the local wave-induced shear stresses in the bed are larger than the yield stress of the aggregate structure. Shear stresses in the bed caused by the streamwise variation in wave-induced pressures on the bed play an important role in this process (De Wit, 1994). The break-up seems to involve an increase in volume due to a rearrangement of the particles or aggregates, for the pore-pressure decreased and the permeability of the mud is quite low. However, due to the weight of the overlying mud the pore pressure showed a gradual build-up to compensate for the reduced effective stress. This excess pore-pressure did not dissipate directly because of the low permeability of the mud.
- Significant wave damping was only measured in tests carried out on April 22nd. The low viscosity of the fluid mud and the relatively thin layer of fluid mud were probably the reason for the fact that no wave damping was measured in the other tests although liquefaction was observed. Only a thin layer of fluid mud was formed in the tests carried out on May 3rd and 6th, which indicates that the yield stress of the consolidated fluid-mud layer formed on April 22nd is greater than that of the initial bed. The peaks in the concentration profiles measured in the bed (figure 3.4.35) seem to confirm this.

- The experiments showed that the Westwald Clay had strong adhesive properties and a special affinity for glass, for it stuck firmly to the glass sidewalls of the flume. Consequently, visual observations were impossible. China Clay used in previous experiments showed a similar behaviour. Therefore, it has to be stated that observations or measurements made near the sidewall of an experimental set-up are not representative of the actual physical processes away from the sidewalls.
- The calculated velocities in the fluid-mud layer using the modified model of Gade (1958) agreed quite well with the measured values. The calculated wave damping underestimated the measured wave damping which may be caused by an underestimation of the thickness of the fluid-mud layer or the viscosity of the fluid mud.
- The automatic traversing units proved to be very reliable and flexible instruments, apart from the break-down of the DA-converter which was necessary to generate an analogue signal proportional to the position of the traversing unit. The operation set with which these instruments can be programmed is adequate and consequently most of the user demands can be programmed very easily although the available user memory is rather limited.

Chapter 4

The second experiment on Westwald Clay

The experimental set-up was cleaned after the first experiment on Westwald Clay and the leakages were stopped (as best as possible). Furthermore, the boards used to separate the test section from the rest of the flume were adjusted and cemented in the flume using a silicone-based sealant in order to eliminate the possibility of a leakage. The experimental set-up was not changed and the same instruments were used as in the first experiment. More information on the locations and the specifications of the instruments used and some calibration data are given in appendix C. The preparation of the bed is described in section 4.1. The experimental procedure and program for the second experiment on Westwald Clay are discussed in section 4.2, whereupon the results of the different tests are presented and discussed in section 4.3. Finally, the conclusions drawn from this experiment are summarized in section 4.4.

4.1 Preparation of the bed

The mixing tank was filled on 11 May 1993 with 2940 dm³ of tap water, 14.7 kg sodium chloride and 441 kg Westwald Clay. The suspension was pumped into the test section after a mixing period of approximately 5 weeks. The remaining parts of the set-up were simultaneously filled with tap water. No leakages of some importance were observed. The filling was stopped when the height of the suspension in the test section was 42.5 cm. The initial concentration of the suspension was 134 kg·m⁻³. Subsequently, the suspension was mixed again for about half an hour using a mixer installed on a measuring carriage mounted on top of the flume. Then four pore-pressure transducers, fixed at several levels on a frame (figure 3.3.2), were placed in the suspension and finally the suspension was allowed to consolidate.

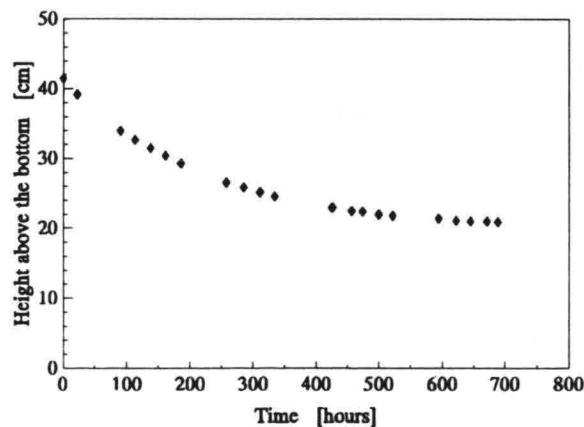


Figure 4.1.1 *The position of the water-mud interface during the consolidation process in the flume prior to the second experiment on Westwald Clay.*

As in the first experiment, an interface was formed between the mud and the clear water during the consolidation process. Small craters were formed and after roughly one week cracks in the mud surface became visible, especially near the walls of the test section. In figure 4.1.1 the position of the water-mud interface during the consolidation process is shown. After 13 days the tap water in the remaining parts of the flume was replaced with saline tap-water (salinity 5‰) which was mixed in the mixing tank. Approximately one week later the boards were removed, which separated the test section from the rest of the flume, after which the second experiment on Westwold Clay was initiated on July 16th 1993. The experimental procedure and program of this experiment are discussed in the following section.

4.2 Experimental procedure and program

The instruments used and procedures followed in this experiment were identical to those in the first experiment (section 3.3), only the exact position of the instruments in the test section differed a little (see appendix C).

The second experiment comprised 8 tests spread over two days. The first test was started on July 16th with the generation of waves with a constant wave height for approximately one hour with the objective to generate a fluid-mud layer. The wave period was set at 1.5 s. The water depth, over the 20 cm thick false bottom, was 30 cm.

In test 2 the wave height was set to a greater value. The waves were generated for roughly one hour. During this part of the test velocity and concentration measurements were made in the fluid-mud layer. Then the wave generator was stopped and concentration profiles were measured in the partly liquefied bed. Subsequently, the wave generator was restarted and waves were generated again for half an hour.

In test 3 the pump was started and the flow rate was set at $12 \text{ dm}^3 \cdot \text{s}^{-1}$. The settings of the wave generator was not changed. Consequently, both waves and current were present in the flume. Velocity and concentration measurements were made simultaneously in and above the mud layer using only one electromagnetic current meter. Subsequently, the flow rate was increased to 24 and $36 \text{ dm}^3 \cdot \text{s}^{-1}$ and similar velocity measurements were made for each setting of the flow rate. After these measurements the pump was stopped.

The wave height was increased again in test 4, which concluded the tests on July 16th. Waves were generated for one hour. At the end of this test velocities were measured in the bed using all electromagnetic current meters. After this test the generation of waves was stopped and the mud was allowed to consolidate for one week, after which the tests were restarted on July 23rd, 1993.

In the first test after the consolidation period (test 5) waves were generated for half an hour. The wave period was 1.5 s.

At the start of test 6 the wave height was increased again and the settings of the wave generator were not altered for one hour. At a later phase of this test velocity measurements were made in the bed using only one electromagnetic current meter.

The wave height was increased again (test 7). The pump was started after generating waves for half an hour. The flow rate was successively set at 12, 24 and $36 \text{ dm}^3 \cdot \text{s}^{-1}$, and for each setting velocities were measured in the bed using three electromagnetic current meters. Subsequently, the pump was stopped.

In the final test (test 8) the wave height was increased again and waves were generated for half an hour. At the end of this phase of the test velocity measurements were made in and over the bed

using three current meters. Then the pump was started and the flow rate was set at $48 \text{ dm}^3\cdot\text{s}^{-1}$ and again velocities were measured in and over the bed. The settings of the wave generator were not changed. Finally, the wave generator and the pump were stopped.

A summary of the experimental program of the second experiment is given in table 4.2.1.

Table 4.2.1 *Experimental program of the second experiment on Westwald Clay.*

test no.	details
1 (16 July 1993)	* No net current. Generation of waves for c. one hour; <i>average wave height 26 mm.</i>
2 (16 July 1993)	* No net current. Generation of waves for c. one hour; <i>average wave height 45 mm.</i> * Wave generation stopped in order to measure concentrations in the bed * No net current. Generation of waves for half an hour; <i>average wave height 44 mm.</i>
3 (16 July 1993)	* Both waves and current. Flow rate increased step by step. Settings of flow rate: 12, 24 and $36 \text{ dm}^3\cdot\text{s}^{-1}$.
4 (16 July 1993)	* No net current. Generation of waves for one hour; <i>average wave height 60 mm.</i>
5 (23 July 1993)	* No net current. Generation of waves for half an hour; <i>average wave height 25 mm.</i>
6 (23 July 1993)	* No net current. Generation of waves for one hour; <i>average wave height 47 mm.</i>
7 (23 July 1993)	* No net current. Generation of waves for three quarter of an hour; <i>average wave height 60 mm.</i> * Both waves and current. Flow rate increased step by step. Settings of flow rate: 24 and $36 \text{ dm}^3\cdot\text{s}^{-1}$.
8 (23 July 1993)	* No net current. Generation of waves for half an hour; <i>average wave height 85 mm.</i> * Both waves and current. Flow rate set at $48 \text{ dm}^3\cdot\text{s}^{-1}$.

4.3 Results

The coordinate system, defined in section 3.4.1, is used to identify the location of each measurement in the following presentation of the experimental results.

4.3.1 Concentration measurements prior to the tests

Prior to the tests concentration profiles were measured in the bed in two cross-sections using a conductivity probe. In figure 4.3.1 the results are presented which were obtained from measurements in the cross-section at $x=2.29$ m. The measurements made at $x=5.72$ m are shown in figure 4.3.2.

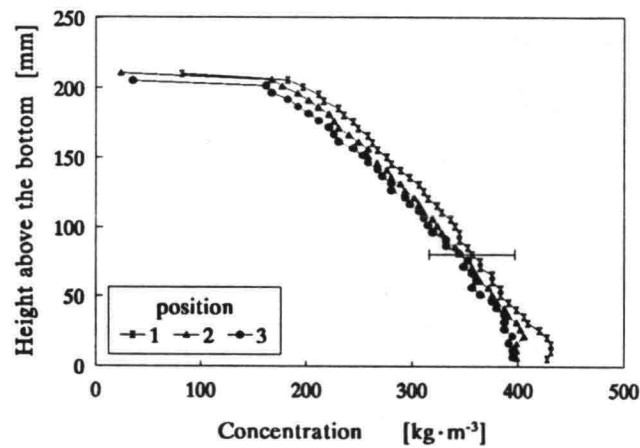


Figure 4.3.1 Concentration profiles in the bed measured at $x=2.29$ m prior to test 1. (Position 1: $y=0.20$ m, position 2: $y=0.40$ m, position 3: $y=0.60$ m)

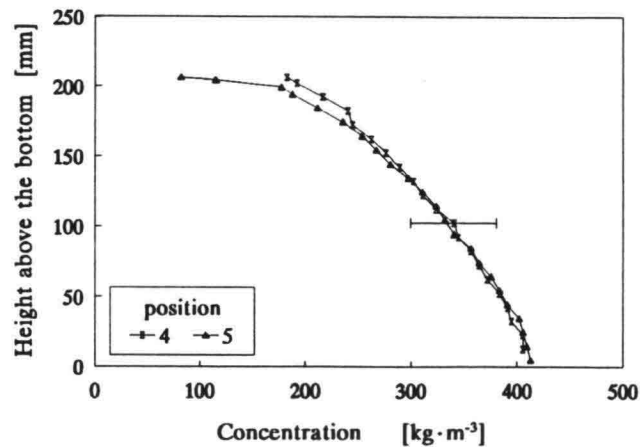


Figure 4.3.2 Concentration profiles in the bed measured at $x=5.72$ m prior to test 1. (Position 4: $y=0.20$ m, position 5: $y=0.60$ m)

Due to the almost ideal consolidation process the bed was quite uniform in longitudinal as well as in a transverse direction as can be concluded from figures 4.3.1 and 4.3.2. The concentration near the bottom of the flume is a little higher than in the first experiment on Westwold Clay (figures 3.4.2 and 3.4.3). The maximal error in the concentration was approximately 10% of the local concentration.

4.3.2 Test 1

Prior to the tests the wave period was set at 1.5 s. The amplitude of the wave generator was increased slowly until the average wave height was approximately 26 mm. As soon as the first waves reached the test section the mud started to liquefy. The liquefaction process was similar to that observed during the first experiment on Westwold Clay (section 3.4.2). After approximately 15 minutes the entire mud-water interface seemed to behave like a fluid.

The results of the wave height measurements during this test are presented in figure 4.3.3. In this graph one-minute averaged wave heights are shown measured at six locations in the test section at various moments during test 1. There was no significant wave damping during this test, although fluid mud was present. Consequently, there was only little dissipation of wave energy in the fluid mud, which indicates that the fluid-mud layer was thin.

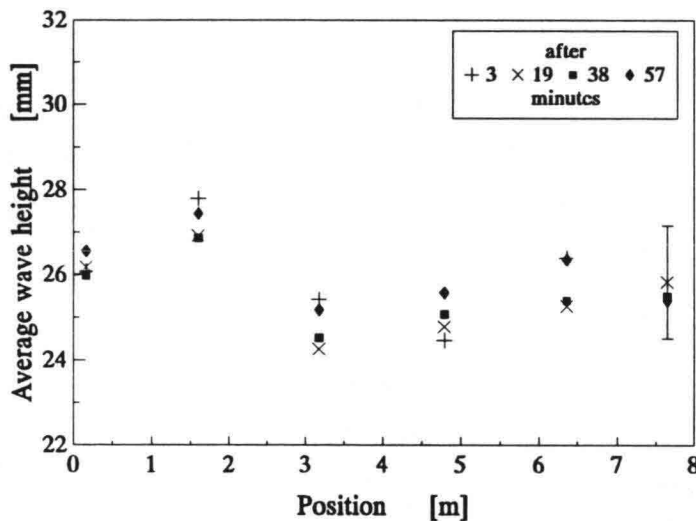


Figure 4.3.3 Average wave heights measured during test 1.

The wave-averaged pore-pressures measured during the first 400 s of this test are shown in figure 4.3.4. The pressure measurements were averaged using a Fast Fourier Technique. The reference pressure measured at $z=21.0$ cm (just above the bed) indicates that there was no change in the average water depth. However, the pore pressure measured at $z=15.0$ cm showed a transient decrease followed by a quick build-up of an excess pore-pressure, which gradually decreased with time. A similar trend was measured at $z=17.3$ cm: a transient decrease followed by a quick build-up of an excess pore pressure followed by a more gradual decrease. Only a gradual build-up was observed at $z=19.3$ cm.

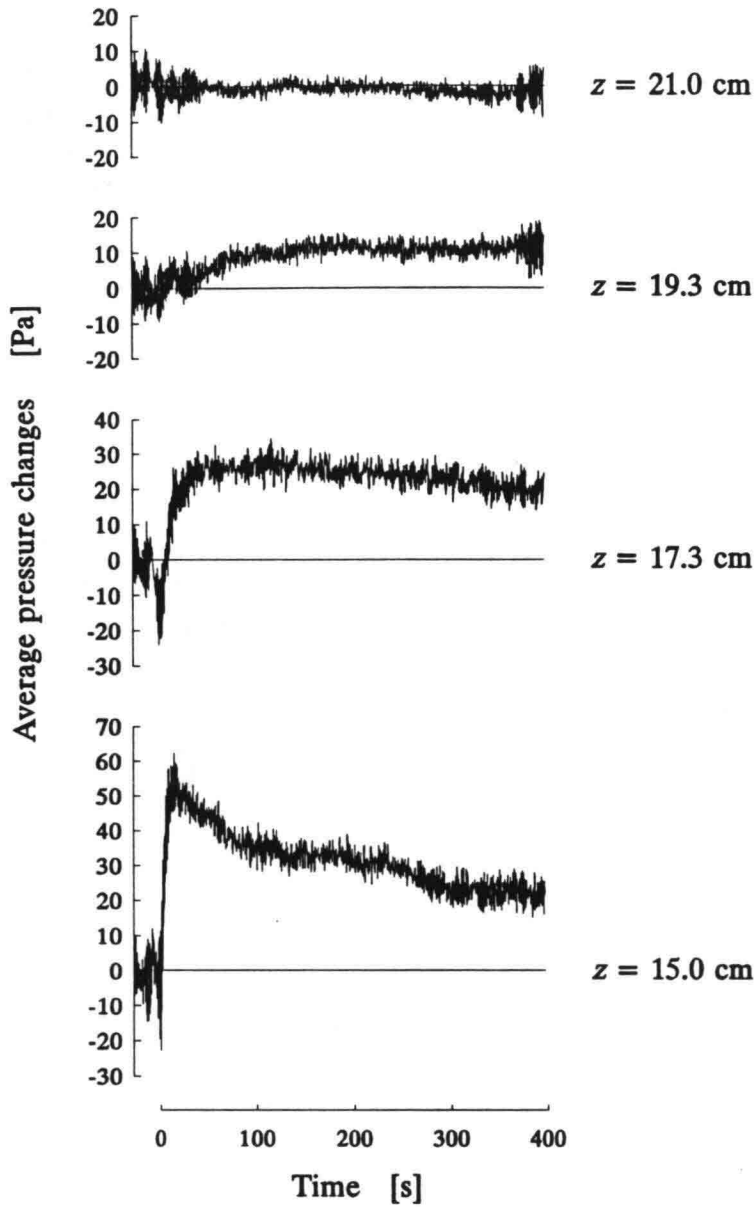


Figure 4.3.4 Wave-averaged pressure changes during the first 400 s of test 1. (The bed surface was at $z=20.5$ cm)

The wave-averaged pressure amplitudes and the average pressures during test 1 are shown in figures 4.3.5 and 4.3.6, respectively. The average pressure amplitudes and average pressures measured at $z=15.0$ cm and $z=17.3$ cm decreased until an apparent equilibrium was formed after approximately 25 minutes.

The suspended sediment concentrations increased quickly and after half an hour the bed surface could not be observed visually any more. Two concentration profiles measured during the first half hour of test 1 are shown in figure 4.3.7. The concentration is seen to increase with time.

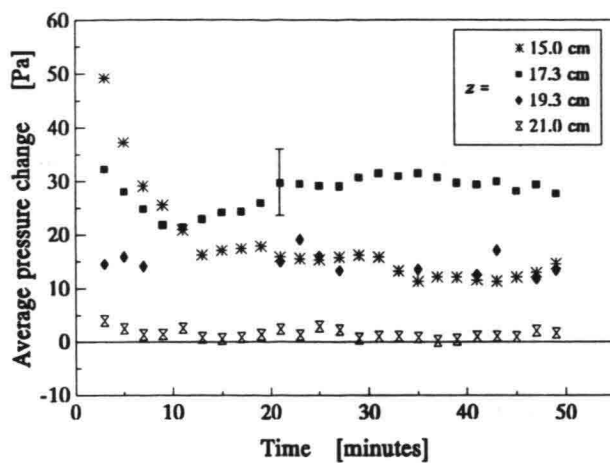


Figure 4.3.5 Average pressure changes during test 1.

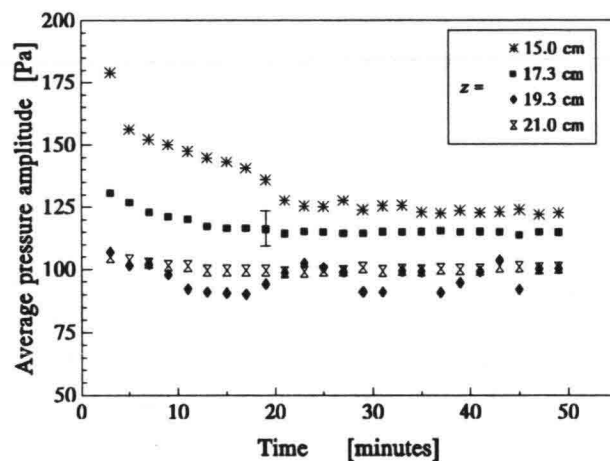


Figure 4.3.6 Average pressure amplitudes during test 1.

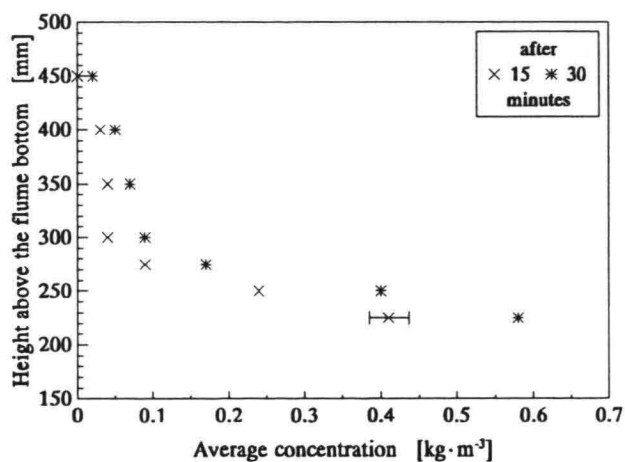


Figure 4.3.7 Suspended sediment concentrations during test 1.

Some typical results of velocity measurements in the water column during the end phase of test 1 are shown in figure 4.3.8. In this graph the longitudinal and vertical components of the velocity amplitudes are shown which were measured at several locations in the test section.

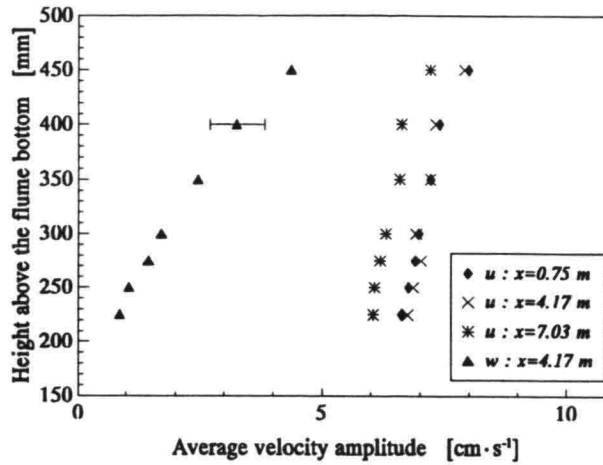


Figure 4.3.8 Velocity amplitudes measured in the end phase of test 1.

4.3.3 Test 2

Directly after test 1 the wave height was increased and the settings of the wave generator were not changed for one hour. The wave heights measured during the first part of test 2 are presented in figure 4.3.9. No significant wave damping can be observed during the first half hour. However, the measurements made in the second half hour clearly show some wave damping. The decrease in wave height as calculated according to the modified Gade model is also shown and it can be observed that the calculated and measured decrease in wave height agree rather well. The parameters used in the calculations are specified later in this section.

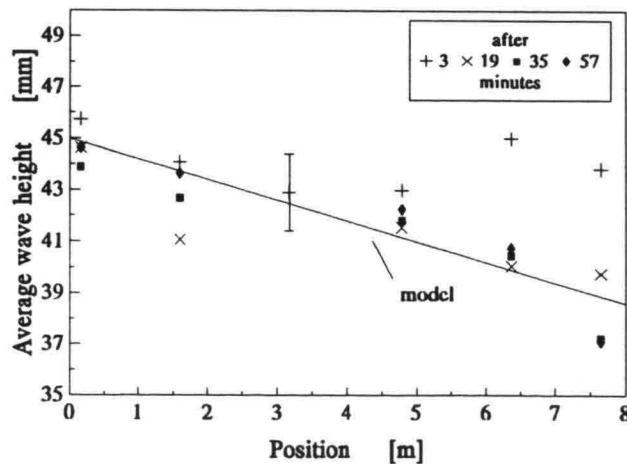


Figure 4.3.9 Wave heights measured during the first part of test 2 and model result.

The average pressure changes and average pressure amplitudes are shown in figures 4.3.10 and 4.3.11, respectively. An excess pore pressure was generated in the first ten minutes of test 2 at $z=15.0$ cm, which decreased when test 2 continued. This decrease was also measured at $z=17.3$ and $z=19.3$ cm. The reference pressure measured at $z=21.0$ cm was constant during this part of the test. The pressure amplitudes (figure 4.3.11) decreased in the first half hour of the test, which corresponds with the measured decrease in wave height during this phase of the test (figure 4.3.9).

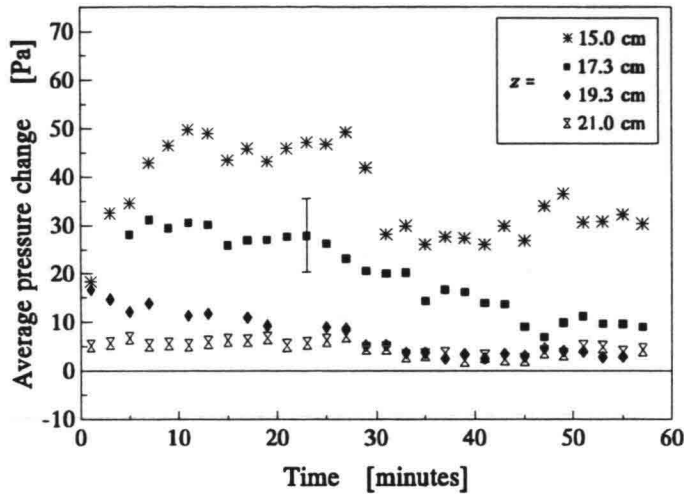


Figure 4.3.10 Average pressure changes during the first part of test 2.

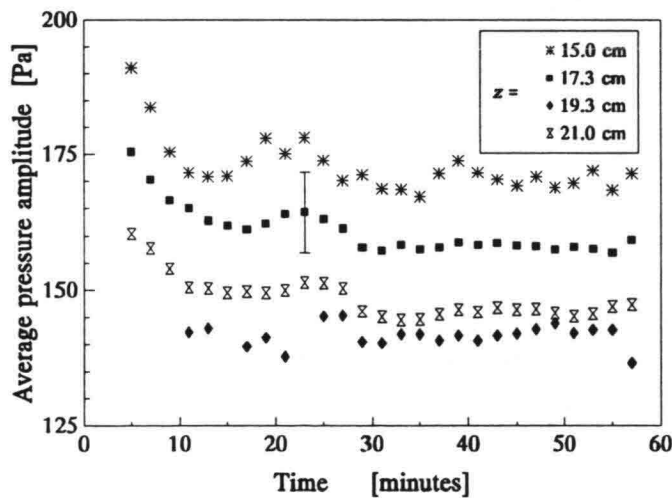


Figure 4.3.11 Average pressure amplitudes during the first part of test 2.

Velocity and suspended concentration measurements were continuously made during this test. Some typical examples of the velocity amplitudes and suspended sediment concentrations measured during the first part test 2 are presented in figures 4.3.12 and 4.3.13, respectively. These profiles are very similar to those measured in test 1.

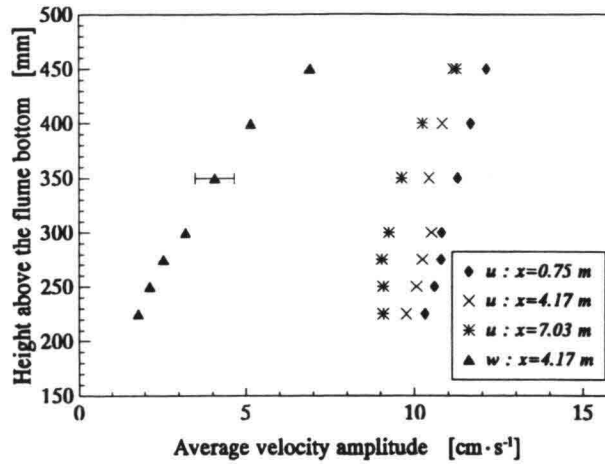


Figure 4.3.12 Average velocity amplitudes measured during the first half hour of test 2. (The bed surface was at $z \approx 190$ mm)

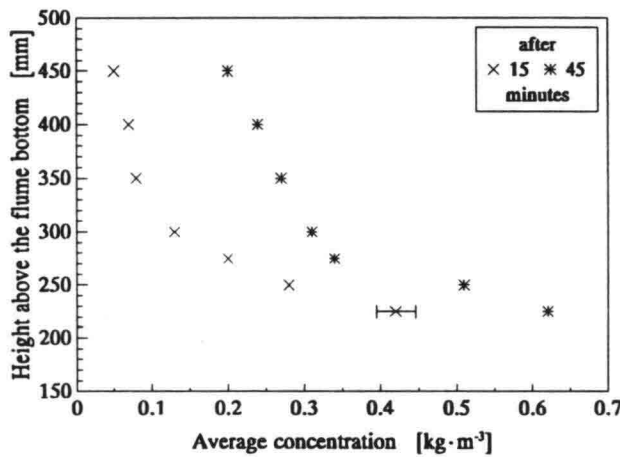


Figure 4.3.13 Suspended sediment concentrations during the first part of test 2. (The bed surface was at $z \approx 190$ mm)

The electromagnetic current meter positioned at $x=7.03$ m was also used to measure velocity components in x direction in the bed during the end phase of the first part of test 2. The local average concentrations were measured simultaneously using the conductivity probe. The results of these measurements are plotted in figures 4.3.14 and 4.3.15. When both figures are compared it can be concluded that the fluid-mud layer was roughly 2.5 cm thick.

The wave generator was stopped after these measurements and the conductivity probe was used to measure two concentration profiles at two locations in the test section. Both measurements were made in the centre-line of the flume ($y=0.40$ m) and the results are shown in figure 4.3.16. The profiles agree with the measurements made prior to the tests (figures 3.4.1 and 3.4.2). However, there seems to be a local maximum in concentration at approximately 17 cm above the bottom of the flume. This increase in concentration may be caused by the consolidation of the fluid-mud layer after wave generation had been stopped. The velocity measurements previously made in the fluid mud, indicated that this layer was about 2.5 cm thick.

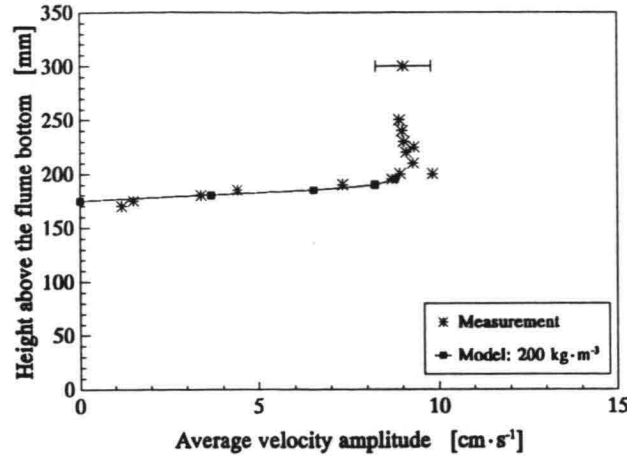


Figure 4.3.14 Average longitudinal velocity amplitudes over and in a partly liquefied bed at the end of the first part of test 2.

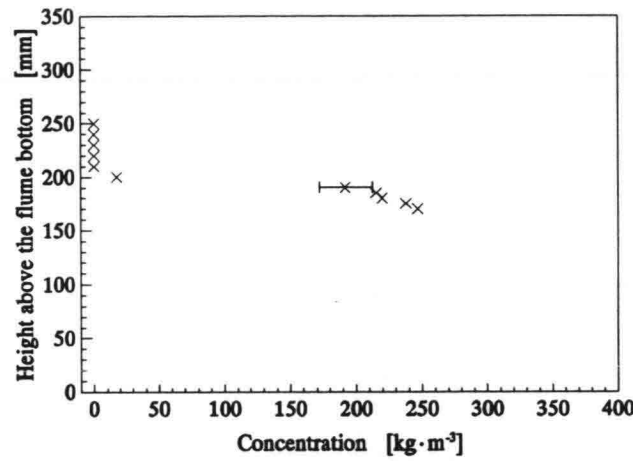


Figure 4.3.15 Concentration profile during the end of the first part of test 2.

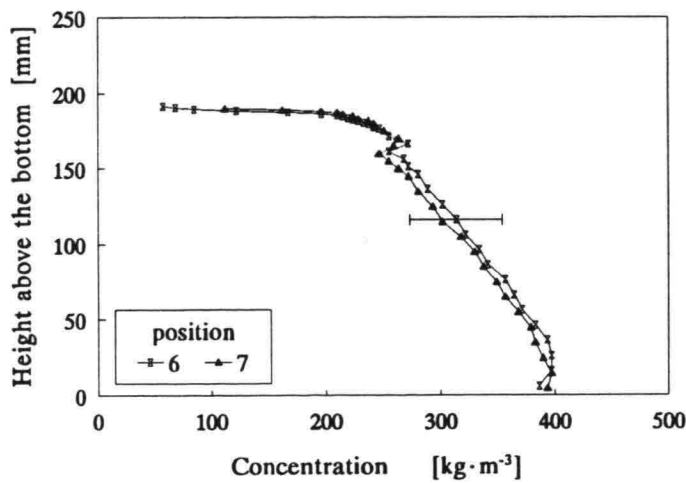


Figure 4.3.16 Concentration profiles measured during test 2 (no waves present). ($y=0.40$ m, position 6: $x=5.42$ m, position 7: $x=6.15$ m)

In figure 4.3.14 the velocity amplitudes calculated using the modified Gade model are also shown and these results agree well with the measured velocity amplitudes. The parameters used in the calculations were: $\bar{h}_1=0.02$ m, $\bar{h}_0=0.32$ m, $\eta_0=0.02$ m, $\rho_1=1000$ kg·m⁻³, $\rho_2=1124$ kg·m⁻³ and $\nu_2=2.91 \cdot 10^{-4}$ m²·s⁻¹.

Test 2 was continued after these concentration measurements. The wave generator was restarted without changing the settings and waves were generated for half an hour. The wave heights measured during the second part of test 2 are shown in figure 4.3.17. Roughly 15 minutes after the wave generator was started the same wave damping was observed as in the end phase of the first part of test 2.

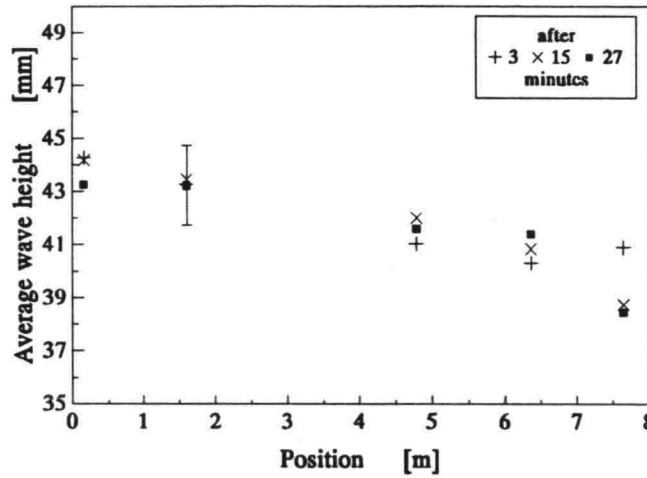


Figure 4.3.17 Wave heights measured during the second part of test 2.

The suspended sediment concentrations during this part of the test are plotted in figure 4.3.18. At first the suspended sediment concentration was almost constant in vertical direction. However, after 30 minutes of wave action a distinct profile had formed, as can be seen in figure 4.3.18.

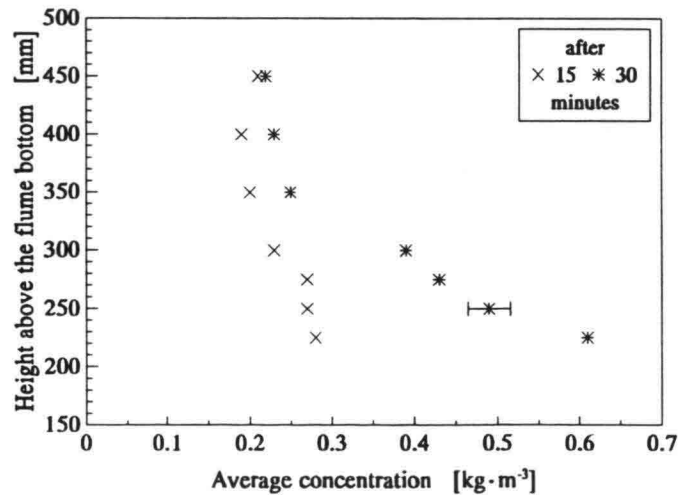


Figure 4.3.18 Suspended sediment concentrations measured at $x=4.35$ m during the second part of test 2.

4.3.4 Test 3

After test 2 the pump was started and the average flow rate was set at $12 \text{ dm}^3 \cdot \text{s}^{-1}$. The settings of the wave generator were not altered. Velocity measurements in and over the partly liquefied bed were measured at $x=7.03 \text{ m}$ approximately 2 minutes after the flow rate was set. Concentrations were simultaneously measured using the conductivity probe. The average amplitude of the longitudinal velocity component are shown in figure 4.3.19. The average velocities are plotted in figure 4.3.20 and in figure 4.3.21 the measured concentrations are presented.

The velocity amplitudes show a similar trend as in test 2. The bed surface was at approximately $z=19.0 \text{ cm}$. The fluid-mud layer was approximately 2 cm thick, because the lowest significant velocity amplitude was measured at $z=17.0 \text{ cm}$. A significant net current was only measured at heights higher than about 18 cm above the bottom of the flume. These measurements indicate that a net current was present only in the upper cm of the fluid-mud layer.

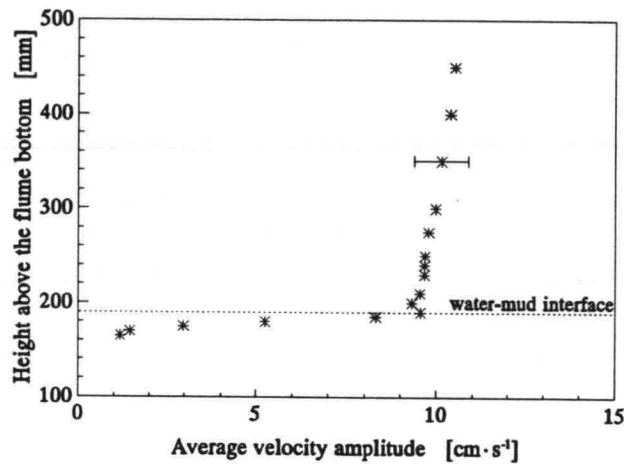


Figure 4.3.19 Average velocity amplitude (u) measured at $x=7.03 \text{ m}$ during test 3. (Average flow rate: $12 \text{ dm}^3 \cdot \text{s}^{-1}$)

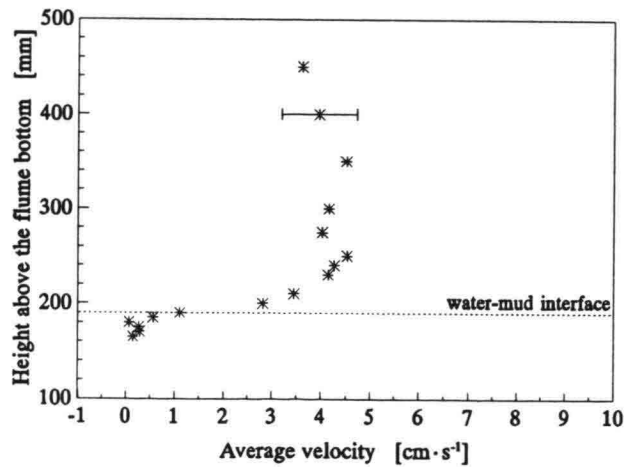


Figure 4.3.20 Average velocity (u) measured at $x=7.03 \text{ m}$ during test 3. (Average flow rate: $12 \text{ dm}^3 \cdot \text{s}^{-1}$)

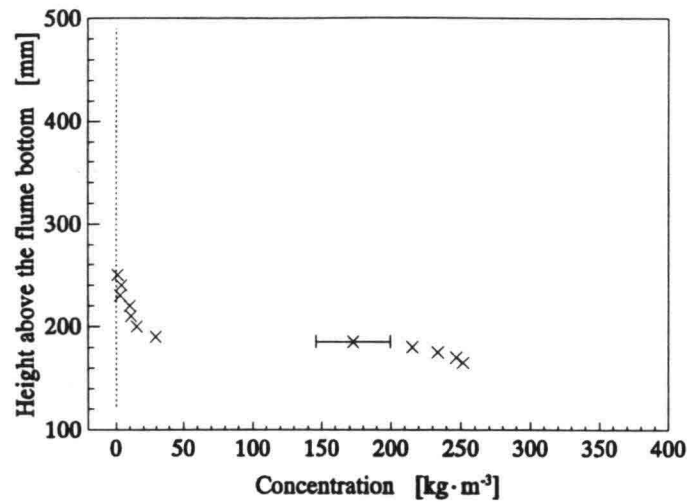


Figure 4.3.21 Concentration profile measured at $x=7.25$ m during test 3. (Average flow rate: $12 \text{ dm}^3 \cdot \text{s}^{-1}$)

The value of the flow rate was increased to $24 \text{ dm}^3 \cdot \text{s}^{-1}$ and the same procedure was repeated: two minutes after the flow rate was set, velocity measurements were made in and over the bed at $x=7.03$ m. The average velocity amplitudes and the average velocities are shown in figures 4.3.22 and 4.3.23, respectively. In these graphs only the velocity components in longitudinal direction are plotted. The concentration profile measured during this phase of test 3 is shown in figure 4.3.24. The bed was approximately 19 cm thick. The velocity measurements showed that there were significant velocity amplitudes at about $z=17$ cm. However, at this level in the bed no net current was measured.

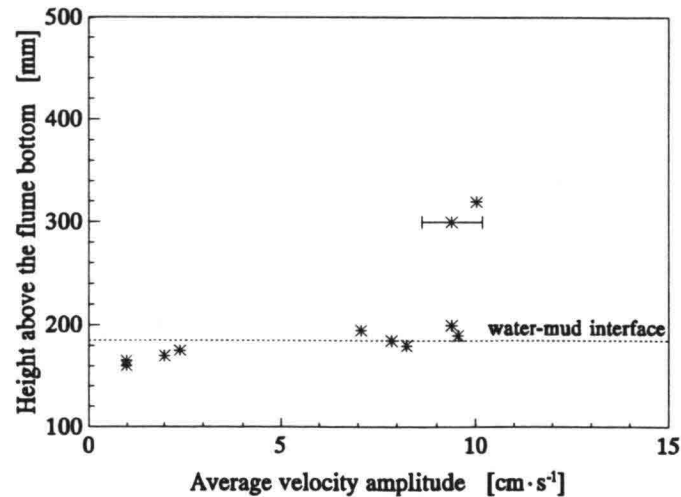


Figure 4.3.22 Average velocity amplitude (u) measured at $x=7.03$ m during test 3. (Average flow rate: $24 \text{ dm}^3 \cdot \text{s}^{-1}$)

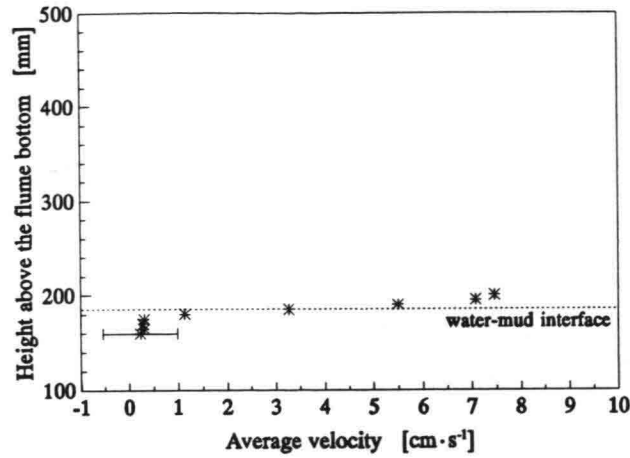


Figure 4.3.23 Average velocity (u) measured at $x=7.03$ m during test 3. (Average flow rate: $24 \text{ dm}^3 \cdot \text{s}^{-1}$)

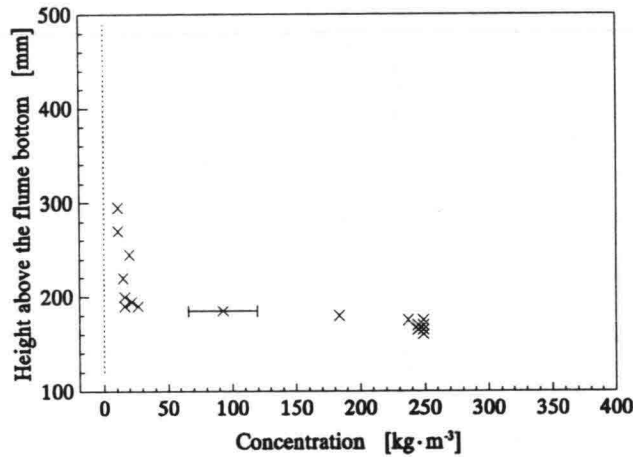


Figure 4.3.24 Concentration profile measured at $x=7.25$ m during test 3. (Average flow rate: $24 \text{ dm}^3 \cdot \text{s}^{-1}$)

This test was concluded with similar measurements for a flow rate of $36 \text{ dm}^3 \cdot \text{s}^{-1}$. The maximum values of the velocity amplitudes (figure 4.3.25) decreased compared to the measurements made for a flow rate of $24 \text{ dm}^3 \cdot \text{s}^{-1}$, which was caused by the decrease in wave height due to the increased flow rate. The increase in flow rate can be clearly observed in figure 4.3.26 (see figure 4.3.20 for comparison) where the average velocities are plotted. The concentration measurements showed that the bed was approximately 18 cm thick (see figure 4.3.27). Consequently, no net current and no velocity amplitudes were observed in the bed, for the first significant average velocities and velocity amplitudes were measured at about 17.5 cm. This result was not unexpected, for the fluid mud was transported in the downstream direction by the current. Therefore, no fluid mud was present any more during this phase of test 3. The pump was stopped as soon as the last measurements had been made.

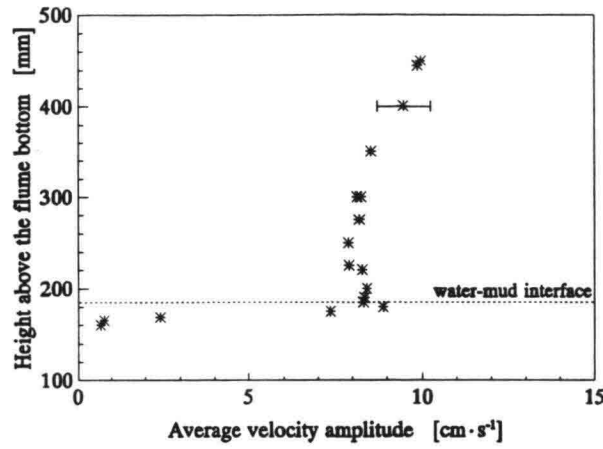


Figure 4.3.25 Average velocity amplitudes measured at $x=7.03$ m during test 3. (Average flow rate: $36 \text{ dm}^3 \cdot \text{s}^{-1}$)

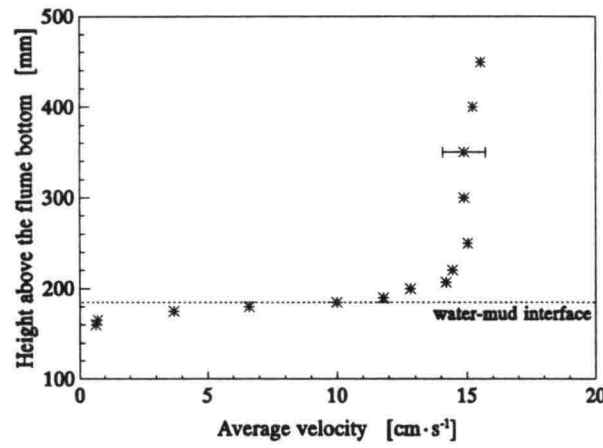


Figure 4.3.26 Average velocities measured at $x=7.03$ m during test 3. (Average flow rate: $36 \text{ dm}^3 \cdot \text{s}^{-1}$)

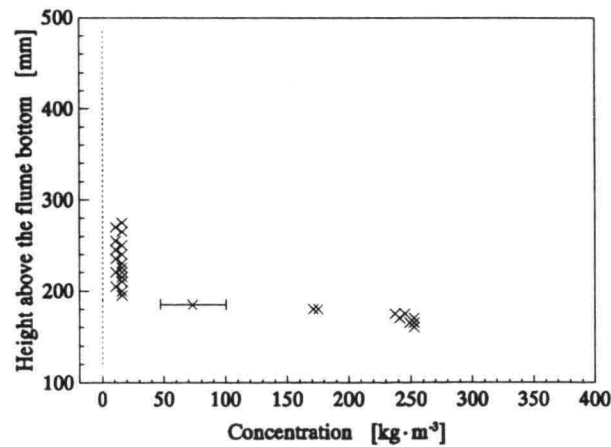


Figure 4.3.27 Concentration profile measured at $x=7.25$ m during test 3. (Average flow rate: $36 \text{ dm}^3 \cdot \text{s}^{-1}$)

4.3.5 Test 4

In the fourth (final) test of 16 July the wave height was increased again and waves were generated for roughly an hour. After about half an hour of wave action all three electromagnetic current meters were used to measure velocities in and over the bed.

The wave heights measured during the entire test are shown in figure 4.3.28. During the first 15 minutes of this test no significant wave damping was observed. This was probably caused by the fact that the fluid mud was transported in the downstream direction during test 3 (waves and current). However, after 30 minutes the waves were heavily damped, for new fluid mud was formed in the test section and the damping increased a little when the test continued. This graph also shows the decrease in wave height as calculated using the modified Gade model. The parameters used in the calculations are specified later in this section. As can be seen the calculated wave damping underestimates the measured wave damping.

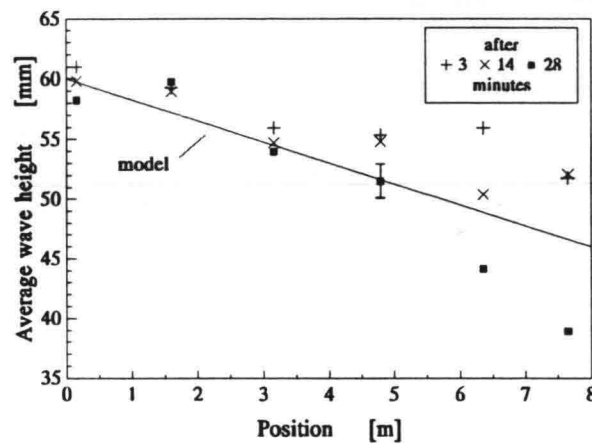


Figure 4.3.28 Average wave heights measured during test 4.

The sudden decrease in wave height can also be observed in the measured pressure amplitudes measured during this test (figure 4.3.29). The average pressure amplitudes suddenly decrease after approximately 15 minutes, which corresponds with the change in wave heights measured. The average pressure showed no significant change as can be seen in figure 4.3.30. The cause of the sudden decrease in pressure amplitudes is unknown.

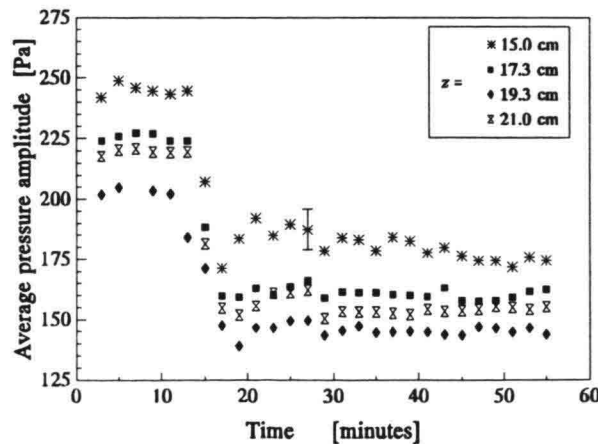


Figure 4.3.29 Average pressure amplitudes during test 4.

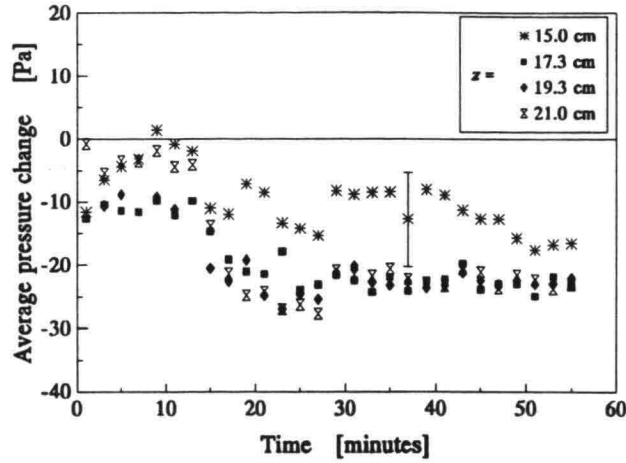


Figure 4.3.30 Average pressure measured during test 4.

The suspended sediment concentrations were measured in the first half hour of test 4 only. The results obtained are shown in figure 4.3.31. During test 3 the water in the flume had been recirculated a number of times and as a result the suspended sediment concentration was almost uniform in the water column. The profile altered into the form measured after 30 minutes, which was probably caused by the settling of the mud particles.

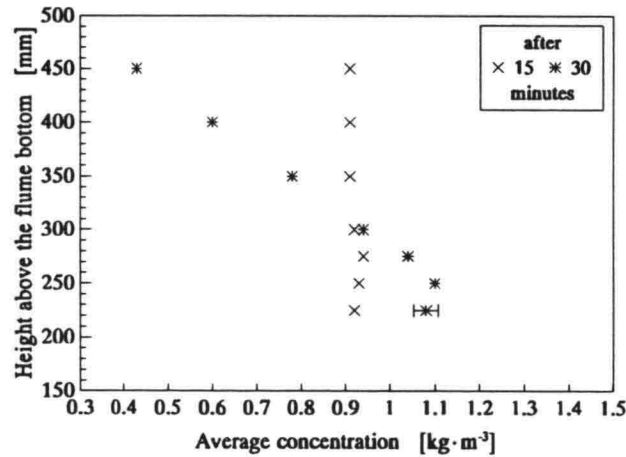


Figure 4.3.31 Average suspended sediment concentrations measured at $x=4.35$ m during test 4.

Thirty minutes after the start of test 4 the optical concentration meters were removed and the electromagnetic current meters were used to measure velocities in and over the bed. Only the velocity components in longitudinal direction were measured. The conductivity probe was mounted on one of the traversing systems in order to simultaneously measure the concentration. The results of the velocity measurements were quite remarkable as can be seen in figures 4.3.32 and 4.3.33. The bed was approximately 17 cm thick, which can be concluded from the concentration measurements (figure 4.3.34). The amplitudes measured over the bed decrease in the downstream direction, which is caused by the damping of the waves (figure 4.3.33). Furthermore, the liquefaction of the bed was not uniform in the longitudinal direction: in an upstream part of the test section the bed seemed to be liquefied down to approximately 4 cm above the bottom of the flume and the velocity amplitudes

increased with the height above the bottom of the flume (figure 4.3.32). According to the velocity measurements the bed in the centre and at the downstream part of the test section oscillated as a whole: the velocity amplitudes were almost constant over the depth in the bed (figure 4.3.33).

The velocity amplitudes calculated using the modified Gade model are also shown in figures 4.3.32 and 4.3.33. The velocity amplitudes shown in figure 4.3.33 were calculated with the following parameters: $\bar{h}_1=0.15$ m, $\bar{h}_0=0.50$ m, $\eta_0=0.02$ m, $\rho_1=1000$ kg·m⁻³, $\rho_2=1186$ kg·m⁻³ and $\nu_2=5.94\cdot 10^{-4}$ m²·s⁻¹. For an explanation of the parameters used see De Wit (1994). As can be seen the calculations correspond well with the measurements. However, the velocity amplitudes measured in the upstream part of the test section could not be reproduced by the calculation using the results of the wave height and concentration measurements. The calculated velocity amplitudes overestimated the measured velocity amplitudes by about 33 percent (figure 4.3.32, parameter set 1) and the profiles did not agree when the following parameters were used: $\bar{h}_1=0.09$ m, $\bar{h}_0=0.46$ m, $\eta_0=0.03$ m, $\rho_1=1000$ kg·m⁻³, $\rho_2=1189$ kg·m⁻³ and $\nu_2=5.94\cdot 10^{-4}$ m²·s⁻¹. The thickness of the fluid mud layer \bar{h}_1 was estimated using the results of the velocity measurements (figure 4.3.32). This discrepancy was probably caused by the fact that the concentration measurements were made in the bed at the downstream end of the test section. However, the bed at $x=0.75$ m was at least 3 cm less thick than the bed at $x=7.25$ m, which can be concluded comparing figures 4.3.32 and 4.3.33. Consequently, the average concentration of the upstream part of the bed may be different too. Furthermore, waves which entered the test section had to adjust because of the increase in water depth at $x=0$ m, which may result in a lower effective wave height near the water-mud surface at $x=0.75$ m than the wave height measured.

The calculations were also made using a different set of parameters, namely $\bar{h}_1=0.09$ m, $\bar{h}_0=0.46$ m, $\eta_0=0.02$ m, $\rho_1=1000$ kg·m⁻³, $\rho_2=1249$ kg·m⁻³ and $\nu_2=2.96\cdot 10^{-3}$ m²·s⁻¹ (parameter set 2). The wave amplitude was set at 0.02 m, and the average concentration was assumed to be 400 kg·m⁻³ which corresponds with a density of 1249 kg·m⁻³. These parameters were also used to calculate the wave damping as shown in figure 4.3.28. The results of these calculations agree well with the measurements.

After these measurements the generation of waves was stopped and two concentration profiles were measured in the test section. The results of these measurements are shown in figure 4.3.35.

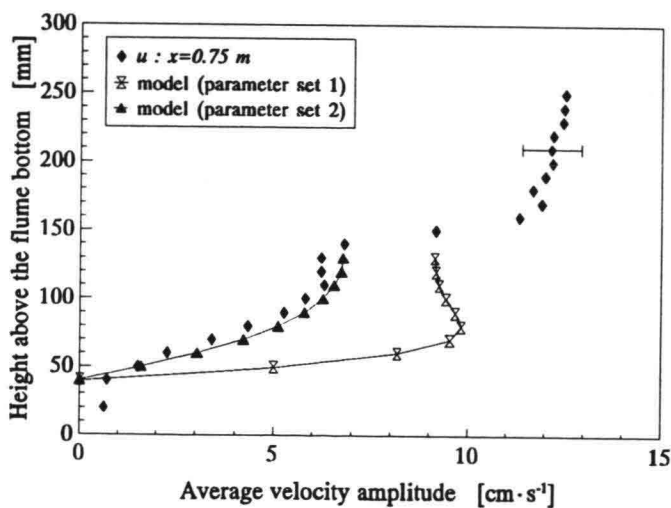


Figure 4.3.32 Velocity amplitudes (u) in and above the bed at $x=0.75$ m during the last half hour of test 4.

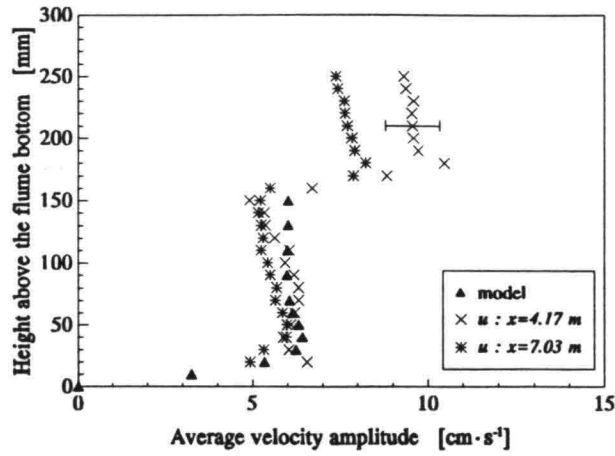


Figure 4.3.33 Velocity amplitudes (u) in and above the bed at $x=4.17$ m and $x=7.03$ m during the last half hour of test 4.

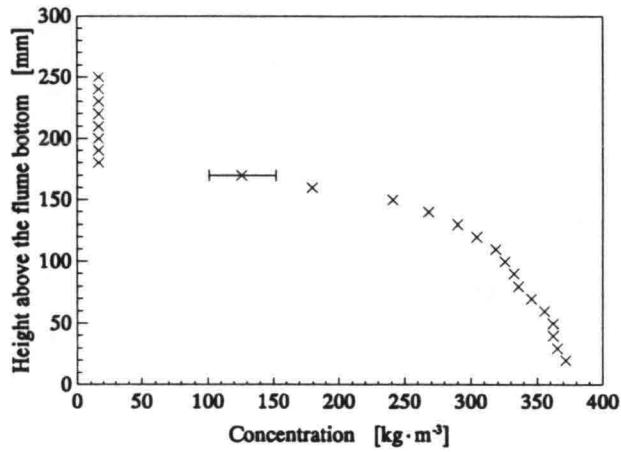


Figure 4.3.34 Concentration profile measured at $x=7.25$ m during the second half hour of test 4.

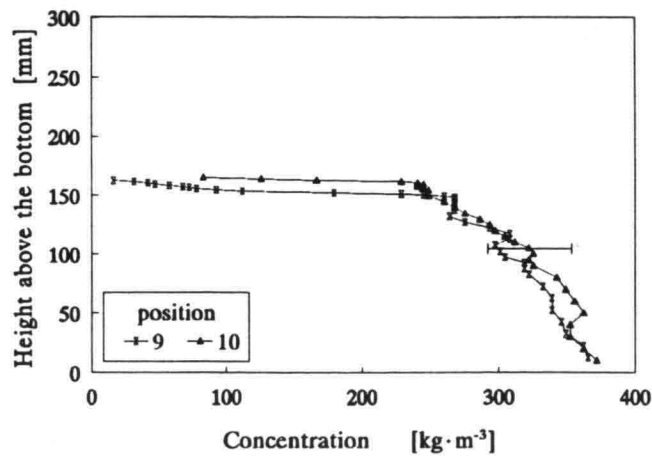


Figure 4.3.35 Concentration profiles measured after test 4.
($y=0.40$ m, position 9: $x=2.37$ m, position 10: $x=6.13$ m)

4.3.6 Concentration measurements prior to test 5

The tests were resumed on July 23rd after a consolidation period of approximately 6 days. As in the first experiment on Westwold Clay the bed surface was not smooth, for lumps of mud, which apparently had not been liquefied during the tests, protruded at various locations from the bed surface. However, the surface of the bed was very smooth between the protruding lumps and presumably had been liquefied during the first four tests.

Prior to the tests concentration measurements were made at six locations in the test section. The results of these measurements are presented in figures 4.3.36 and 4.3.37. These measurements show that the bed was not horizontal in the longitudinal as well as the transverse direction. The fact that the endwalls of the test section, especially the downstream endwall, were not lowered enough during the first four tests was the cause of the increment in the thickness of the bed in the downstream direction. The variation in height of the bed in a cross-section was caused by the lumps of mud which protruded from the bed surface.

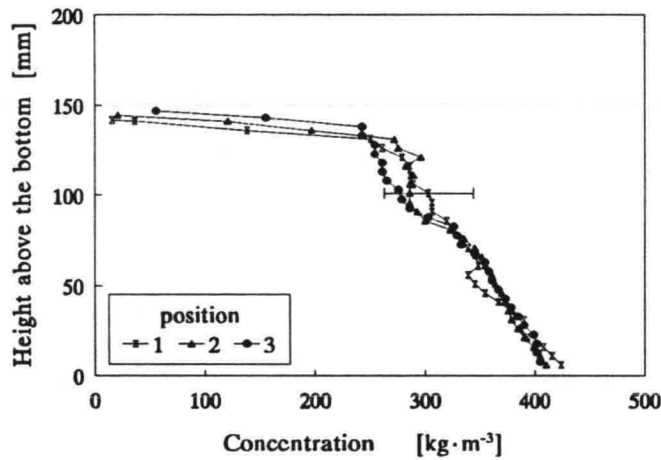


Figure 4.3.36 Concentration profiles measured at $x=2.30$ m prior to test 5.
(Position 1: $y=0.20$ m, position 2: $y=0.40$ m, position 3: $y=0.60$ m)

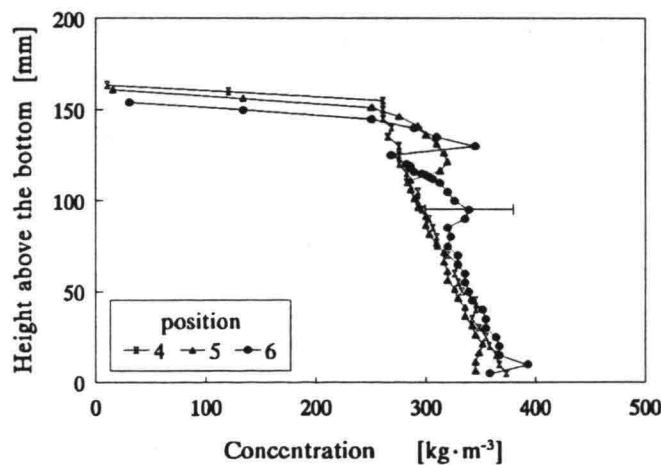


Figure 4.3.37 Concentration profiles measured at $x=5.70$ m prior to test 5.
(Position 1: $y=0.20$ m, position 2: $y=0.40$ m, position 3: $y=0.60$ m)

4.3.7 Test 5

In test 5 the bed was cyclicly loaded for approximately half an hour. The wave height was approximately 25 mm (see figure 4.3.38). As soon as the first waves had reached the test section the mud surrounding the protruding lumps started to make oscillating movements. No movement could be observed in the lumps. No significant wave damping was measured during test 5.

As the bed was partly eroded in the foregoing tests three pressure transducers were no longer situated in the bed. Only one pressure transducers was just at the water-mud interface. From the pressure measurements made at the beginning of test 5 (figure 4.3.39) it may be concluded that the pressure transducer fixed at $z=15.0$ cm was exactly at the water-mud interface for no significant pressure changes were measured although the mud started to liquefy according to visual observations.

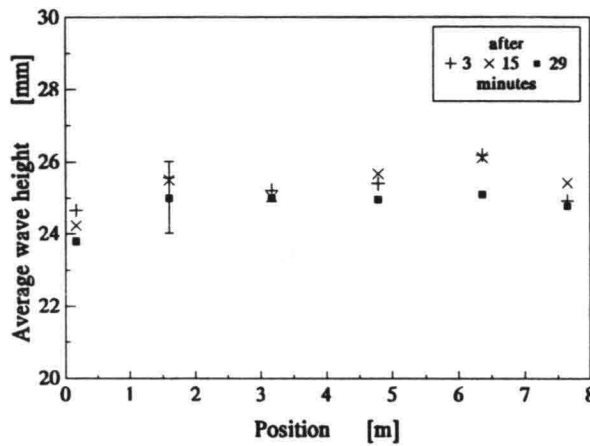


Figure 4.3.38 Average wave heights measured during test 5.

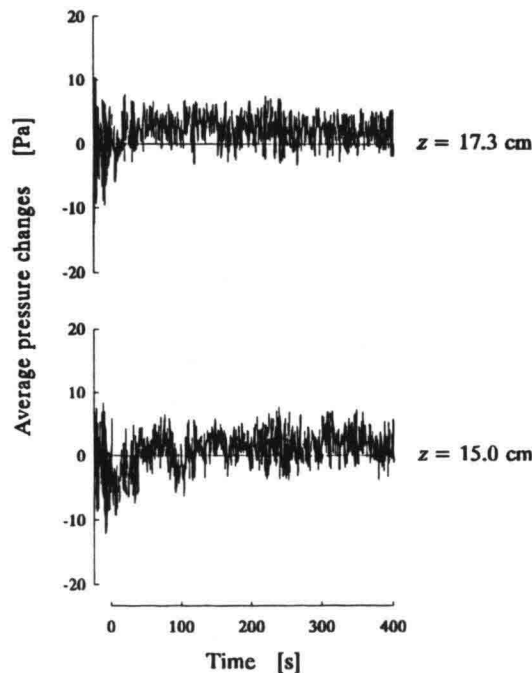


Figure 4.3.39 Wave-averaged pressures during the start of test 5.

No significant increase in suspended sediment concentration was measured during test 5. A typical example of the velocity amplitudes measured in the water column is shown in figure 4.3.40. The water temperature was 19.8°C at the start of test 5.

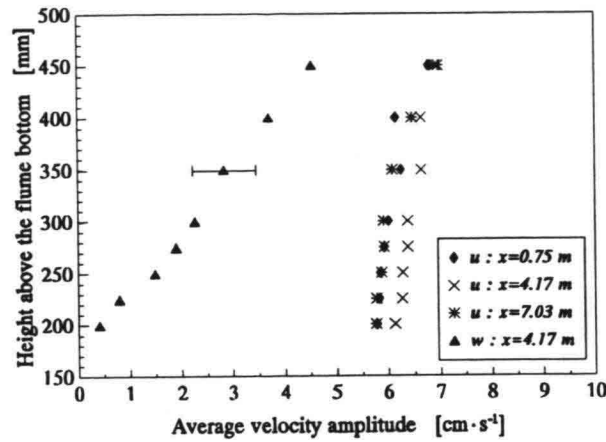


Figure 4.3.40 Average velocity amplitudes measured in the end phase of test 5.

4.3.8 Test 6

The wave height was increased directly after test 5. As in all of the foregoing tests the wave period was 1.5 s, and the average wave height was about 46 mm. No significant decrease in wave height was observed in the downstream direction in an initial phase of test 6, which result is similar to the observations made during test 5. However, after 15 minutes significant wave damping was observed (figure 4.3.41) which was almost constant during the remaining part of the test. The wave damping calculated using the modified Gade model is also plotted in this graph. The model results underestimate the measured decrease in wave height. The parameters used in the calculation are specified later in this section.

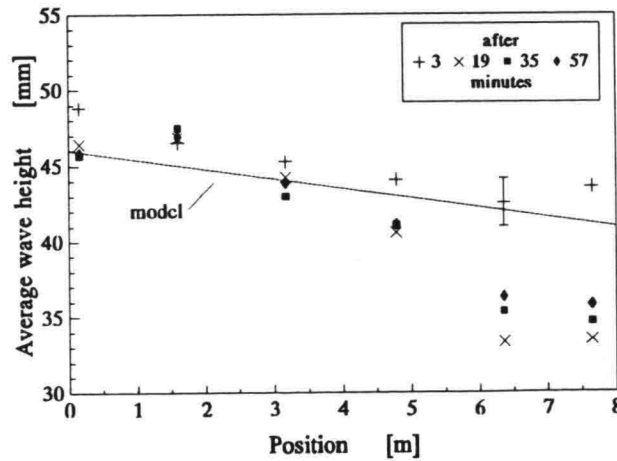


Figure 4.3.41 Average wave heights measured during test 6.

The effects of the wave damping were also clearly noticeable in the measurements of the velocity amplitudes. In figure 4.3.42 the average amplitudes of the velocity components in the longitudinal direction (u -velocity amplitudes) are plotted. These velocities were measured at three locations in the test section about half an hour after the start of this test. The decrease in amplitude in the downstream direction is clearly visible.

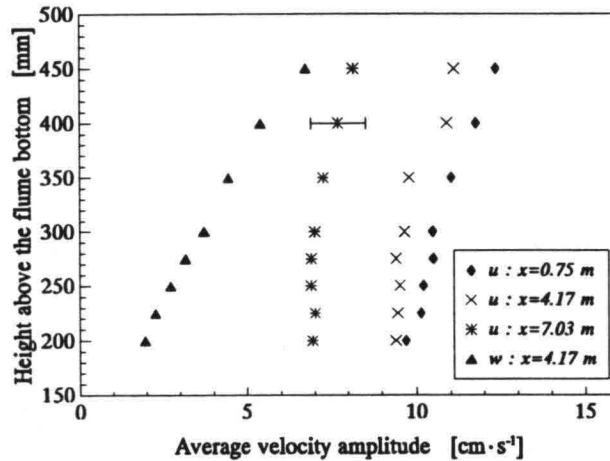


Figure 4.3.42 Average velocity amplitudes measured in the test section 30 minutes after test 6 was started. (The bed surface was at $z \approx 15$ cm)

The suspended sediment concentration increased rapidly as can be seen in figure 4.3.43. In this graph the suspended sediment concentration measure at $x=4.35$ m is shown. After half an hour a distinct concentration profile was formed, which was also observed visually.

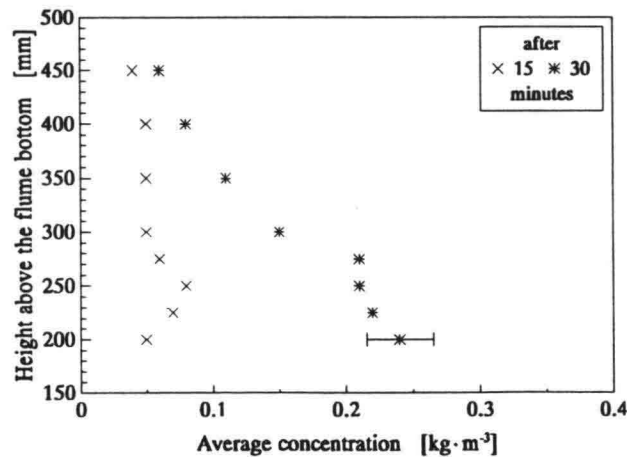


Figure 4.3.43 Suspended sediment concentrations measured at $x=4.35$ during the first half hour of test 6.

An electromagnetic current meter, installed at $x=7.03$ m, was used to measure velocities in the and over the bed during the second half of this test. Concentration measurements were simultaneously made using the conductivity probe. The velocity measurements, presented in figure 4.3.44, showed

that the bed was oscillating as a whole over the bottom of the flume. The results of the concentration measurements are shown in figure 4.3.45. The calculated velocity amplitudes in the fluid layer were also calculated using the modified Gade model. The results of the calculations, which are also shown in figure 4.3.44, correspond very well with the measurements. The parameters used in the calculations were: $\bar{h}_1=0.15$ m, $\bar{h}_0=0.50$ m, $\eta_0=0.0175$ m, $\rho_1=1000$ kg·m⁻³, $\rho_2=1186$ kg·m⁻³ and $\nu_2=5.94 \cdot 10^{-4}$ m²·s⁻¹. For an explanation of the parameters used see De Wit (1994).

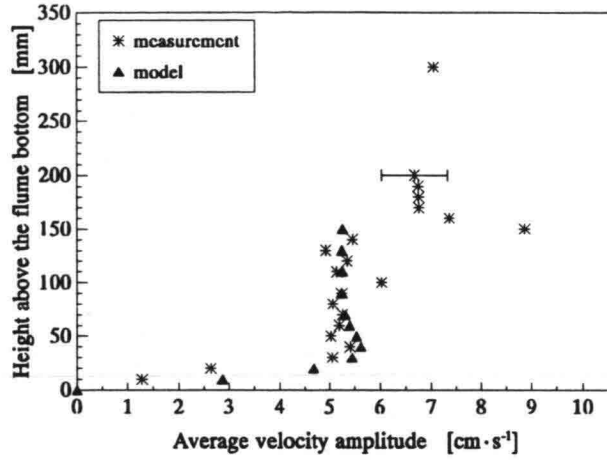


Figure 4.3.44 Average velocity amplitudes measured at $x=7.03$ m during the second half of test 6.

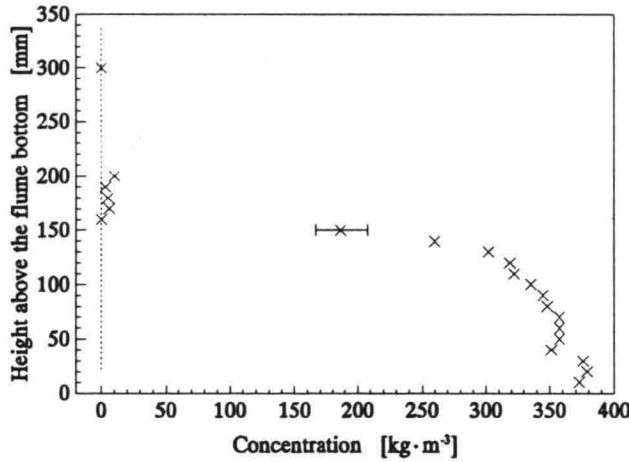


Figure 4.3.45 Concentration profile measured at $x=7.25$ m during the second half of test 6.

4.3.9 Test 7

The wave height was increased again in test 7. The wave height measurements during the first half hour of wave action are shown in figure 4.3.46. In this test there was also significant wave damping.

The suspended sediment concentration increased during the first half hour as can be seen in figure 4.3.47 where the suspended sediment concentration measured during this phase of the test is shown. The effect of the wave damping on the velocity amplitudes was also striking. In figure 4.3.48 the results of the velocity measurements are shown.

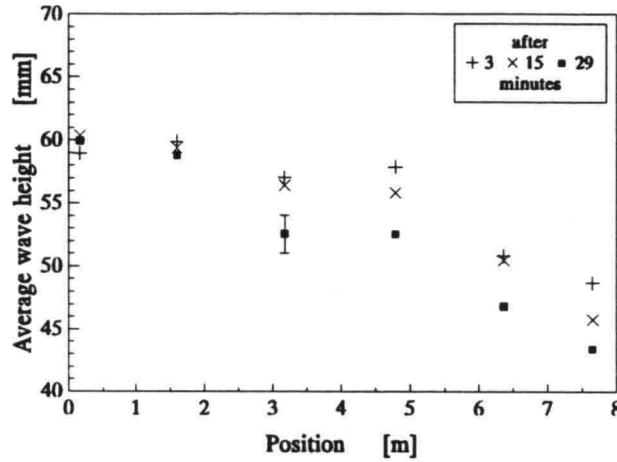


Figure 4.3.46 Average wave heights measured during the first half hour of test 7.

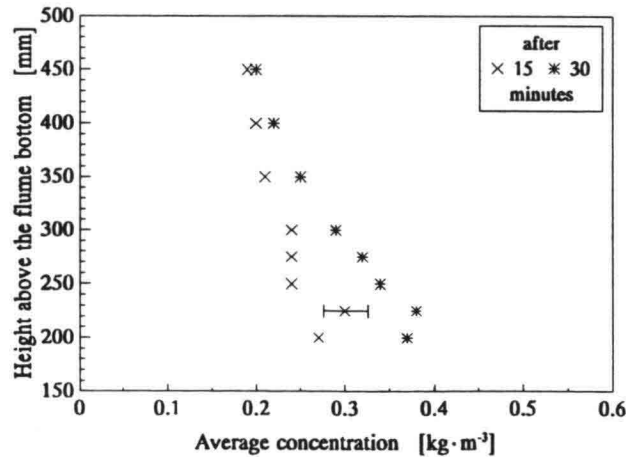


Figure 4.3.47 Average suspended sediment concentrations measured at $x=4.35$ m during the first half hour of test 7.

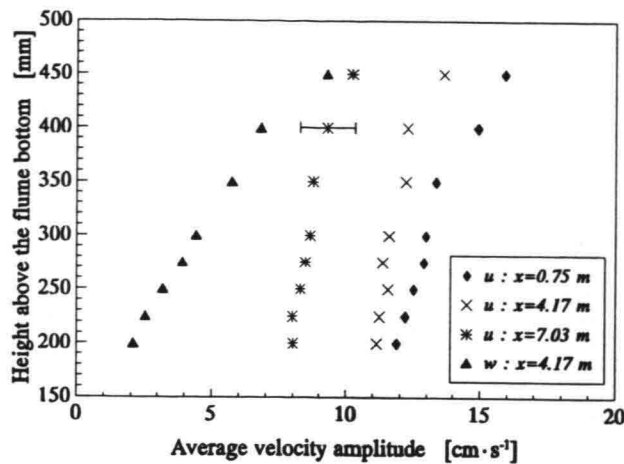


Figure 4.3.48 Average velocity amplitudes during the first half hour of test 7.

Subsequently, the electromagnetic current meters were lowered into the mud layer with the objective to measure velocities in the bed. The conductivity probe was used to measure simultaneously the local concentration at only one location. The wave heights measured during this operation are shown in figure 4.3.49. The wave damping is substantial. The decrease in wave height was calculated according to the modified Gade model for two different parameter sets. These parameter sets are specified later. The wave damping calculated underestimates the measured wave damping.

The velocity profiles measured in the bed are plotted in figures 4.3.50 and 4.3.51. Note the difference between the profile measured at the upstream end of the test section (figure 4.3.50) and the profiles measured in the middle and the downstream end of the test section (figure 4.3.51). These measurements seem to indicate that the upstream part of the bed was not liquefied to the same degree as the rest of the bed. However, this result may also have been caused by the fact that the electromagnetic current meter was lowered into a lump of mud which was not liquefied in the previous tests. Furthermore, the influence of the upstream endwall on the flow at the location of the measurement may be significant. The results of the concentration measurements are shown in figure 4.3.52.

The velocity amplitudes were also calculated according to the modified Gade model for two parameter sets. The amplitudes plotted in figure 4.3.50 were calculated using the following parameters: $\bar{h}_1=0.15$ m, $\bar{h}_0=0.50$ m, $\eta_0=0.0215$ m, $\rho_1=1000$ kg·m⁻³, $\rho_2=1186$ kg·m⁻³ and $\nu_2=5.94 \cdot 10^{-4}$ m²·s⁻¹. The agreement between the measured and calculated values was good. The amplitudes in figure 4.3.51 were calculated with the following parameter set: $\bar{h}_1=0.05$ m, $\bar{h}_0=0.44$ m, $\eta_0=0.03$ m, $\rho_1=1000$ kg·m⁻³, $\rho_2=1249$ kg·m⁻³ and $\nu_2=2.96 \cdot 10^{-3}$ m²·s⁻¹. Here the measured and calculated velocity amplitudes agree well. For an explanation of the parameters used see De Wit (1994).

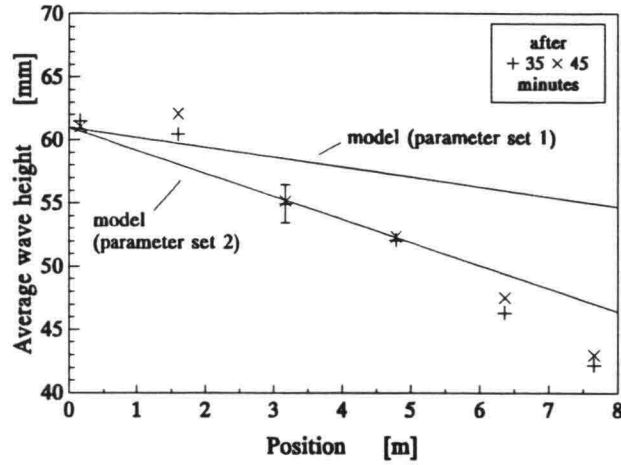


Figure 4.3.49 Average wave heights during test 7.

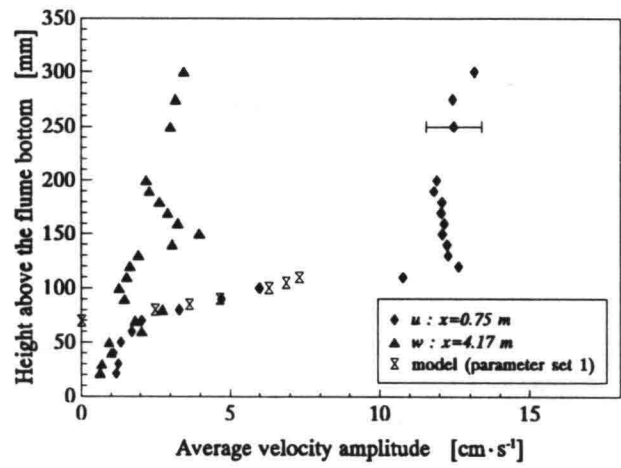


Figure 4.3.50 Average velocity amplitudes measured during test 7 (waves only).

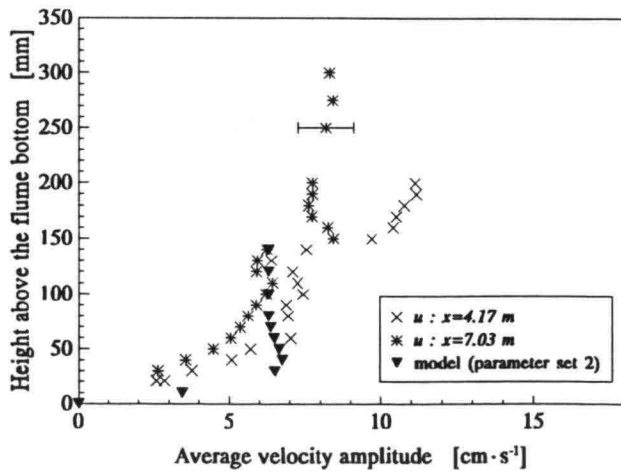


Figure 4.3.51 Average velocity amplitudes measured during test 7 (waves only).

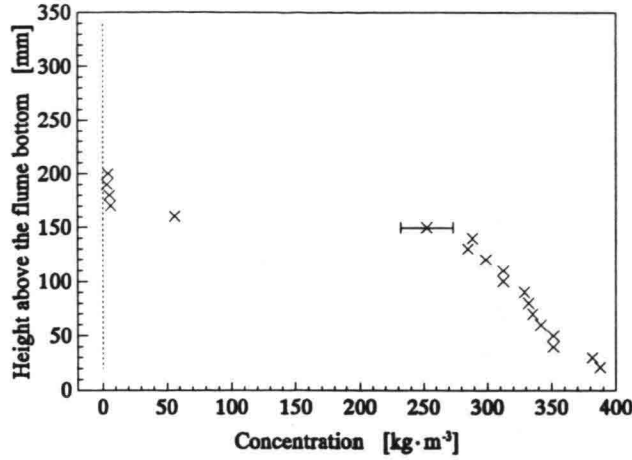


Figure 4.3.52 Concentration profile measured during test 7 (waves only).

The pump was started as soon as the velocity measurements in the bed were completed and the flow rate was set at $24 \text{ dm}^3 \cdot \text{s}^{-1}$. The settings of the wave generator were not changed. Velocity measurements started at $z=450 \text{ mm}$ two minutes after the flow rate had been set. The average velocity amplitudes are shown in figure 4.3.53. The average velocities are presented in figure 4.3.54. This graph shows that there was only a net current in the upper part of the fluid-mud layer. The vertical average velocities (not shown in this figure) were equal to zero. The concentration profile measured during this phase of the test is plotted in figure 4.3.57 together with the profile measured when the flow rate was set at $36 \text{ dm}^3 \cdot \text{s}^{-1}$.

The velocity amplitudes measured when the flow rate was set at $36 \text{ dm}^3 \cdot \text{s}^{-1}$ are presented in figure 4.3.55. The profile measured is similar to the profile measured when the flow rate was set at $24 \text{ dm}^3 \cdot \text{s}^{-1}$ (figure 4.3.53). The average velocities are shown in figure 4.3.56.

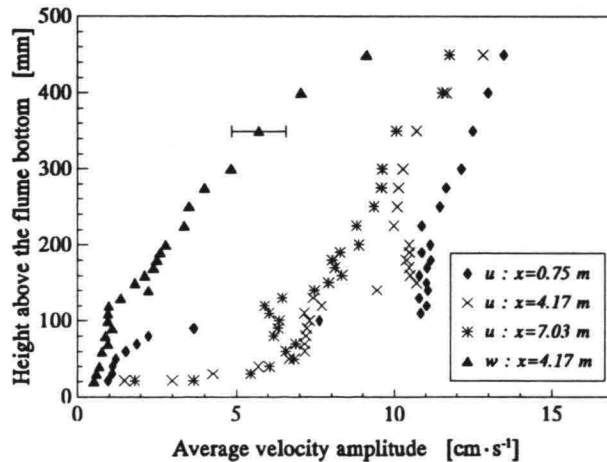


Figure 4.3.53 Average velocity amplitudes measured during test 7. (Waves and current, flow rate: $24 \text{ dm}^3 \cdot \text{s}^{-1}$)

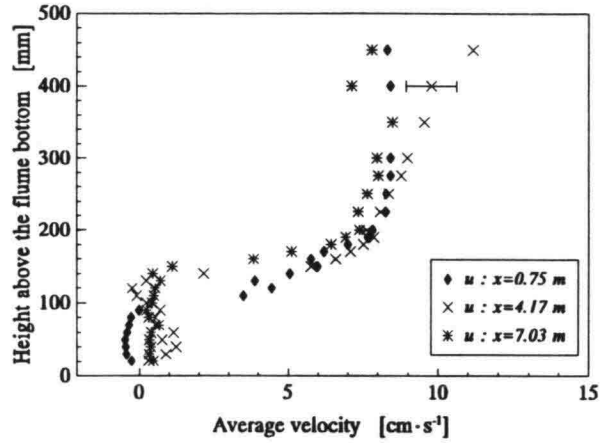


Figure 4.3.54 Average velocities measured during test 7.
(Waves and current, flow rate: $24 \text{ dm}^3 \cdot \text{s}^{-1}$)

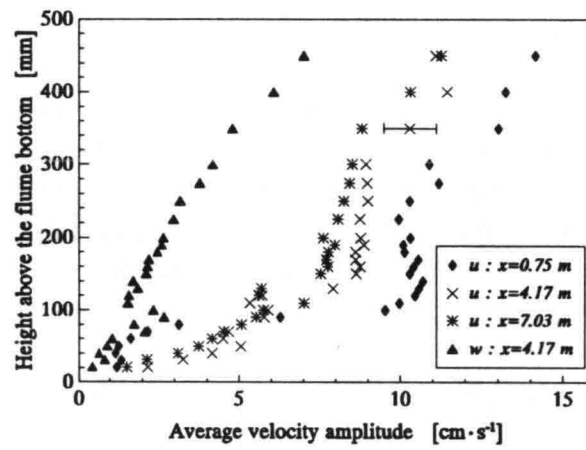


Figure 4.3.55 Average velocity amplitudes measured during test 7.
(Waves and current, flow rate: $36 \text{ dm}^3 \cdot \text{s}^{-1}$)

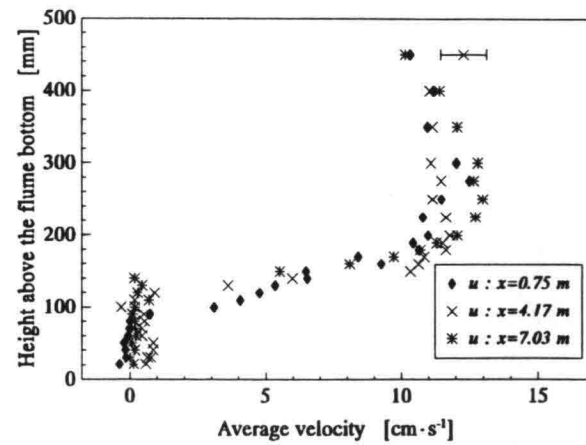


Figure 4.3.56 Average velocities measured during test 7.
(Waves and current, flow rate: $36 \text{ dm}^3 \cdot \text{s}^{-1}$)

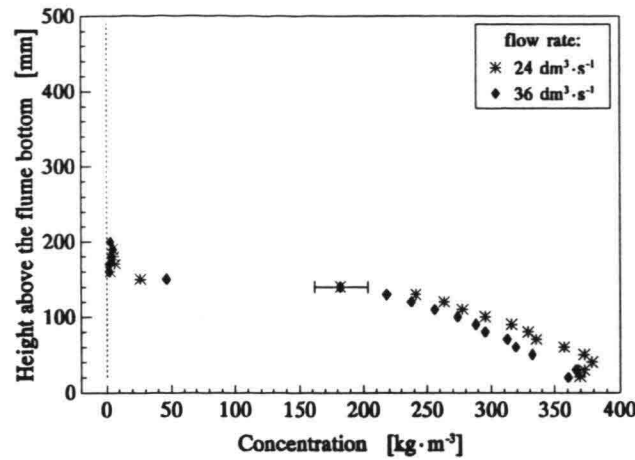


Figure 4.3.57 Concentration profiles during test 7. (Waves and currents)

4.3.10 Test 8

The flow rate was carefully reduced to zero. Subsequently, the wave height was increased, which started the final test on Westwold Clay in the wave/current flume. In the first phase of this test waves were generated for half an hour. The wave heights measured during this phase are shown in figure 4.3.58. The concentration profile measured 15 minutes after the start of this test is plotted in figure 4.3.59.

Velocity measurements were made in and over the bed directly after the concentration measurements. The results of these measurements and the concentration measurements made using the conductivity probe are shown in figures 4.3.60 and 4.3.61, respectively.

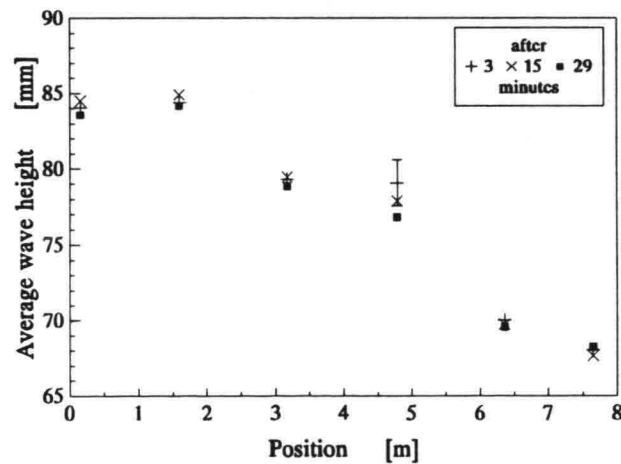


Figure 4.3.58 Average wave heights measured during test 8. (Waves only)

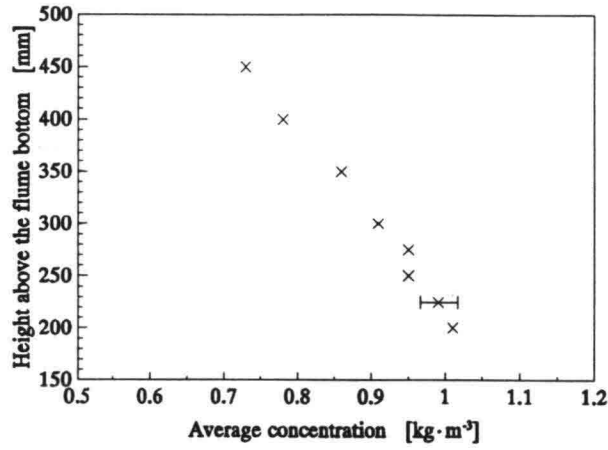


Figure 4.3.59 Suspended sediment concentrations measured at $x=4.35$ m during test 8. (Waves only)

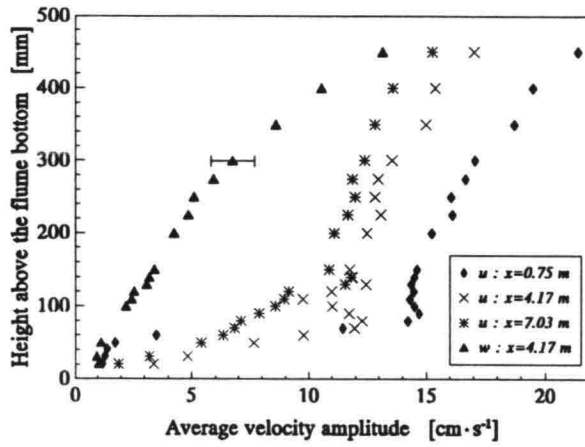


Figure 4.3.60 Average velocity amplitudes during test 8. (Waves only)

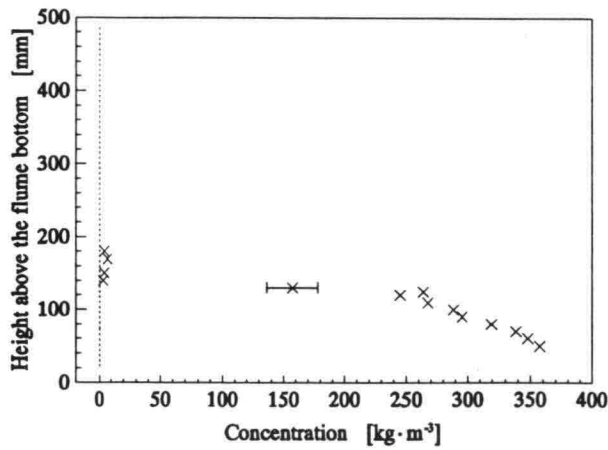


Figure 4.3.61 Concentration profile measured during test 8. (Waves only)

After these measurements the pump was started and the flow rate was set at $48 \text{ dm}^3 \cdot \text{s}^{-1}$. The settings of the wave generator were not altered. Again two minutes after the flow rate was set velocity measurements were made in and over the bed. The results of the measurements are shown in figures 4.3.62 and 4.3.63. In figure 4.3.62 the average velocity amplitudes are plotted and in figure 4.3.63 the average velocities are shown. A net current was only measured at $x=0.75 \text{ m}$. These measurements concluded the experiments on Westwold Clay. The water temperature at the end of test 8 was 20.2°C .

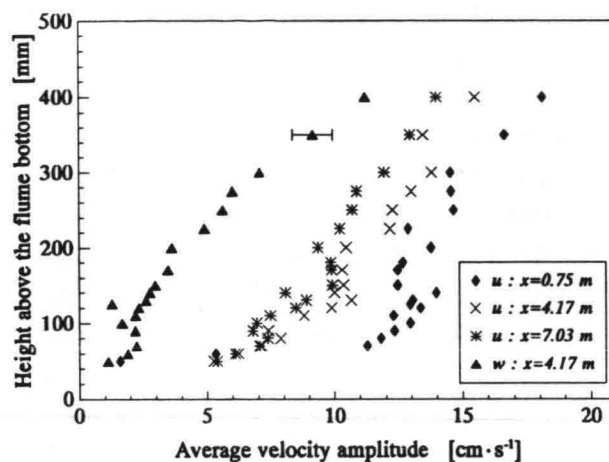


Figure 4.3.62 *Average velocity amplitudes during test 8.*
(Waves and current, flow rate: $48 \text{ dm}^3 \cdot \text{s}^{-1}$)

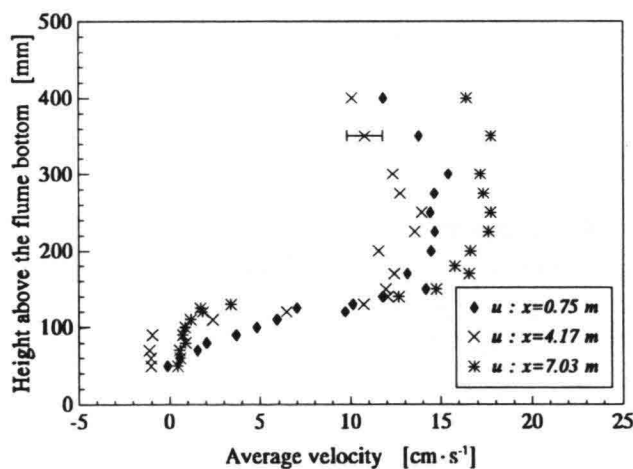


Figure 4.3.63 *Average velocities measured during test 8.*
(Waves and current, flow rate: $48 \text{ dm}^3 \cdot \text{s}^{-1}$)

4.4 Conclusions

The following conclusions may be drawn from the results of the second experiment on Westwald Clay.

- The concentration measurements made prior to the first test showed that the bed was almost uniform in both longitudinal and transverse directions. This uniformity is likely to be due to an almost ideal consolidation process, for there were no leakages during this experiment.
- As soon as the first waves had reached the test section the mud started to liquefy, which behaviour was similar to the observations made in the first experiment. The pore pressures measured during the liquefaction process showed similar trends as measured in the first experiment on Westwald Clay: initially a decrease in the average pressure followed by a transient build-up of an excess pore pressure. This excess pore-pressure decreased gradually with time. For a possible explanation of these results see section 3.5.
- Although fluid mud was present, no significant wave damping was measured during test 1 and the begin phase of test 2, which was probably caused by the fact that the layer of fluid mud was relatively thin. The concentration of the upper part of the bed was approximately $200 \text{ kg}\cdot\text{m}^{-3}$ (figures 4.3.1 and 4.3.2). Consequently, little wave energy was dissipated in the fluid mud, because the viscosity of the fluid mud was relatively low (figure 2.2.1).
There was also no significant wave damping in the begin phase of test 4 (figure 4.3.28), although fluid mud was present in the previous test 3. In test 3 both waves and current (flow rate up to $36 \text{ dm}^3\cdot\text{s}^{-1}$) were present in the flume. As a result the fluid mud was transported out of the test section in the downstream direction. Consequently, hardly any fluid mud was present at the start of test 4 and no wave damping was measured. However, fluid mud was formed during the test which resulted in a significant wave damping.
- The model results and the measured velocity amplitudes in the fluid-mud layer agree very well. Consequently, the assumption made that suspensions of Westwald Clay behave as a viscous fluid seems to be validated with these results. However, in general the calculated decrease in wave height was underestimated by this model. An underestimation of the viscosity of the fluid mud may have caused this effect. An increase in viscosity will lead to an increase in the dissipation of wave energy. However, an increase in viscosity leads to a different velocity profiles as the measurements showed. Another cause for the underestimation of the wave damping may be the adaptation of the incoming waves to the instantaneous increase in water depth.
- The velocity measurements made during test 4 indicated that the thickness of the fluid-mud layer was not uniform in the longitudinal direction: in the upstream part of the test section the fluid-mud layer was roughly 9 cm thick whereas, the fluid-mud layer was approximately 15 cm thick in the downstream part of the test section. Furthermore, the velocity profiles measured in the upstream part of the test section were different from the profiles measured in the downstream part (figure 4.3.33).

- In the experiments on China Clay (De Wit, 1994) it was observed that a layer of fluid mud was easily transported by a current in the downstream direction and hardly any mud was entrained during this process. During tests 3, 7 and 8 velocities were measured in the fluid mud when both waves and current were present in the flume. Although the bed was completely liquefied in some tests, only a net current was generally measured in the upper part of the fluid-mud layer, which was probably caused by the downstream endwall of the test section. The heights of the endwalls, in particular the downstream one, were very critical during these measurements: on one hand, the mud would not leave the test section if the endwalls were too high and, on the other hand, a gravitational current would be generated if the endwalls were too low. The adjustments of these endwalls was not easy, for estimating the thickness of the mud layer was hampered by the highly opaque suspension in later phases of the experiment. Furthermore, measurements in the fluid mud had to be made very quickly when both waves and current were present, because the fluid mud was rapidly transported out of the test section.
- The suspended sediment concentrations increased very rapidly in the first two tests. The concentration measurements made during test 4 showed that, unlike the suspended sediment concentrations measured in tests 1 and 2, the suspended sediment concentrations were almost uniform in the water column. This unusual concentration profile was formed during test 3, where waves and current were present in the flume. During this test the eroded mud was recirculated and a uniform suspension was formed which reentered the test section.

Chapter 5

General conclusions

Two major experiments were made on Westwald Clay in a wave/current flume. Mineralogical analysis and rheological measurements showed that Westwald Clay is a more cohesive sediment than the China Clay used in the foregoing experiments (De Wit, 1994). Preliminary consolidation tests showed that Westwald Clay had to be mixed with saline tap-water (salinity 5‰) for at least 3 weeks to form an equilibrium suspension.

The beds were formed by deposition from a suspension. The suspended sediment concentration was about $135 \text{ kg}\cdot\text{m}^{-3}$. The consolidation periods in the first and second experiment were 20 and 28, respectively. The average bed concentrations in the experiments on Westwald Clay were roughly $\pm 300 \text{ kg}\cdot\text{m}^{-3}$, which is half the value of the bed concentrations encountered in the China Clay experiments.

Fluid mud was generated in both experiments when the first waves (wave height $\pm 3 \text{ cm}$) had reached the test section, which was probably caused by the rather low yield strength of the Westwald Clay.

The pore pressures measured during the liquefaction process showed initially a decrease in the average pressure, which may be induced by a break-up and rearrangement of the particles and aggregates. Shear stresses in the bed caused by the streamwise variation in wave-induced pressures on the bed play an important role in this process (De Wit, 1994). The break-up seemed to involve an increase in volume due to a rearrangement of the particles or aggregates, for the pore-pressure decreased and the permeability of the mud was quite low. However, due to the weight of the overlying mud the pore pressure showed a gradual build-up to compensate for the reduced effective stress. This excess pore-pressure did not dissipate directly because of the low permeability of the mud.

In general waves were dampened when fluid mud was present. However, in some tests no significant wave damping was observed although fluid mud was present. The low viscosity of the fluid mud and the relatively small thickness of the fluid-mud layer were likely to be the causes for the absence of significant wave damping during these tests.

The calculated velocities in the fluid-mud layer using the modified model of Gade (1958) agreed quite well with the measured values. The calculated wave damping underestimated the measured wave damping which may be caused by an underestimation of the thickness of the fluid-mud layer or the viscosity of the fluid mud.

Westwald Clay had strong adhesive properties and a special affinity for glass, for it stuck to the glass sidewalls of the flume. Consequently, no visual observations concerning the state of the bed could be made during the tests, which made it very difficult to adjust the heights of the endwalls of the test section in a correct way.

The automatic traversing units proved to be very reliable and flexible instruments. The operation set with which these instruments can be programmed is adequate and consequently most of the user demands can be programmed easily, although the available user memory is rather limited.

Appendix A

Traversing unit

Three motorised traversing units were used to position automatically the electromagnetic velocity meters and the optical concentration meters during the experiments on Westwald Clay. A traversing unit comprised two parts: a mechanical part where the actual traversing was made and an electronic part, which controlled the translation. The specifications of the units used are discussed in section A.1. All of the functions of the electronic controller were controlled by software. A user program was built using a special instruction set. A listing of the control program used in the experiments and some information on the instruction set are found in section A.2. A special device was built, which generated an analogue signal proportional to the position of the traversing unit. This device was used to log the position of the traversing units during the experiments. The operation of the device is discussed in section A.3.

A.1 Specifications of the traversing unit

The mechanical part of the traversing unit was a motorised elevating stage based on the standard B2500 series of Unislide (type B2536LP). The B2500 series stage was basically assembled of a slider and a so-called base, both constructed from high specification aluminium alloy (figures A.1.1 and A.1.2). The slider (length 76 mm) was translated in the base by the rotation of a stainless steel leadscrew, which was connected to a leadscrew nut in the slider. The slider was provided with a Nulatron GS lamination to improve the wear resistance of this assembly. The base was fixed in a vertical position by a u-shaped bar fitted on an aluminium base plate. The total weight of a unit was approximately 11 kg. Two limit switches were installed at both ends of the base and furthermore a home switch was installed just below the upper limit switch. The function of these switches is explained later. A brushless servo motor with an integrated resolver and break (GSC, type BL-SM60/B24) was used to rotate the leadscrew.

The servo motor was controlled by a digital amplifier (Elmo DBA-12/160RRI, power supply Elmo PSS-12/160R) which was based on a 16 bit micro-processor. The resolver integrated in the servo motor was required for the proper operation of the digital amplifier. All the amplifier functions could be controlled by software, such as current control, protective functions and position control. The controller was provided with a battery-backed RAM-memory for storing user programs and parameters. The execution of user programs could be changed by 7 inputs, furthermore 10 outputs and a 4-digit display could be controlled by software. The programs could be stored in the RAM-memory of controller via RS232 or RS485. The maximum number of program lines was 50 and the maximum length of a program line was 39 characters. A special software packet called DCB was provided with which user programs could be easily built and sent to the controller via the serial port of a personal computer. The accuracy of the traversing unit was ± 0.1 mm.

A custom-made electronic circuit was added to the controller which could be activated with a switch mounted at the back of the controller when the slider had activated one of the limit switches.

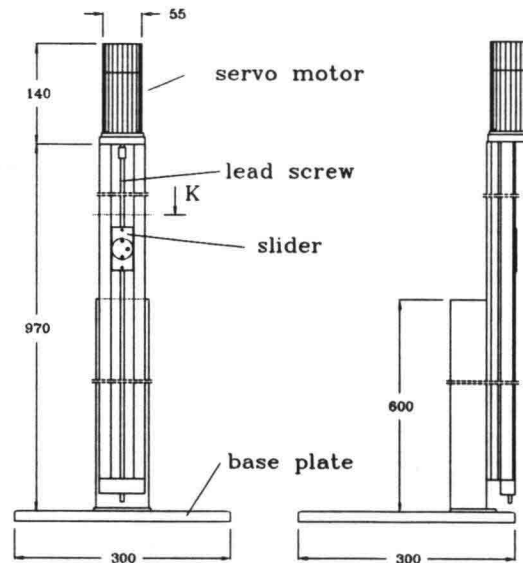


Figure A.1.1 Front (left) and side (right) view of the mechanical part of a traversing unit. (Dimensions in mm)

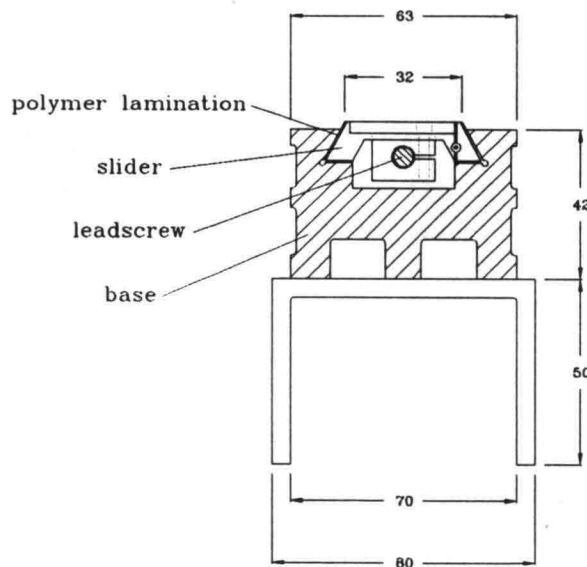


Figure A.1.2 Enlarged cross-section K (figure A.1.1) of the mechanical part of the traversing unit.

As a result the slide was translated in such direction that the limit switch was deactivated, i.e. in upward direction when the lower limit switch was activated and in downward direction when the upper limit switch was activated. Without this emergency circuit the controller stopped all operations if one of the limit switches was activated and the characters "INHB" (INHibited) appeared on the display. The controller would not start any other operations unless the limit switch was deactivated, consequently the slide had to be translated manually. However, when an automatic error routine was stored in the memory of the controller this routine was started when one of the limit switches was activated and in this way the same result could be achieved by software as the custom-made electronic circuit. By adding this circuit the error subroutine could be omitted from the user program, which

was very convenient for the RAM memory was rather limited (maximal 50 lines).

The electromagnetic velocity meter and the intake and output pipes of an optical concentration meter were mounted on a frame especially built for the traversing unit which is shown in figure A.1.3. Under an aluminium tray fixed to the slider, a PVC frame was installed in which the electromagnetic velocity meter and the pipes of the concentration meter could be easily fixed using knurled bolts. This frame proved to be very rigid in preliminary tests, although it was quite light (c. 2 kg).

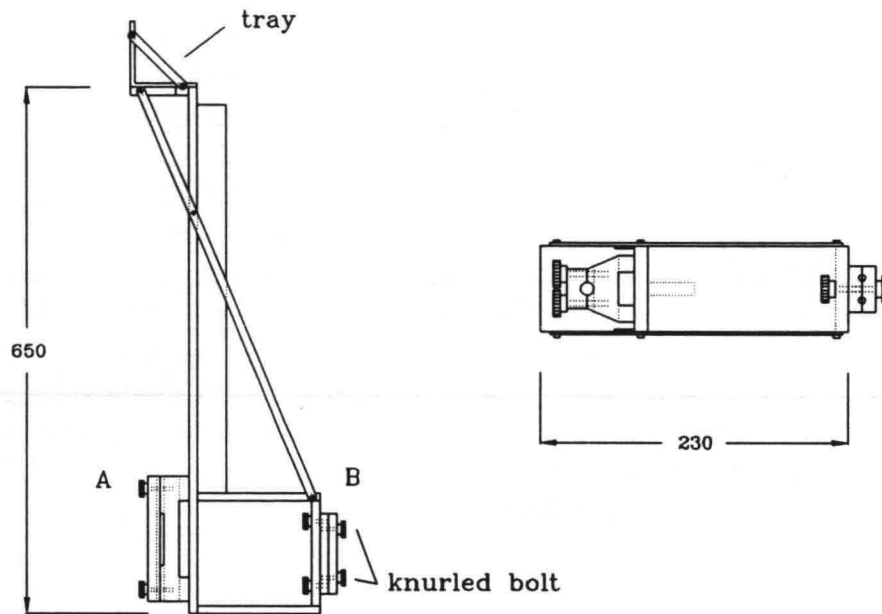


Figure A.1.3 Side (left) and enlarged view from below (right) of the construction made to hold an electromagnetic velocity meter (A) and the pipes of an optical concentration meter (B). (dimensions in mm).

As stated before, the user program was built using the program DCB on a personal computer. Via the serial port of the personal computer the user program was sent to the controller and stored in its memory. The program used in the experiments on Westwald Clay is listed and explanations of several instructions are given in the next section.

A.2 Traversing program used in the experiments on Westwald Clay

In the experiments on Westwald Clay the employment of the traversing units had to be flexible: standard measurements, such as the measurements of velocity profiles in the water layer as well in a fluid-mud layer, had to be easily made automatically. However, it should also be possible to abort these automatic traversing routines in order to traverse manually, for instance when other instruments were fixed to the traversing units or when measurements at certain locations were preferred. In both cases the user should be able to determine the measuring position from the data logged on the personal computer. A user program and a special device were built which answered the criteria mentioned above. The device was controlled by the digital amplifier via the available outputs (10) and

it generated an output voltage proportional to the position of the traversing unit. The operation of this device was based on a simple digital to analogue conversion, as a result this device was called the DA-converter. The listing of the program used in the experiments is listed next. The amplifier-controlled device (DA-converter) is discussed in section A.3.

A special instruction set had to be used to program the digital amplifier. See DCB (1991) for a complete list of the instructions which can be used to program the amplifier. Some details on the hardware configuration are discussed first in order to understand the program used in the experiments on Westwald Clay.

A home switch was installed just below the upper limit switch. This home switch can be used as a reference point in a user program. If a homing sequence is required the Index (connector J3, pin 15) must be connected to Input 5 (connector J4, pin 6) (DCB, 1991). Consequently, 6 inputs can be used as inputs for a user program. A switchboard was built on which 6 switches were mounted; one selector switch (input 1) and five push buttons (inputs: 2, 3, 4, 6 and 7). Pushing a button resulted in setting the input port high as long as the button was pushed. The inputs were either high or low (TTL-levels), just as the 10 outputs. The switchboard was connected with a 25 pins connector to each controller. Consequently, the traversing units could be activated simultaneously by pushing a button on the switchboard when the same user programs were stored in the memories of the digital amplifiers. The outputs of the digital amplifier were used to control the device which generated an analogue signal proportional to the position of the traversing unit (outputs 1-9) and to control the trigger for the data-acquisition set (output 10).

The general user program employed in the experiments on Westwald Clay is listed next. The line numbers are only used for explanatory reasons and have to be omitted when programming the digital amplifier. An explanation of the settings, the variables and the in- and output ports is found in tables A.2.1, A.2.2 and A.2.3, respectively.

1	<i>#@;HX;AC640DC0;GN28;SP9C40;R0=FA0</i>	Hexagonal definition of constants
2	<i>I17;DSWAIT;HM;AM;R1=1721E0;R8=C3500;DC</i>	
3	<i>R1=-1*R1;PAR1;BG;AM;DH;R1=0;R5=1;JS#A</i>	Go to the start position
4	<i>#I;R45=0;JP#U,I1=1</i>	<u>Main program</u>
5	<i>SB10;DSMAN</i>	traverse manually or automatically
6	<i>#J;JP#M,I1=0</i>	
7	<i>JP#I</i>	
8	<i>EN</i>	
9	<i>#M;JS#O,I2=1</i>	<u>Traverse manually</u>
10	<i>JS#N,I3=1</i>	#O: go in positive direction (up)
11	<i>JS#L,I4=1</i>	#N: go in negative direction (down)
12	<i>JP#J</i>	#L: change interval (1 or 25)
13	<i>#L;WT250;JP#K,R5=25</i>	
14	<i>DSD=25;R5=25;RT</i>	
15	<i>#K;DSD=1;R5=1;RT</i>	
16	<i>#O;JP#P,R1+R8>512-R5*R0</i>	<u>Go upward if possible</u>
17	<i>R1=R0*R5+R1;PAR1;CB10;BG;AM;SB10</i>	
18	<i>#P;JS#A</i>	
19	<i>RT</i>	
20	<i>#N;JP#Q,R1+R8<R5*R0</i>	<u>Go downward if possible</u>

```

21  R1=-1*R0*R5+R1;PAR1;CB10;BG;AM;SB10
22  #Q;JS#A
23  RT
24  #U;CB10;R14=1;DSAUTO;JS#R,I4=1
25  R12=5000;R13=60000;R6=260*R0;JS#Y,I6=1
26  JP#I
27  #R;DSPRG1;R10=25*R0;R6=8*R10;R11=4
28  R7=1;R12=7500;R13=30000;JS#E
29  R15=150*R0;JS#S
30  R15=200*R0;JS#S
31  #T;RT
32  #S;JP#T,R45=1
33  R1=R6+R15-R8;PAR1;BG;AM;JS#A
34  WTR12;SB10;WTR13;CB10;JP#T
35  #Y;DSPRG2;R10=10*R0;R11=24;R7=-1
36  #E;R1=R7*R10*R14+R6-R8;PAR1;BG;AM;JS#A
37  WTR12;SB10;WTR13;CB10;JP#Z,R45=1
38  R14=R14+1;JP#E,R14<R11+1
39  #Z;RT
40  #A;R2=R1+R8/R0;SSR2;DS,SS;JP#B,R2<4
41  JP#C,R2<512
42  R3=127;R4=127;JP#D
43  #B;R3=R2*32;R4=0;JP#D
44  #C;R4=R2-3/4;V4=R2-3/4;V4=V4-R4*10;
45  R3=-4*R4+R2*32;JP#D,V4<2;
46  R4=R4+1;R3=-4*R4+R2*32;JP#D
47  #D;CB9;OPR3;WT25;SB9;OPR4;SB8;WT25
48  CB8;RT
49  #^;R45=1;RI
50  E

```

Traverse automaticallyProgram 1

Measurements at positions 225, 250, 275, 300, 350 and 400 mm;
 adjusting time: 7.5 s
 measuring time: 30 s

Program 2

Measurements at positions 250, 240, 230, 220, ..., 30, 20, 10 mm;
 adjusting time: 5 s
 measuring time: 60 s

Subroutine Digital

Convert the decimal position to a digital 9 bit value.

Calculate the 7 low-order and high-order bits.

Export the 7 low-order and high-order bits.

Interrupt routine activated when input 7 is high (line 2: II7)

Table A.2.1 System settings used in the traversing program.

instruction	hexadecimal value	decimal value	description
AC	640DC0	11800000	acceleration
SP	9C40	40000	speed
GN	28	40	gain

Table A.2.2 *Explanation of the variables used in the traversing program.*

variable	description
R0	Constant: number of pulses per mm decimal value: 4000, hexadecimal value: FA0
R1	Absolute position, a multiple of R0
R2	Distance (mm) from zero position: R1/R0
R3	7 low-order bits
R4	7 high-order bits
R5	Interval (mm)
R6	Start position - R7*R10
R7	Multiplier: -1 (down) or 1 (up)
R8	Initial starting position (C3500 ~ 200 mm)
R10	Interval size
R12	Adjustment time (ms), maximal 65 s
R13	Measuring time (ms), maximal 65 s
R14	counter (number of measuring points)

Table A.2.3 *Function of the in- and output ports of the digital amplifier.*

Port	Function
In 1	Manually or automatically traversements low: manually
In 2	Manually traversements: go upwards when high
In 3	Manually traversements: go downwards when high
In 4	Automatically: program 1 when high Manually: interval change when high
In 5	Required for homing sequence
In 6	Automatically: program 2 when high
In 7	Abort automatically traversements when high
Out 1-7	7 bit number; LSB: Out 1, MSB: Out 7
Out 8	Low-order bits when low High-order bits when high
Out 9	Clock puls: conversion when high
Out 10	Trigger: start data logging when high

A.3 Operation of the DA-converter

The accuracy of the DA-converter was chosen with respect to the accuracy of the data-acquisition set used in the experiments. The data-acquisition set was based on a signed 12 bits analogue-digital converter (-10V ~ -2048, +10V ~ +2047) and the accuracy of the set was ± 1 bit. Consequently, the maximal resolution of the data-acquisition set was 1024. Only 512 data points had to be determined during an experiment for the minimal interval of the traversing unit was only 1 mm, and the total span of the traversements was approximately 500 mm. Nine output ports of the digital amplifier were available to send the position of the traversing unit to a DA-converter, for output 10 was reserved as a trigger for the data-acquisition set. As a result only 256 different values could be send from the digital amplifier in one setting of the ports, which was inadequate. This problem was solved by sending the position of the traversing unit in a multiplex way to a DA-converter: first the low-order part and subsequently the high-order part of the position was sent. Output 8 was used to indicate whether the data sent were the low-order (output 8 low) or high-order bits. Output 9 was used as a trigger for the conversion of the digital value to an analogue voltage. Consequently, a 14 bit (2x7) value could be send in this way to the DA-converter. As a result the so-called DA-converter was based on a 14-bit digital-to-analog converter AD7840. For further specifications on this converter see DAT (1992). The electronic circuit is schematically shown in figure A.3.1.

The upper octal latch (74LS373) is enabled when output 9 (OUT 9, figure A.3.1) is low. Then the state of the output ports 1 up to 7 inclusive (low-order bits) will be stored and the pins 1Q up to 7Q inclusive are set. The lower octal latch (U6) is enabled when the state of output 9 changes to low. The high-order bits can be set. As soon as these bits are stored the state of output 8 is changed from low to high, resulting in a conversion cycle of the digital-to-analog converter (AD7840) of the digital

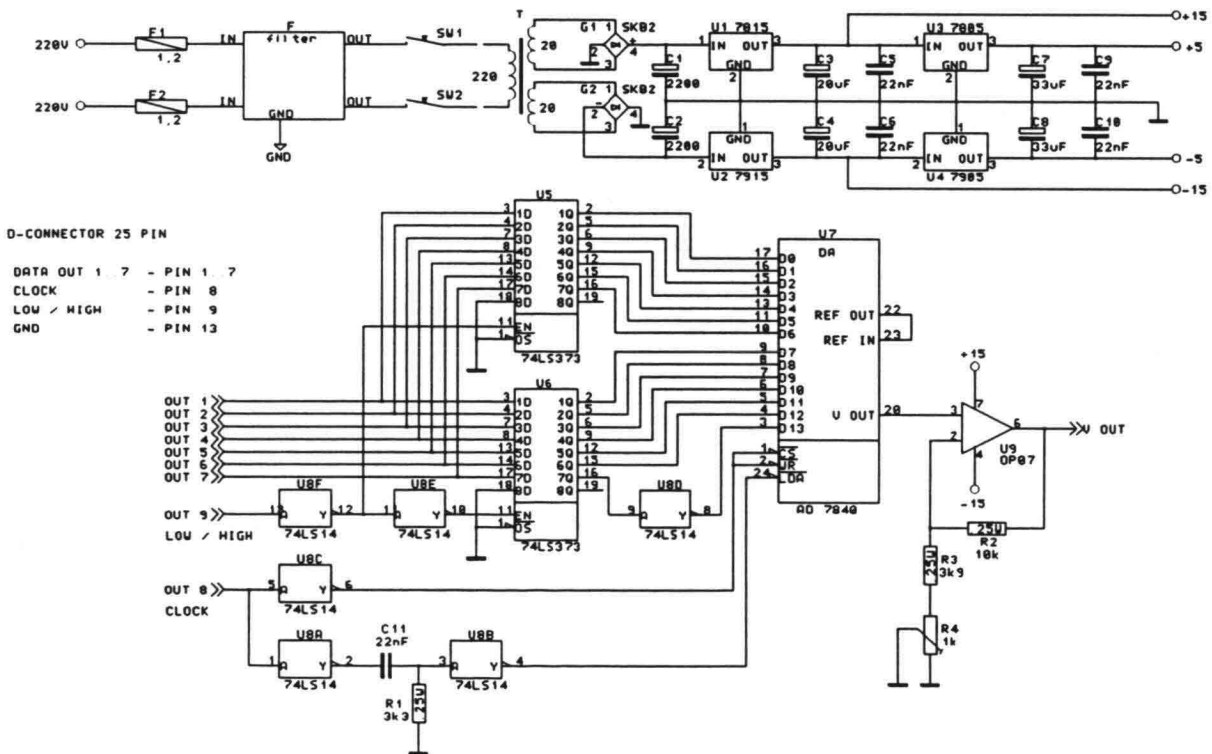


Figure A.3.1 Circuit of the DA-converter.

input to an analogue output voltage (V OUT). An adjustable amplifier is added to adjust the span of the DA-converter to the span of the data-acquisition set, for the data-acquisition sets used in the Hydromechanics Laboratory had slightly different operating ranges during the period when the experiments were made.

The subroutine Digital included in the user program (lines 40-48) as discussed in section A.2 was built in such a way that it could be used with this DA-converter. In the first seven lines of this subroutine (#A, #B and #C) the low-order bits (R2) and the high-order bits (R3) are calculated from the position of the traversing unit. In line 47 the low-order bits are sent to the DA-converter (output 9: low) using the OP command (Output Port). Subsequently, output 9 goes high and the high-order bits are send (OPR3) and finally output port 8 goes from low to high and the conversion is made.

Appendix B

Additional information on the first experiment

In the first experiment on Westwald Clay 6 wave height meters, 3 electromagnetic current meters, 3 optical concentration meter, 4 pressure meters, 1 thermometer and 1 conductivity meter were used. The signals generated by these instruments and the signal generated by the traversing unit were recorded on two personal computers using a data-acquisition system. The signals generated by the instruments which were fixed, such as the wave height meters, the pressure meters and the thermometer, and the signals from the optical concentration meters were continuously logged on computer 1. Computer 2 was used to record the signals of those instruments which were traversed in the water column, i.e. the velocity and concentration meters. In tables B.1 and B.2 specifications are given on the exact location, the number and the channel on which the signal of every instrument was recorded for the computers used. The original measurements, can be found on tape no. 1 under session entitled "The first experiment on Westwald Clay". This backup was made using the Interpreter TapeXchange TX120 tape backup system with Txplus Software version 5.14.

The calibration measurements of the wave height meters for the ranges 5, 10 and 20 cm are saved under the directories "CALWHM\RANGE05", "..\RANGE10" and "..\RANGE20", respectively. The filename of each measurement contains the position of the wave gauge relative to the mean water level; every name starts with "CWHM" (Calibration Wave Height Meter) followed by "U" or "D", which refers to the change in position of the gauge with respect to the mean water level: U for Upward and D for Downward. The remaining digits indicate the vertical displacement in millimetres.

The measurements from which the zero-flow drift of the electromagnetic current meters was determined are saved under directory "DRIFTEMS". Measurements of the X and Y-channels were made in quiescent water prior to the and after the tests and were saved as "EMSNIL.LOG" and "EMSEND.LOG", respectively.

The data-acquisition sets were also calibrated prior to the experiments. The files used to calibrate the two data-acquisition sets are saved under directory "CALAD" (CALibration Data-Acquisition set). The single calibration measurements were saved as "CALAD@@", where @@ indicates the number of the measurement. The input voltage, measured using an accurate potential meter, was saved under the item "remarks" of every file.

The traversing units were also calibrated prior to the experiments. The files used for the calibration are saved under directory "CALTRAV" (CALibration TRAVersing unit). The single calibration measurements were saved as "CALTRA@@", where @@ indicates the number of the measurement. The displayed position of the traversing unit for every single measurement was saved under the item "remarks".

The data needed to process the measurements using the conductivity probe are listed in table B.3. The optical concentration meter were calibrated using the data listed in table B.4.

The measurements made during the different tests are saved under the subdirectories "TEST@", where @ denotes the number of the test.

Table B1 *Additional information on the instruments used during the first experiment on Westwald Clay (computer 1).*

Instrument	number of gauge	number of main amplifier	location on flume ¹⁾ [m]	signal recorded on channel no.
wave height meter	A-M?-032	010/004	0.10	1
wave height meter	75B046	MS76004	1.60	2
wave height meter	78AP93	MS76006	3.17	3
wave height meter	78AP94	MS76003	4.78	4
wave height meter	75G045	MS76007	6.38	5
wave height meter	070	MS76010	7.65	6
pressure meter ²⁾	5830	11219/92-10	4.15	7
pressure meter ³⁾	6812	11222/92-10	4.15	8
pressure meter ⁴⁾	6813	11051/92-9	4.15	9
pressure meter ⁵⁾	5938	7461/91/2	4.15	10
thermometer ⁶⁾	390Pt RTD	Fluke model 2180A	5.43	11
concentration meter	-	2	0.93	12
concentration meter	-	0194	4.35	13
concentration meter	-	0591	7.24	14
position traversing unit	-	-		15

¹⁾ Maximal error: ± 0.01 m, instruments installed at $y = 0.40$ m, except for the pressure transducers. See section 3.4 for the definition of the coordinate system.

²⁾ Range: 0-75 mbar ($\sim 0-7.5$ Vdc), installed at 15.0 cm above the bottom of the flume.

³⁾ Range: 0-75 mbar ($\sim 0-7.5$ Vdc), installed at 17.5 cm above the bottom of the flume.

⁴⁾ Range: 0-75 mbar ($\sim 0-7.5$ Vdc), installed at 19.3 cm above the bottom of the flume.

⁵⁾ Range: 0-75 mbar ($\sim 0-10$ Vdc), installed at 21.0 cm above the bottom of the flume.

⁶⁾ 100 mV per degree Celsius

Table B.2 *Additional information on the instruments used during the first experiment on Westwald Clay (computer 2).*

Instrument	number of gauge	number of main amplifier	location on flume ¹⁾ [m]	signal recorded on channel no.
current meter ²⁾	E127	-	7.02	1
current meter ₃₎	E127	-	7.02	2
current meter ²⁾	E075	E075	4.16	3
current meter ³⁾	E075	E075	4.16	4
current meter ²⁾	E125	-	0.74	5
current meter ³⁾	E125	-	0.74	6
concentration meter	-	2	0.93	7
concentration meter	-	0194	4.35	8
concentration meter	-	0591	7.24	9
conductivity probe	-	-	7.24	10
position traversing unit	-	-	-	11

¹⁾ Maximal error: ± 0.01 m, instruments installed at $y = 0.40$ m.

²⁾ X channel

³⁾ Y channel

Table B.3 *Calibration data used for the conductivity probe.*

date	output in clear water [V]	output in sample [V]	concentration sample [kg·m ⁻³]
22 April	3.14	3.74	260
3 May	2.95	3.84	365
5 May	2.99	3.60	276

Table B.4 Calibration data used for the optical concentration meters.

date	Number 2		Number 0591		Number 0194	
	concentration [kg·m ⁻³]	output voltage [V]	concentration [kg·m ⁻³]	output voltage [V]	concentration [kg·m ⁻³]	output voltage [V]
22 April (tests 1-2)	0.283	2.19	0.0934	0.62	0.0208	0.14
	0.300	2.46	0.0726	1.14	0.0652	0.68
	0.261	2.00	0.214	1.47	0.159	1.65
	0.893	7.10	0.308	2.38	0.182	1.80
			0.327	2.22	0.280	2.61
			0.922	7.20	0.274	2.91
				0.620	6.02	
22 April (tests 3-4)	1.02	7.90	0.766	2.70	0.627	2.00
	1.48	7.55	0.997	3.50	0.916	3.00
	1.10	5.50	1.37	4.90	1.47	4.80
	1.28	6.20	1.74	6.10	1.70	5.50
	0.337	4.90	2.03	7.15	1.99	6.15
3 May	0.0884	0.11	0.0174	0.02	0.0152	0.03
	0.351	0.56	0.625	0.87	0.668	1.06
	0.434	0.68	0.696	1.07	0.853	1.48
	0.527	0.81	0.376	0.49	0.541	0.87
	0.815	1.44	1.38	1.96	1.23	1.85
5 May	0.299	0.38	0.294	0.42	0.203	0.26
	0.294	0.48	0.261	0.41	0.258	0.39
	0.490	0.79	0.610	0.88	0.692	1.06
	0.634	0.93	0.748	0.98	0.784	1.22
	0.787	1.44	0.880	1.08		
	0.938	1.38	0.789	1.14		

Appendix C

Additional information on the second experiment

In the second experiment on Westwald Clay 6 wave height meters, 3 electromagnetic current meters, 3 optical concentration meter, 4 pressure meters, 1 thermometer and 1 conductivity meter were used, just as in the first experiment. The procedure followed to log and backup the data is identical to the procedure described in appendix B. In tables C.1 and C.2 specifications are given on the exact location, the number and the channel on which the signal of every instrument was recorded for the computers used. The original measurements, can be found on tape no. 1 under session entitled "The second experiment on Westwald Clay".

The data needed to process the measurements using the conductivity probe are listed in table C.3. The optical concentration meter were calibrated using the data listed in table C.4.

Table C.1 *Additional information on the instruments used during the second experiment on Westwald Clay (computer 2).*

Instrument	number of gauge	number of main amplifier	location on flume ¹⁾ [m]	signal recorded on channel no.
current meter ²⁾	E125	-	0.75	1
current meter ₃	E125	-	0.75	2
current meter ²⁾	E075	E075	4.17	3
current meter ³⁾	E075	E075	4.17	4
current meter ²⁾	E127	-	7.03	5
current meter ³⁾	E127	-	7.03	6
concentration meter	-	2	0.94	7
concentration meter	-	0194	4.35	8
concentration meter	-	0591	7.25	9
conductivity probe	-	-	7.25	10
position traversing unit	-	-	-	11

¹⁾ Maximal error: ± 0.01 m, instruments installed at $y = 0.40$ m.

²⁾ X channel

³⁾ Y channel

Table C.2 *Additional information on the instruments used during the second experiment on Westwald Clay (computer 1).*

Instrument	number of gauge	number of main amplifier	location on flume ¹⁾ [m]	signal recorded on channel no.
wave height meter	A-M?-032	010/004	0.16	1
wave height meter	75B046	MS76004	1.60	2
wave height meter	78AP93	MS76006	3.17	3
wave height meter	78AP94	MS76003	4.79	4
wave height meter	75G045	MS76007	6.36	5
wave height meter	070	MS76010	7.65	6
pressure meter ²⁾	5830	11219/92-10	4.19	7
pressure meter ³⁾	6812	11222/92-10	4.19	8
pressure meter ⁴⁾	6813	11051/92-9	4.19	9
pressure meter ⁵⁾	5938	7461/91/2	4.19	10
thermometer ⁶⁾	390Pt RTD	Fluke model 2180A	2.80	11
concentration meter	-	2	0.94	12
concentration meter	-	0194	4.35	13
concentration meter	-	0591	7.25	14
position traversing unit	-	-	-	15

¹⁾ Maximal error: ± 0.01 m, instruments installed at $y = 0.40$ m, except for the pressure transducers. See section 3.4 for the definition of the coordinate system.

²⁾ Range: 0-75 mbar ($\sim 0-7.5$ Vdc), installed at 15.0 cm above the bottom of the flume.

³⁾ Range: 0-75 mbar ($\sim 0-7.5$ Vdc), installed at 17.5 cm above the bottom of the flume.

⁴⁾ Range: 0-75 mbar ($\sim 0-7.5$ Vdc), installed at 19.3 cm above the bottom of the flume.

⁵⁾ Range: 0-75 mbar ($\sim 0-10$ Vdc), installed at 21.0 cm above the bottom of the flume.

⁶⁾ 100 mV per degree Celsius

Table C.3 *Calibration data used for the conductivity probe.*

date	output in clear water [V]	output in sample [V]	concentration sample [$\text{kg}\cdot\text{m}^{-3}$]
16 July	2.96	3.64	340
23 July	2.88	3.73	344

Table B.4 Calibration data used for the optical concentration meters.

date	Number 2		Number 0591		Number 0194	
	concentration [kg·m ⁻³]	output voltage [V]	concentration [kg·m ⁻³]	output voltage [V]	concentration [kg·m ⁻³]	output voltage [V]
16 July	0.042	0.07	0.090	0.18	0.034	0.06
	0.071	0.10	0.186	0.41	0.204	0.44
	0.314	0.57	0.258	0.50	0.478	0.73
	0.248	0.63	0.372	0.65	0.478	1.10
	0.900	1.52	0.974	1.57	0.864	1.38
	1.29	2.19	1.05	1.78	0.976	1.52
23 July	0.206	0.36	0.226	0.36	0.138	0.22
	0.230	0.39	0.420	0.74	0.196	0.29
	0.436	0.76	0.654	1.12	0.368	0.62
	0.630	1.07	0.772	1.32	0.482	0.78
	0.764	1.26	0.978	1.70	0.644	1.02
	1.14	1.97	1.50	2.42	0.758	1.24
	1.43	2.40			0.916	1.48
				1.46	2.31	

References

- Dacon, (1990a), *DACON Data-acquisition software vers. 1.2*, Delft University of Technology, Hydromechanics Laboratory, The Netherlands.
- Dacon, (1990b), *DACON Program listings vers. 1.2*, Delft University of Technology, Hydro-mechanics Laboratory, The Netherlands.
- DAT, (1992), *1992 Data converter reference manual*, Vol. 1, Analog Devices, Inc., 1992
- DCB, (1991), *Digital servo amplifier DCB series operating instructions*, ELMO, Rev 91/9, preliminary.
- De Wit, P.J., (1992a), *Rheological measurements on artificial muds*, Report no. 9-92, Delft University of Technology, The Netherlands.
- De Wit, P.J., (1992b), *Instruments used in the research on cohesive sediments*, Report no. 8-92, Delft University of Technology, The Netherlands.
- De Wit, P.J., (1994), *Liquefaction and erosion of mud due to waves and current - experiments on China Clay*, Report no. 10-92, Delft University of Technology, The Netherlands.
- Gade, H.G., (1958), *Effect of a nonrigid, impermeable bottom on plane surface waves in shallow water*, Journal of Marine Research, Vol. 16, No. 2, pp. 61-82.
- Van Olphen, H., (1977), *An introduction to clay colloid chemistry*, Second edition, 1977, John Wiley & Sons, Inc., ISBN 0-471-01463-X.
- Winterwerp, J.C., (1994), *Calibration of the Haake CV100 Rheometer*, Report no. VR682.94, Delft Hydraulics, The Netherlands.

